BAW-10177

Topical Report
October 1990

Mark-BW Reload LOCA Analysis for the Trojan Plant

B&W Fuel Company
P. O. Box 10935
Lynchburg, Virginia 24506-0935

B&W Fuel Company
P. O. Box 10935
Lynchburg, Virginia 24506-0935

Topical Report BAW-10177

October 1990

Mark-BW Reload LOCA Analysis for the Trojan Plant

Key Words: Large Break, LOCA, Transient, Water Reactors

ABSTRACT

The B&W Fuel Company will be delivering reload fuel to the Portland General Electric Trojan plant beginning in 1991. This report presents a complete LOCA evaluation for operation of the Trojan nuclear plant with Mark-BW reload fuel. Compliance with the criteria of 10 CFR 50.46 is demonstrated. Operation of the unit while in transition from Westinghouse-supplied fuel to BWFC-supplied Mark-BW fuel is also justified. Other BWFC topical reports describe the Mark-BW fuel assembly design; the mechanical, nuclear, and thermal-hydraulics methods supporting the design; and ECCS codes and methods. The analyses and evaluations presented in this report serve, in conjunction with the other topical reports, as a reference for future reload safety evaluations applicable to cores with BWFC-supplied fuel assemblies.

ACKNOWLEDGEMENTS

The B&W Fuel Company wishes to acknowledge the efforts put forth by J. R. Biller, J. J. Cudlin, B. M. Dunn, J. A. Klingenfus, R. J. Lowe, C. K. Nithianandan, N. H. Shah, and K. C. Shieh in preparing and documenting the material contained in this report.

Topical Report Revision Record

Documentation Revision	Description
0	Original Issue

TABLE OF CONTENTS

List of Tables

List of Figures

List of Figures (Con't)

List of Figures (Con't)

List of Figures (Con't)

List of Figures (Con't)

List of Figures (Con't)

1. Introduction

The B&W Fuel Company (BWFC) will be delivering reload fuel to the Portland General Electric Trojan plant beginning in 1991. The Mark-BW reload fuel will be similar in design and performance to fuel assemblies already licensed and operating in Trojan. In accordance with the requirements of 10 CFR 50.46 and 10 CFR 50, Appendix K, an evaluation of the emergency core cooling system (ECCS) performance has been performed for BWFC reload fuel for the Trojan plant. In presenting that analysis, this report complements other BWFC topical reports that describe the Mark-BW fuel design; the mechanical, nuclear, and thermal-hydraulics methods supporting the design; and ECCS codes and methods. The analyses and evaluations presented in this report a intended to serve, in conjunction with these other topical reports, as a reference for future reload safety evaluations of the Trojan plant applicable to cores with BWFC-supplied fuel assemblies.

The Trojan nuclear power plant uses a nuclear steam supply system designed by Westinghouse that is representative of the standard Westinghouse four-loop, 3411 Mwt design. The ECCS provided for the plant consists of the conventional combination of high pressure pumped injection, pressurized water storage tanks, and low pressure pumped injection, all connected into the reactor coolant piping just upstream of the reactor vessel. The Trojan containment is of the dry type.

The results of calculated predictions of LOCAs must meet the criteria imposed by 10 CFR 50.46. At the time of initial operation, the Trojan plant was fueled with Westinghouse-supplied fuel and compliance was demonstrated by calculations performed by Westinghouse. This report documents compliance to 10 CFR 50.46 when the plant is fueled by BWFC-supplied fuel with the simulated rated power for the plant set to 3558 Mwt. In this report, possible LOCAs are divided into two groups depending on the

assumed break size. For breaks larger than 1.0 ft^2, compliance is demonstrated by calculations and analyses performed in accordance with the BWFC Large Break LOCA Evaluation Model for recirculating steam generator plants, BAW-10168 (Reference 1). For breaks smaller than 1.0 ft^2, compliance is shown by validating that the calculations performed in support of the plant prior to the loading of the Mark-BW fuel remain applicable when the Mark-BW is in use.

A summary of the results of the analyses is presented in Chapter 2. Chapter 3 provides a general description of the Trojan plant. The analysis parameters used for the large break calculations are discussed in Chapter 4 and system sensitivity studies in Chapter 5. The large break spectrum analysis to determine the most limiting break is documented in Chapter 6. Chapter 7 presents the LOCA limit calculations which confirm adherence to the first two criteria of 10 CFR 50.46. The evaluation of maximum hydrogen generation, coolable geometry, and long-term cooling are presented in Chapters 8, 9 and 10, respectively. Validation of the applicability of the earlier small break LOCA studies is provided in Chapter 11.

During the transition from Westinghouse fuel to the Mark-BW assembly, the core will for some time consist of a mix of the two fuel assembly types. For such cycles, Appendix A shows that the mixing of the assemblies does not alter the LOCA performance of either fuel assembly to any degree approaching the criteria of 10 CFR 50.46.

2. Summary and Conclusion

10 CFR 50.46 specifies that the emergency core cooling system (ECCS) for a commercial nuclear power plant must meet five criteria. The calculations and evaluations documented in this report demonstrate that the Trojan plant continues to meet these criteria when operated with Mark-BW fuel. Large break LOCA calculations performed in concurrence with an approved evaluation model (BAW-10168 and revisions) demonstrate compliance for a full Mark-BW core for breaks up to and including the double-ended severance of the largest primary coolant pipe. The small break LOCA calculations used to license the plant operation during previous fuel cycles are shown to be unaffected by the change in fuel design, and therefore, demonstrate that the plant meets 10 CFR 50.46 for small breaks when loaded with Mark-BW fuel. The coexistence of the Mark-BW assembly and the Westinghouse standard 17 x 17 assembly in the same fuel cycle is shown to be inconsequential and does not cause the calculated temperatures for either assembly to approach the limits of 10 CFR 50.46.

Specifically, this report demonstrates that when the Trojan plant is operated with Mark-BW fuel:

1. The calculated peak cladding temperatures for the limiting cases are less than 2200 F (Chapter 7).

2. The maximum calculated local cladding oxidation is less than 17.0 % (Chapter 7).

3. The maximum amount of core-wide oxidation does not exceed 1.0 % of the fuel cladding (Chapter 7).

4. The cladding remains amenable to cooling (Chapter 9).

5. Long-term cooling is established and maintained after the LOCA (Chapter 10).

The results of the large break sensitivity studies and the break spectrum studies performed with the BWFC evaluation model show that the double-ended guillotine break at the pump discharge with a discharge coefficient of 1.0 and maximum ECCS is the most limiting case. Table 2-1 shows the results of this accident on the Mark-BW fuel design when the assumed axial location of peak power is varied along the length of the pin. As the local power for the Mark-BW assemblies is controlled such that it cannot exceed the Mark-BW LOCA limits curve, this table lists the results of the large break LOCA calculations which demonstrate compliance with the first four criteria of 10 CFR 50.46. Compliance with the long-term cooling criterion (as described in Chapter 10) is through the use of a pumped injection system that can be recirculated, drawing water from the containment sump through a heat exchanger, to provide extended energy removal. The concentration of boric acid is held below its solubility limit by starting hot leg injection within 13 hours of the accident.

During the transition from the Westinghouse standard 17 x 17 to the Mark-BW, both fuel assemblies will reside in the core simultaneously for several fuel cycles. Appendix A demonstrates that the results and conclusions presented above are also applicable to the Mark-BW assemblies in the transition core. Similarly, Appendix A demonstrates that insertion of Mark-BW fuel with the Westinghouse standard 17 x 17 does not adversely affect the cooling of the Westinghouse fuel. Thus, the original calculations showing that the Westinghouse standard 17 x 17 meets the criteria of 10 CFR 50.46 remain valid for that fuel through the transition period.

TABLE 2-1 SUMMARY OF RESULTS (LOCA Limit Runs)

Core Elevation, ft	Peak Cladding Temperature, F	Maximum Oxidation, % Local	Whole Core
2.9	1894	3.4	0.43
4.6	2028	4.8	0.63
6.3	2047	6.8	0.79
8.0	1993	5.3	0.74
9.7	2119	7.4	0.84

3. Plant Description

The Trojan nuclear power plant uses a nuclear steam supply system (NSSS) designed by Westinghouse that is representative of the standard Westinghouse four-loop, 3411 Mwt design. The ECCS provided for the plant consists of the conventional combination of high pressure pumped injection, pressurized water storage tanks, and low pressure pumped injection all connected into the reactor coolant piping just upstream of the reactor vessel. The plant uses a dry containment system.

3.1 Physical Description

The reactor coolant system is enclosed entirely within the containment and is arranged into four heat transport loops, each of which has one recirculating steam generator and one reactor coolant pump. The reactor coolant is directed through the nuclear core within the reactor vessel, transported to the steam generators via four pipes (hot legs), cooled within the steam generator tubes, and returned to the reactor vessel through four cold leg pipes. Flow through the system is driven by four reactor coolant pumps, one per coolant loop. System pressure is maintained by a pressurizer connected to the loop two hot leg.

Reactor Vessel

The reactor vessel configuration is that of a cylindrical shell with a hemispherical bottom head and a removable hemispherical upper head. Major regions of the reactor vessel are the inlet and outlet nozzles, the downcomer, the lower plenum, the core, the upper plenum, and the upper head. Coolant enters the vessel through four inlet nozzles and passes downward through the downcomer to the lower plenum. From the lower plenum, coolant is directed upward, passing either through the core or the baffle bypass region, to the upper plenum. Within the upper plenum, the

coolant mixes with a small amount of flow that was bypassed directly from the downcomer to the upper head and exits the reactor vessel through the hot leg nozzles.

Reactor Core and Fuel Assembly

The reactor core comprises 193 fuel assemblies, with each fuel assembly consisting of 264 fuel rods, 24 guide thimbles, and one instrument tube. Each fuel rod consists of stacked fuel pellets contained in a Zr-4 fuel rod with a gap between the fuel pellet and the fuel rod. Fifty three of the fuel assemblies have rod cluster control assemblies used for power control and shutdown capability. Trojan has silver-indium-cadmium control rods. The Trojan plant will be replacing the Westinghouse standard 17 X 17 fuel assembly with the Mark-BW fuel assembly. Both fuel assemblies are 17 x 17 fuel rod arrays with active lengths of approximately 12 feet. A comparison of fuel rod geometries for both fuel types is provided in Appendix A.

Reactor Coolant Loops

The coolant loop piping is connected to the reactor vessel through eight nozzles, all of which are located at the same elevation, approximately six feet above the top of the core. The outlet piping (hot legs) runs from the reactor vessel in a horizontal plane and undergoes an upward bend as it attaches to the steam generator inlet plenum. The steam generators are of the recirculating or U-tube type with vertical tubes and inlet and outlet plenums at a common elevation. The steam generator outlet pipe is bent to vertically downward at the plenum and continues downward for about 10 feet. At this point, the piping is bent through a 180 degree turn to vertically upward and rises to meet the reactor coolant pump casing (refer to FSAR Figure 3.6-2 in Reference 8). Discharge from the reactor coolant pump is horizontal and at the same elevation as the reactor vessel

inlet nozzles, making the run of piping from the reactor coolant pump to the reactor vessel horizontal.

Steam Generators

The Trojan steam generators are of the recirculating or U-tube design. Preheated feedwater enters the steam generator above the tube region, travels down the downcomer mixing with fluid being recirculated by the separators, and enters the tube region at the tube sheet. The two-phase mixture from the tube bundle then enters the separators wherein the steam is allowed to proceed to the steam generator upper dome, and the liquid is recirculated to the downcomer and back to the tube bundle.

3.2 Description of Emergency Core Cooling System

The ECCS provided for the plants consists of the conventional combination of high pressure pumped injection, pressurized water storage tanks, and low pressure pumped injection all connected to the reactor coolant piping upstream of the reactor vessel.

The high pressure injection capability of the plants is achieved through two systems: the centrifugal charging system (CC) and the safety injection system (SI). The centrifugal charging system is the highest pressure system of the ECCS, capable of injecting above normal operating system pressure, and is part of the makeup and purification system during normal operation. The system includes sufficient redundancy such that one full train remains operative under the assumption of a single active failure. Emergency operation is activated automatically after receiving a safety injection systems "SIS" signal, indicating low reactor coolant system pressure or high containment pressure. The safety injection system operates in the middle pressure range, capable of injecting up to about 1430 psia. It has two separate pumping sources with sufficient redundancy in the number

of components to provide the required flow rate assuming a single active failure. The system is also actuated by the safety injection systems "SIS" signal.

The accumulator system consists of four tanks, each containing about a thousand cubic feet of borated water and four hundred cubic feet of nitrogen pressurized to 600 psi. The tanks are connected to the reactor coolant system at the reactor coolant pump discharge via pipes. Reverse flow during normal operation is prevented by in-line check valves. The system is, therefore, self-contained, self-actuating and passive. Flow into the RCS occurs whenever the reactor coolant system pressure falls below the tank pressure.

Low pressure injection is achieved with the residual heat removal system (RHR). Normally used for cooling when the reactor is not operating, the system also serves the low pressure ECC injection function by providing borated water through the four accumulator injection nozzles. In emergency operation, the RHR pumps initially inject water from the refueling water storage tank (RWST). When the RWST low level set point is reached, the RHR pumps are aligned to take suction from the containment sump. During recirculation, injection flow is passed through a heat exchanger before being returned to the reactor coolant system. The system contains sufficient redundancy such that one full train is available under a single active failure. Actuation is by the safety injection systems "SIS" signal on low reactor coolant system pressure or high containment pressure. In its recirculation mode, the RHR injection system provides for long-term core cooling.

In the recirculation mode, only the RHR pump is capable of taking suction from the containment sump. However long-term, high pressure cooling is possible because both the centrifugal charging pumps and the Safety Injection pumps can take suction

from the RHR pump discharge and deliver coolant through their cold leg connections to the RCS.

3.3 Plant Parameters

The major plant parameters and operating conditions are presented in Table 3-1.

TABLE 3-1 PLANT PARAMETERS AND OPERATING CONDITIONS

Reactor Power	3411 Mwt *
Operating Core Outlet Pressure	2280 psia
Highest Allowable Total Peaking (F_Q)	2.50
System Flow	135.4 x 10^6 lbm/hr
Core Heat Transfer Area	59973 ft^2
Average Linear Power Generation Rate	5.58 Kw/ft **
Fuel Assembly	Mark-BW, 17 x 17 array
Fuel Pin OD	0.374"
Hot Leg Temperature	619 F
Cold Leg Temperature	551 F
Steam Generator Pressure	842 psia

* The LOCA evaluation performed within this report was conducted for a rated power of 3558 Mwt in anticipation of a possible power upgrade for Trojan. Currently, it is the intention of PGE to operate the Trojan unit at a rated power of 3411 Mwt.

** The operational gamma flattening factor (0.974) has been applied to compute this value. The value therefore represents the average heat deposited in the fuel pellets.

4. Analysis Inputs and Assumptions

The Trojan plant evaluation performed for this report was conducted in accordance with the B&W Fuel Company recirculating steam generator LOCA evaluation model (Reference 1). This chapter provides a brief discussion of the computer codes, plant parameters, and assumptions used in the evaluation. Although the chapter is oriented to the analysis of large breaks, the information supplied applies widely to both large and small break calculations. Specific assumptions for the SBLOCA calculations are provided within Chapter 11 or in the referenced SBLOCA analyses reports.

4.1 Computer Codes and Methods

For the evaluation of cladding temperature transients and local oxidation, the B&W Fuel Company LOCA evaluation model consists of a group of computer codes. Figure 4-1 illustrates the interrelation between and among the computer codes used for the large break analyses. The RELAP5/MOD2-B&W code calculates system thermal-hydraulics and core power generation during blowdown. The thermal-hydraulic transient calculations are continued with the REFLOD3B code to determine refill time and core reflooding rates for the remainder of the transient. The FRAP-T6-B&W code is used to determine the hot pin temperature response during blowdown. The BEACH code is used to determine the hot pin cladding temperature response during refill and reflood with core flooding rates from the REFLOD3B outputs.

The evaluation model and previous analyses employ FRAP-T6 through the end-of-adiabatic-heatup, not making the transfer to BEACH until the beginning of reflooding. The switch from FRAP-T6 to BEACH during the refill phase strictly represents a change to the evaluation model. However, during this period the cladding is evaluated adiabatically, no heat transfer is allowed from the

fuel pin, a condition within the range of the applications for which either code has already been approved. No change in predicted cladding temperature or other governing parameters results from the shift to BEACH for the hot channel calculation during the refill period. Therefore, the switch is considered an evaluation model alteration of nonconsequence with the results approvable under the evaluation model as documented in BAW-10168 Revision 1 Approved. In order to maintain clear and unambiguous documentation of the evaluation model, a package of changes that will allow the use of either code for the refill period will be submitted with the next request for change of the evaluation model.

4.2 Inputs and Assumptions

The major plant operating parameters used in the LOCA codes are:

1. Power Level - The plant is assumed to be operating in steady-state at 3629 Mwt (102% of 3558 Mwt).

2. Total System Flow - The initial RCS flow is 135.4×10^6 lbm/hr.

3. Fuel Parameters - The initial fuel pin parameters are taken from TACO3 runs performed for the fuel assembly burnup which produces the highest peak cladding temperature. Studies discussed in Chapter 5 show that fuel conditions at the beginning of life are the most severe for large break LOCA.

4. ECCS - The ECCS flows are based on the worst case between the assumption of a single active failure and the assumption of no failure. Sensitivity studies discussed in Chapter 6 show that the condition of maximum ECCS is the most severe assumption.

5. Total Peaking Factor (F_Q) - The maximum total peaking factor assumed by this analysis is 2.50.

6. The moderator density reactivity coefficient is based on beginning-of-cycle conditions to minimize negative reactivity.

7. The cladding rupture model is based on NUREG-0630.

4.2.1 RELAP5/MOD2-B&W Modeling

The RELAP5/MOD2-B&W computer code is used to analyze RCS thermal-hydraulic behavior during the blowdown phase of a LOCA. RELAP5/MOD2-B&W, a modified version of the RELAP5/MOD2 code, is documented in BAW-10164 (Reference 2). RELAP5 permits the user to select model representation that results in a suitable finite difference model for the fluid system being analyzed. The nodalization for the plant evaluation, shown in Figure 4-2, was developed in accordance with the BWFC LOCA evaluation model (Reference 1).

The control volume inputs generally consist of volume geometry (area and height), flow-related parameters (resistance, hydraulic diameter, surface roughness), primary metal heat data, and initial conditions (pressure, temperature and flow). The non-equilibrium, non-homogenous option is used throughout, except for the core region, where the equilibrium, homogeneous option is selected in order to generate blowdown thermal-hydraulic data consistent with the formulation of the FRAP-T6 code. Flow paths are defined between control volume geometric centers. The B&W-developed SAVER computer code (Reference 3) is used to determine the initial pressure drops and flow distribution. RELAP5/MOD2-B&W is run in steady-state to assure proper initialization.

Core

As shown on Figure 4-2b, the reactor core model consists of an average channel (Nodes 426-445), a hot channel (Nodes 326-345), a core bypass region (Pipe 346), and a baffle gap region (Pipe 350). The hot channel consists of one assembly and the remaining 192 assemblies are modeled in the average channel. Axially, the powered regions are represented by twenty approximately equal-length segments and the unpowered regions by three equal-length segments. Crossflow is allowed between the average core and the hot assembly using crossflow junctions. The resistance for these junctions is developed from the experimental correlation given in Section 2.2.7 of BAW-10092 (Reference 4). For the sensitivity studies and the break spectrum, the power distribution in the core is based on a symmetric chopped cosine with an axial peak of 1.5. For the LOCA Limits studies, where the position of the axial peak varies with the case, the power shapes and peaking correspond to the case (refer to Chapter 7). Initial fuel temperatures, pressure, gas composition, and dimensions are based on beginning-of-life TACO3 calculations.

Previously submitted calculations, those in the evaluation model report BAW-10168 and in the McGuire/Catawba applications report BAW-10174, have used six axial nodes to represent the core hot and average channels in the RELAP5 model while using 20 nodes in FRAP-T6 and BEACH. With common noding schemes a substantial portion of the core inputs are the same for RELAP5 and BEACH. The use of the more refined spacial modelling in RELAP5 reduces costs, improves accuracy, and reduces opportunities for input mistakes. The noding increase is considered a model improvement within the scope of the original evaluation model. The noding sensitivity studies documented in Appendix A of the evaluation model report, BAW-10168, show that a doubling of the axial detail in the core from 6 to 12 nodes does not alter the RELAP5 solution. An additional doubling of the noding detail, 24 nodes,

although not specifically evaluated, is not expected to deviate in result from the base studies. Thus, the increase in core noding detail to 20 nodes is considered within the range of convergence established by the evaluation model sensitivity study and not a change to the evaluation model.

Reactor power during a LOCA transient is calculated using the RELAP5/MOD2-B&W kinetics option. The rate of heat generation within the fuel is computed by the code and is the sum of the fission power and fission product decay power. The point kinetics model used in the code accounts for changes in reactivity due to the effects of fuel temperature and coolant density. The action of control or safety rods is not credited by the BWFC LBLOCA evaluation model. The Doppler coefficient is developed from end-of-life reactor physics calculations, so that fuel temperature decreases during LOCA maximize power generation.

Reactor Vessel

The reactor vessel model consists of a downcomer (Nodes 300-308), the lower head (Node 310), the core inlet plenum (Nodes 312 and 314), the core outlet plenum (Nodes 352 and 356), and the upper head (Nodes 358 to 364). In the downcomer, Nodes 300 and 302 are centered at the core inlet nozzles. In the upper plenum, Nodes 352 and 356 are centered at the vessel outlet nozzles. Reactor coolant bypass between the downcomer and upper head is taken into account by connecting Node 300 to Node 358.

Reactor Coolant Loops

The loop noding scheme is a result of the loop noding and break noding sensitivity studies performed in Appendix A of BAW-10168. The four RCS loops are modeled as two by combining the three loops that do not contain the break simulation together. The 100-Series nodes model the unbroken loops, and the 200-Series

models the broken loop. Within each loop, the hot legs are separated into 4 nodes; the RSG inlet plenum (Nodes 120 and 220) and RSG outlet plenum (Nodes 130 and 230) are single nodes. The RSG tubes (Nodes 125 and 225) are separated into sixteen segments. The tube flow area is based on the assumption that 11.5 percent of the tubes have been plugged on the primary side and removed from service. The cold leg reactor coolant pump suction consists of 5 nodes, and the reactor coolant pump (Nodes 160 and 260) is a single node. The cold leg from the reactor coolant pump to the reactor vessel is modeled as four nodes for the broken loop and as two volumes for the unbroken loop.

Reactor Coolant Pumps

The reactor coolant pump performance is developed from homologous relationships adjusted for two-phase degradation based on the data in Table 2.1.5-2 of BAW-10164. This is the same degradation data in NUREG/CR-4312 (Reference 5). In accordance with the LOCA evaluation model, the reactor coolant pumps are assumed to trip at the time of a LOCA.

Pressurizer

The pressurizer model consists of three parts: the surge line (Node 400), an eight-section pressurizer (Node 410), and a valve model (Junction 415 and Node 420). The initial condition for the pressurizer is saturated steam over saturated liquid with a void fraction specified in the interface node. The initial inventory for the pressurizer is set to approximate the normal operating level.

Recirculating Steam Generator

In agreement with the loop noding arrangement, the three steam generators associated with the unbroken loops are modeled as a

combined region (700-Series nodes) with the broken loop containing a single generator (600-Series nodes). The tube riser section is modelled by four-volumes (Nodes 630 and 730) which span the height of the generator tubes. Two volumes (Nodes 635, 640 and 735, 740) are modeled below the separators. Nodes 650 and 750 are separator volumes. The steam domes are each modelled by two nodes (660, 670 and 760, 770). The separator component in RELAP5/MOD2 acts as a steam separator and dryer with two-phase fluid entering from the bottom, steam exiting upward, and saturated fluid going back to the downcomer through Nodes 655 and 755. Nodes 625 through 665 and 725 through 765 form the steam generator downcomer. Main and auxiliary feedwater is supplied at Nodes 620 and 720. Nodes 675 to 680 and 775 to 780 provide simulation of the steam lines and the safety valves.

The heat structures which model the steam generator tubes are reduced in heat transfer area by about 5000 square feet to simulate 11.5 percent tube plugging. Heat structures of characteristic volume and surface area are also included for the shell, the downcomer walls, and separator components.

Break Characteristics

The four-node break location configuration is a result of the break nodding sensitivity study in Appendix A of BAW-10168. Referring to Figure 4-2a, a double-ended guillotine break is modeled with leak paths from both Nodes 270 and 275 to the containment. For a split-type break, the leak is modeled as a single path that leaves Node 275. For the double-ended break, no flow is permitted between the leak nodes following the break. The switching criterion from subcooled (Extended Henry-Fauske) to two-phase (Moody) discharge models is based on a leak node quality of 0.1 percent.

Primary Metal Heat Model

All major components within the reactor vessel, loops and steam generators are considered. Within a specific region, primary metals are grouped together based on similar thickness and geometry. The exterior surfaces of the primary and secondary systems' pressure boundaries are assumed adiabatic to maximize stored energy in metal slabs.

ECCS

The accumulators, centrifugal charging, safety injection, and residual heat removal systems are modeled by Nodes 900 through 915. For LBLOCA injection is allowed only into the unbroken loops at the cold leg. The injection which would take place in the broken loop is assumed to flow directly into the containment. The accumulator is a passive system, check valve controlled, and activates automatically when the primary pressure falls below the tank pressure. The pumped systems are activated by the Safety Injection Systems signal of the Engineered Safety Features Activation System. Appropriate time delays for signal generation, electrical supply startup, and injection pump startup are accounted for in the initiation of the pumped injection systems.

4.2.2 REFLOD3B Modeling

The REFLOD3B code simulates the thermal-hydraulic behavior of the primary system during the core refill and reflood phases of the LOCA. The noding, shown in Figure 4-3, is consistent with the LOCA evaluation model and consists of reactor vessel and loop models. The reactor vessel is represented by a four fixed-nodes model; Nodes 1R and 2R are volumes above and below the steam-water interface in the inner vessel region, and Nodes 4R and 3R represent steam and liquid volumes, respectively, in the

downcomer region including the lower plenum. The primary system piping is represented by two loops similar to the RELAP5 blowdown model with a reduced number of volumes. Values for volume geometry and flow path hydraulic parameters are developed from the RELAP5 model.

RELAP5 results at the end of blowdown (EOB) define the starting point for the REFLOD3B calculations. The core and system initial conditions for REFLOD3B are derived from those of the associated RELAP5 run at EOB with appropriate accounting given for the differing noding details. In defining initial liquid inventory for REFLOD3B, the excess bypass and liquid remaining in the reactor vessel at EOB in RELAP5 is placed in the lower plenum of REFLOD3B. The initial flow rates, gas volumes, liquid inventories, and pressures of the accumulator tanks are taken directly from RELAP5. The reactor vessel (RV) steam volumes (1R and 4R) are initialized with saturated steam corresponding to containment pressure, and the loops contain superheated steam corresponding to the containment pressure and fluid temperature of the secondary sides.

The primary metal heat structures are also taken from the RELAP5 model with the initial conditions in REFLOD3B matching those in RELAP5 at the end of blowdown. The secondary side metal structures include a representation of the shell material. In mostly stagnant regions, such as the downcomer or lower head, the heat transfer coefficient is based on pool boiling or natural convection to vapor. In regions with flow, such as the hot legs or the steam generator, the surface heat transfer coefficient is set to 1000 Btu/hr-ft^2-F for both vapor and liquid. These selections insure that the fluid leaving the steam generator is continuously dry steam superheated to the secondary side temperature.

For a double-ended pump discharge break, two leak paths are modeled, one from the RV upper downcomer (Node 4R) and the other from the pump side of the break (Node 28). The pump rotor resistance is based on the locked rotor condition. A 0.85 psi pressure drop is imposed on cold leg pipe junctions to account for momentum losses due to steam-ECC water interaction during the accumulator injection phase. This value is reduced to 0.50 psi for the pumped injection once the accumulators have fully discharged.

The containment backpressures as a function of time from the Trojan FSAR are used in the REFLOD3B calculations. This assumption was originally employed in 1989 for the evaluation of the McGuire and Catawba Units, BAW-10174. For those units a detailed comparison of the calculated mass and energy releases with those in the respective FSAR's was made. The comparison showed no significant differences between the BWFC and Westinghouse calculations, justifying use of the containment pressures previously calculated by Westinghouse for use in the REFLOD3B analysis.

4.2.3 FRAP-T6-B&W Modeling

The FRAP-T6 code is used to predict thermal responses of the hot fuel rod for the blowdown phase of the LOCA. It is a boundary data-driven code with inputs taken from RELAP5. The fuel rod axial and radial nodalization is identical to that of the BEACH model (Figure 4-4). Prior to transient calculations, the fuel rod is initialized, and the fuel temperature, fuel rod geometry and pin pressure are compared with the data predicted by TACO3. The boundary data inputs from RELAP5 are core power, hot channel flows, hot channel enthalpies, and system pressure.

4.2.4 BEACH Modeling

The BEACH code is used to determine the hot fuel rod cladding temperature response during the refill and reflooding phases of the LOCA. BEACH heat transfer models used to determine the peak cladding temperature are overly conservative following the initiation of cladding cooldown and cannot be used directly to predict cladding quench. Rather, the occurrence of core quenching is determined from the core quench height as predicted by the REFLOD3B code. For these analyses, the latest version of BEACH as documented in Revision 3 of the BEACH topical, Reference 6, has been used. This version provides an option, used for these analyses, to reduce discontinuities in the reflooding heat transfer coefficient selection logic. The discontinuities of the previous BEACH version can lead to excessive cladding temperature oscillations and non-physical heatup of the cladding at upper pin elevations when the void fraction of a quenched node is around 0.999. In previous submittals the effect was not problematic because of the incrementally lower local power levels analyzed. At the local power levels for this application the difficulty required correction. Revision 3 of the BEACH topical fully documents the option and provides revised calculations that show that use of the option does not alter the results of the experimental benchmarks upon which code approval is based.

The BEACH model consists of a hot fuel rod and a flow channel with time-dependent inlet and outlet volumes to permit inputs of boundary data from the REFLOD3B calculations. The fuel rod is axially divided into 20 segments, as shown in Figure 4-4, with variable nodal length such that each grid is located at the bottom of a node and three nodes are used to cover a grid span. The nodalization is basically that used in the code benchmarks in Appendixes C, D, E, and F of the BEACH topical report, BAW-10166 (Reference 6). Radially, the fuel pellet is divided into 7

equally spaced mesh points and two equally spaced mesh points for cladding.

The initial temperature distribution in the fuel rod and fuel pellet-clad gap conductance are obtained from the FRAP-T6 calculations at the beginning of refill. The boundary data inputs from the REFLOD3B calculations are inlet and outlet pressures, flooding rate, inlet water temperature, and core decay heat. The initial temperature of the steam surrounding the fuel rod is set equal to the cladding surface temperature.

If rupture occurs, BEACH is run in two passes. First, the code is run to the time of rupture. At this point, the cladding surface area at the location of rupture is increased, the blockage model applied, and BEACH restarted to the end of the analysis.

TABLE 4-1 LOCA MODEL GEOMETRIC VALUES

Parameter	Model Value
OVERALL SYSTEM	
Total System Volume Including Pressurizer, ft^3	12,100 *
Total System Liquid Volume Including Pressurizer, ft^3	11,400 *
REACTOR VESSEL	
RV I.D. at Flange, in	167.0
RV I.D. of Lower Shell, in	173.0
RV Inlet Nozzle I.D., in	27.5
RV Outlet Nozzle I.D., in	29.0
REACTOR COOLANT LOOP	
Hot Leg Pipe I.D., in	29.0
Cold Leg Pump Suction Pipe I.D., in	31.0
Cold Leg Pump Discharge Pipe I.D., in	27.5
Pump Volume, ft^3	56.0
RECIRCULATING STEAM GENERATOR	
U-Tube Outer Diameter, in	0.875
Tube Wall Thickness, in	0.05
Number of U-Tubes	3,388 *
Heat Transfer Area, ft^2	51,500 *

* The values provided for the table are at standard temperature and without tube plugging. The actual evaluation used values adjusted to hot full power operation reduced to account for the assumed degree of tube plugging.

FIGURE 4-1. LARGE BREAK ANALYSIS CODE INTERFACE.

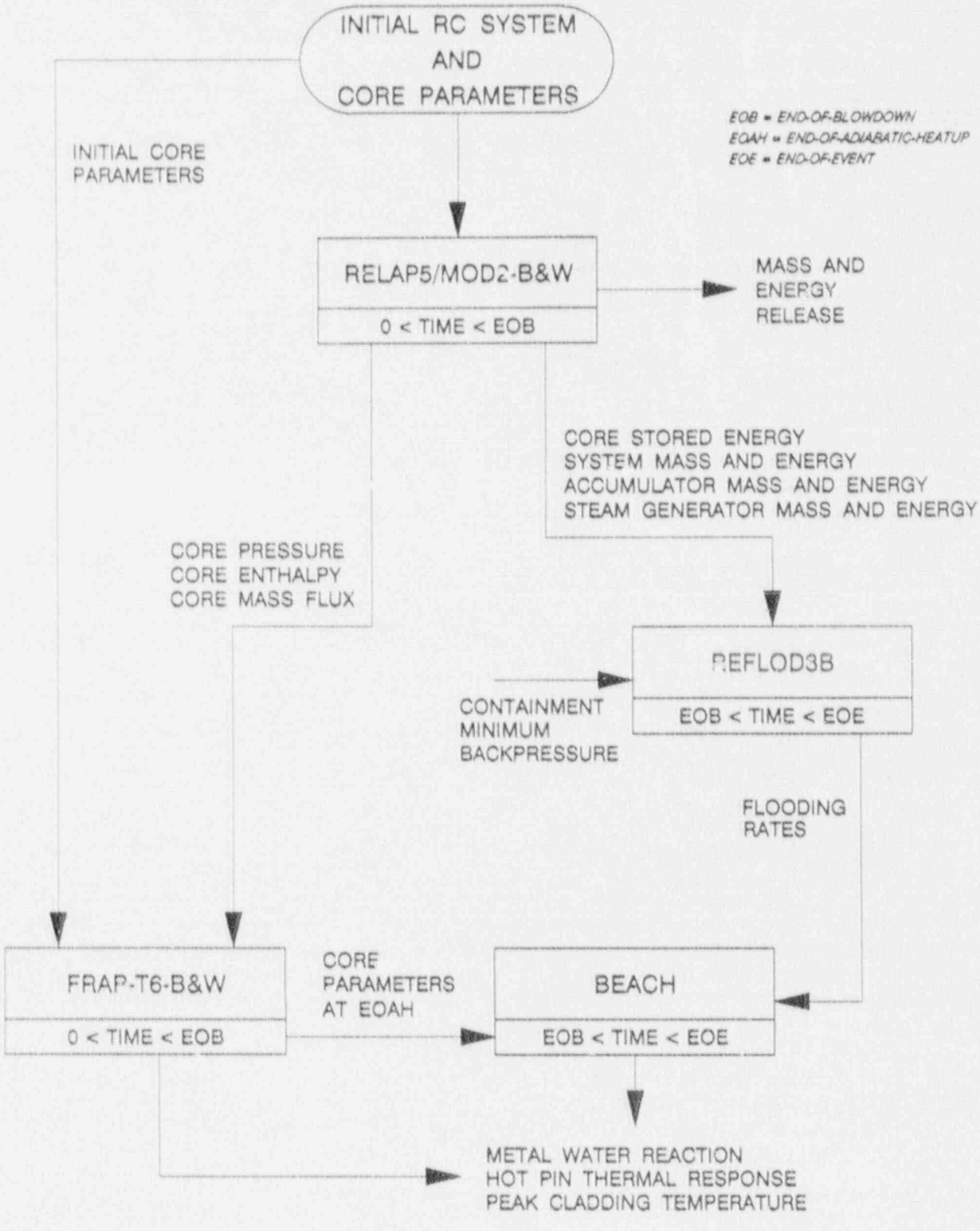

FIGURE 4-2a. RELAP5/MOD2-B&W LBLOCA NODING DIAGRAM, REACTOR COOLANT LOOPS.

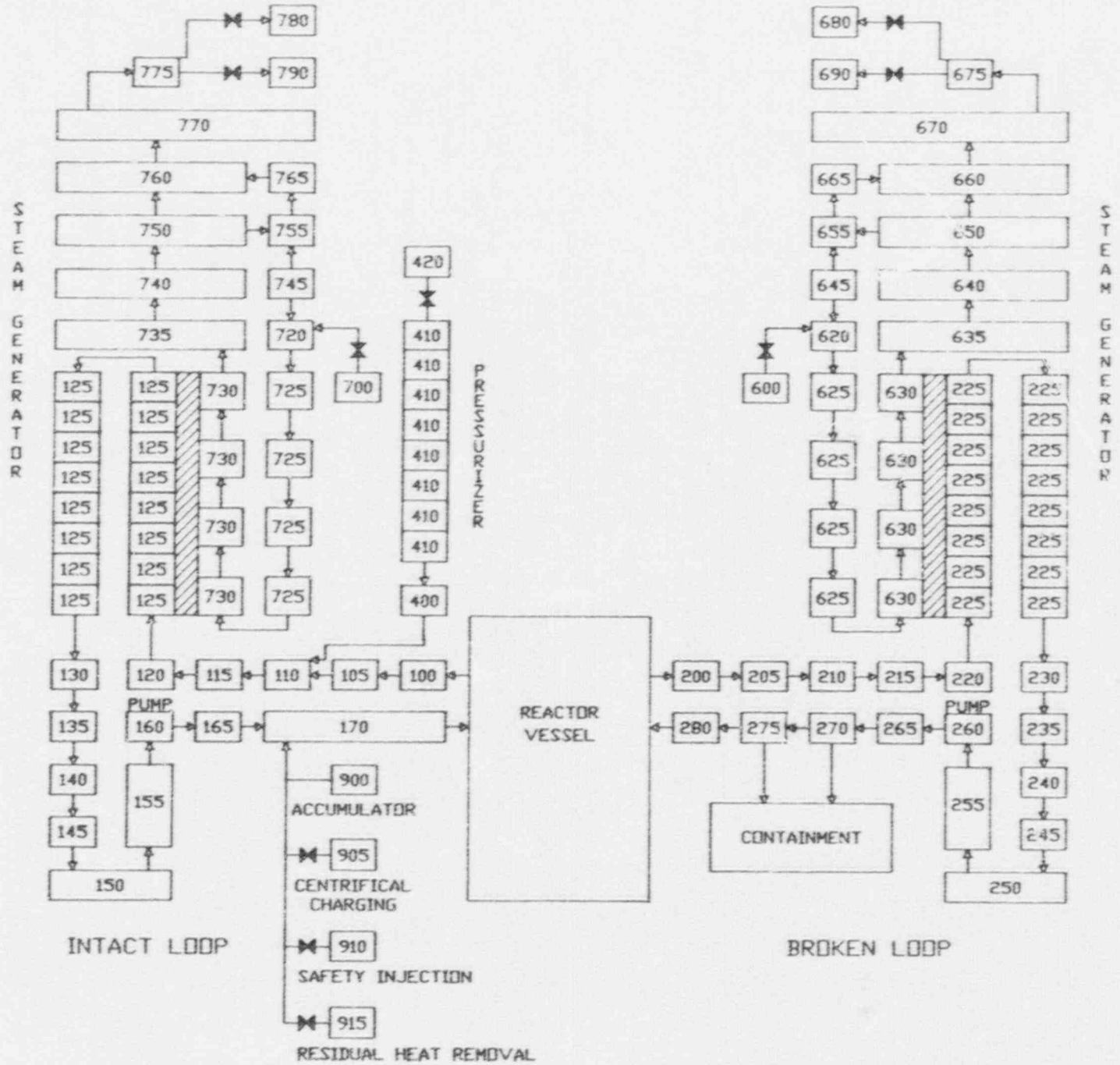

FIGURE 4-2b. RELAP5/MOD2-B&W LBLOCA NODING DIAGRAM, REACTOR CORE.

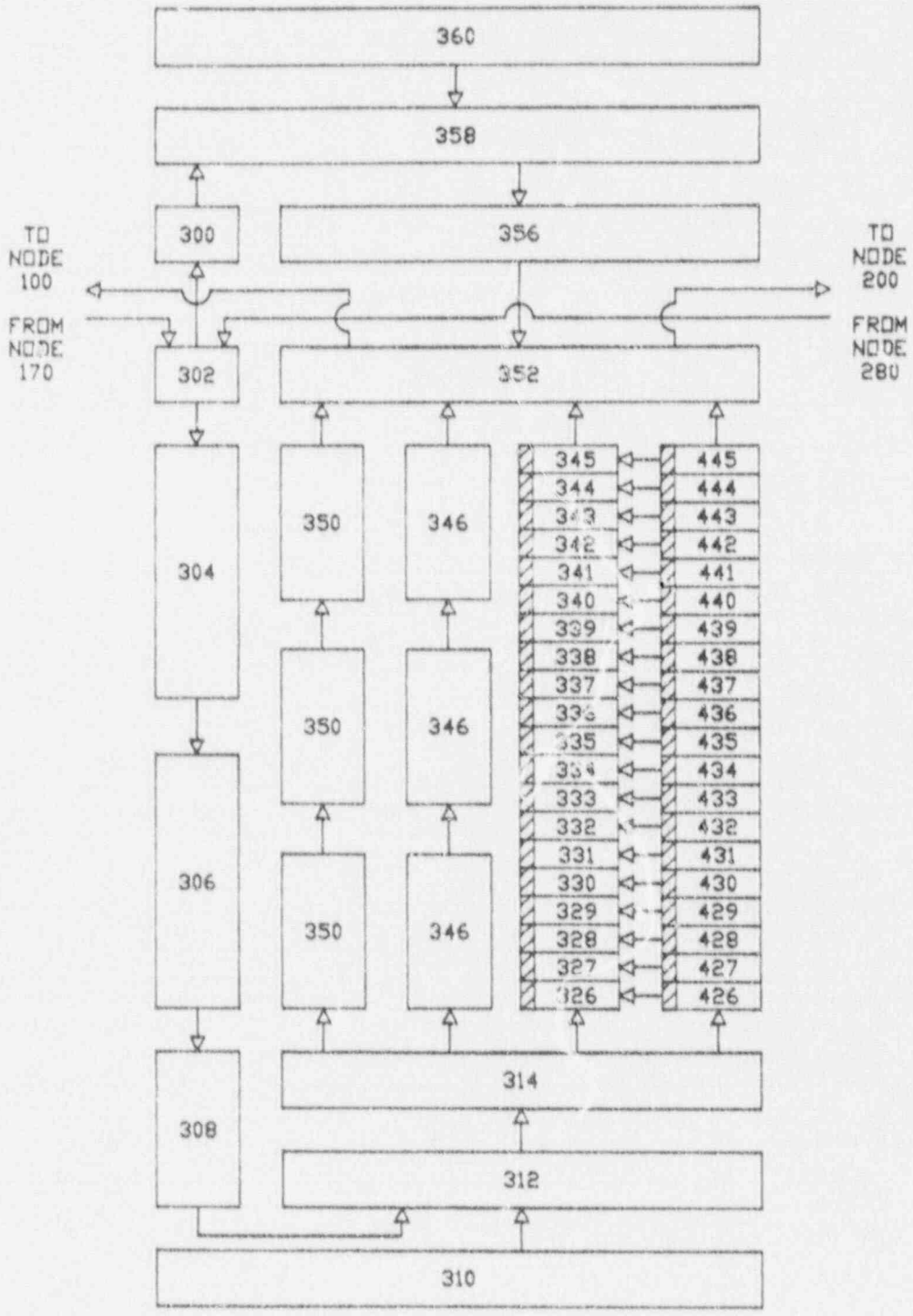

FIGURE 4-3. REFLOD3B NODING DIAGRAM.

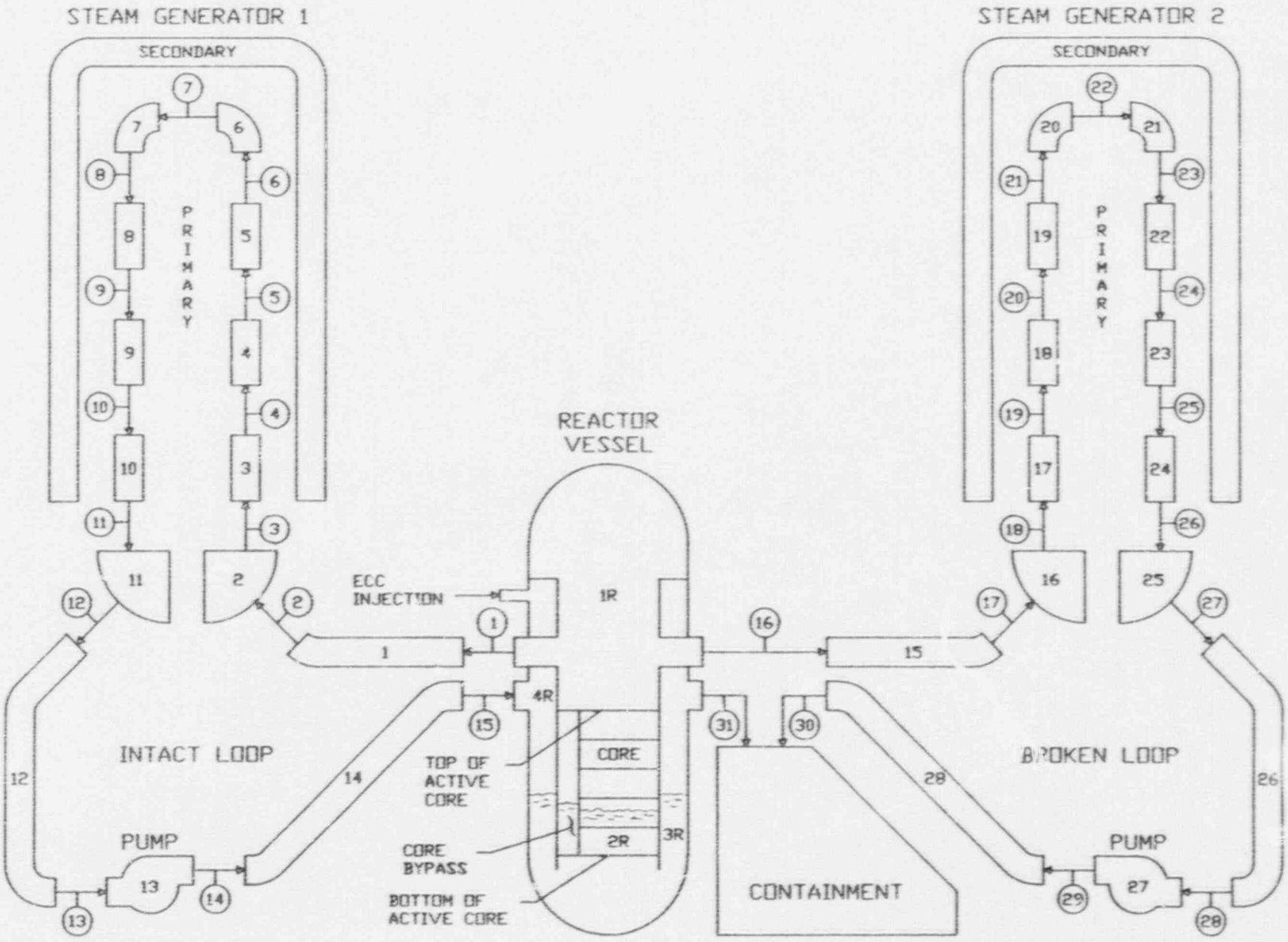

FIGURE 4-4. BEACH AND FRAP-T6-B&W NODING DIAGRAM FOR MARK-BW FUEL ASSEMBLY.

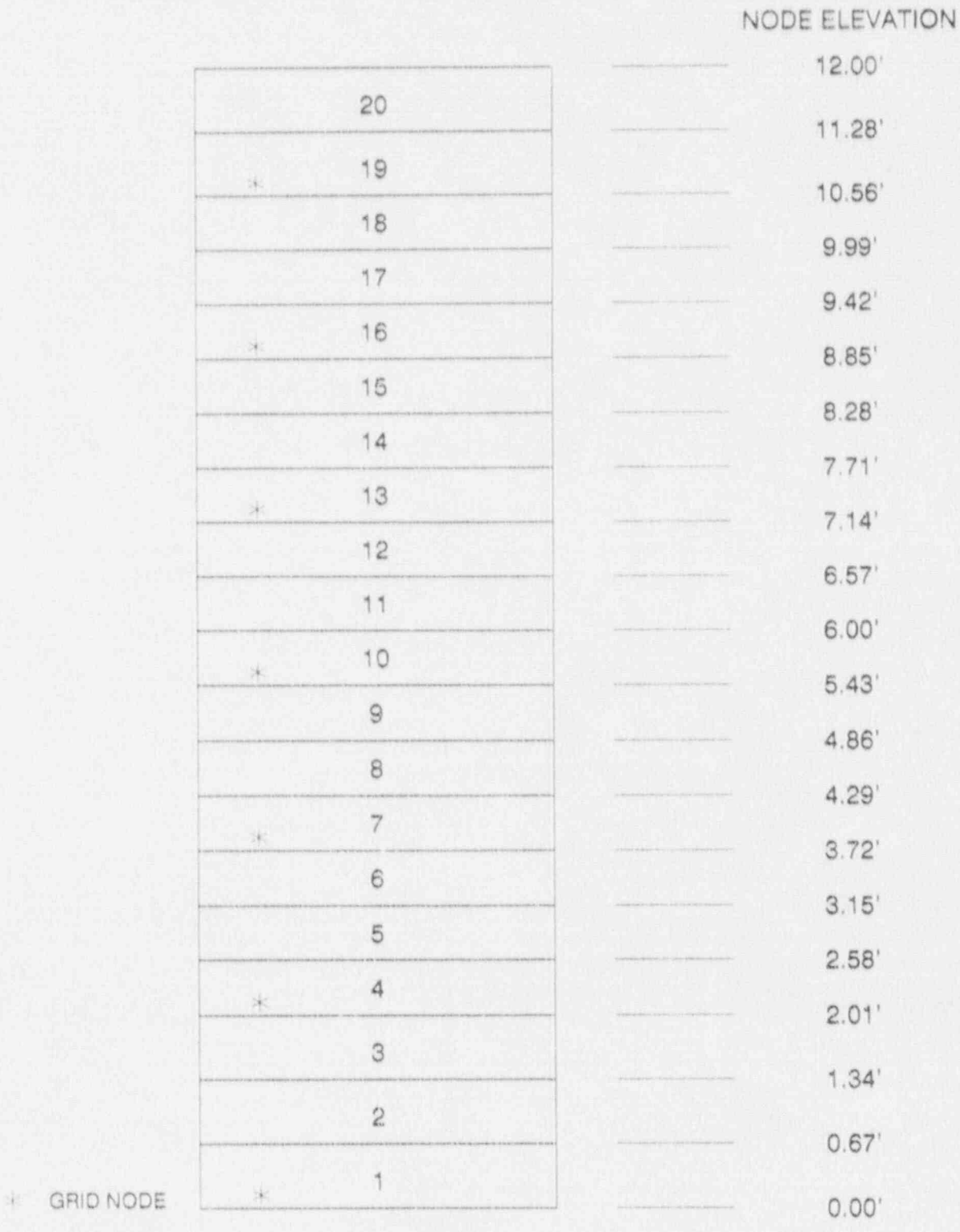

5. Sensitivity Studies

LOCA evaluations require that a substantial number of sensitivity studies be performed with the evaluation model in order to establish model convergence and conservatism. Most of the studies upon which the evaluations in this report are based are generic and were documented in the evaluation model report, BAW-10168 (Reference 1). Studies such as break spectrum and worst case ECCS configuration are considered plant-specific and are documented in this report. This chapter provides a discussion of the generic sensitivity studies from the reference evaluation model report that have been applied. The plant-specific sensitivity studies are presented in Chapter 6.

5.1 Evaluation Model Generic Studies

Of the sensitivity studies presented in the original evaluation model topical report (Reference 1), the majority are generic and would apply to any plant evaluated. Those studies considered generic each demonstrate results that are characteristic of the evaluation model--the codes and interfaces--and that are not plant dependent. An example of this is the RELAP5/MOD2-B&W time step study, which demonstrated that the automatic time step selection in RELAP5/MOD2-B&W would produce converged results. This demonstration need not be repeated for plant-specific applications wherein the modeling techniques used are represented by those in the evaluation model studies. Furthermore the studies being referenced in the Evaluation Model Report were conducted with a standard 3411 Mwt class Westinghouse plant meaning that they were in essence conducted on the Trojan plant. The following is a listing of the sensitivity studies considered to be generic, with a discussion of why the conclusions of the study are applicable for this applications report. For convenience of review, each discussion is referred to the section in the evaluation model report where the study is documented.

RELAP5/MOD2-B&W Time Step Study

This study (BAW-10168, Appendix A, Section A.2.1) verified that for light water reactor geometry, the RELAP5 time step controller governs the code solution sufficiently to assure converged results. Alternate system designs within the range of designs covered by the evaluation model will not change that result. Therefore, the study remains applicable.

RELAP5/MOD2-B&W Loop Noding Study

This study (BAW-10168, Appendix A, Section A.2.2) verified the general noding requirements within the loop for recirculating steam generator plants. In conjunction with the break noding study, the results can be applied to the separate regions of the hot leg, the steam generator, and the cold leg. Alternate system designs within the range of designs covered by the evaluation model will not change the noding requirements. Therefore, the study remains applicable.

RELAP5/MOD2-B&W Break Noding Study

This study (BAW-10168, Appendix A, Section A.3.1) verified that hydraulic stability is achieved by providing at least one control volume in the pipe between any adjacent component and the break node. The break noding study is applicable to all plants covered by the evaluation model. Therefore, the study remains applicable.

RELAP5/MOD2-B&W Pressurizer Location Study

Although the assumption placing the pressurizer in one of the intact loops was somewhat conservative, this study (BAW-10168, Appendix A, Section A.3.[illegible]) showed that there is little difference in results when the pressurizer is modeled in the broken loop.

The lack of sensitivity to pressurizer location is expected to hold for all designs covered by the evaluation model. Therefore, the study remains applicable.

RELAP5/MOD2-B&W Core Crossflow Study

This study (BAW-10168, Appendix A, Section A.3.4) verified that cross flow in a light water reactor is limited and does not alter the course of a LOCA evaluation substantially. The study is dependent only on the basic aspects of the fuel design, which are consistent across the range of designs considered by the evaluation model. Therefore, the study remains applicable.

RELAP5/MOD2-B&W Core Noding Study

In conjunction with the core crossflow study, this study (BAW-10168, Appendix A, Section A.3.5) verified that modeling of the reactor core with six or more axial segments with a hot and an average channel provides sufficient spacial detailing for both model convergence and result accuracy. The study, specifically addressing axial noding patterns of 6 and 12 nodes, showed that there was no substantial change in results between the two nodings and that the model was already converged with a 6-node modelling. Therefore, the 20-node pattern used in the analyses in this report will not effect the solution other than to resolve spacial detail more accurately. As the basic core arrangement and fuel design are not altered across the range of designs to be considered, the results of the study are applicable to all plants considered by the evaluation model. Therefore, the study remains applicable.

RELAP5/MOD2-B&W RCS Pumps Powered/Unpowered Study

This study (BAW-10174; response to NRC question number 16) verified that the pumps unpowered (tripped) is a reasonable

configuration for the calculation of large break LOCA. The study also concluded that the status of the pumps is a minor determinant of the calculated cladding temperature and that plant-specific pump status sensitivity studies are unnecessary. Therefore, the study remains valid.

REFLOD3B Primary Coolant Pump Rotor Resistance Study

This study (BAW-10168, Appendix A, Section A.2.4) showed a considerable reduction in flooding under a locked rotor assumption. The study affirms the generally accepted data on loop resistance effects on reflooding rates and is applicable for all plant types covered by the evaluation model. Therefore, the study remains applicable.

FRAP-T6-B&W Time Step Study

This study (BAW-10168, Appendix A, Section A.3.6) verified that the time step selection for FRAP-T6-B&W provided converged results for the spatial detail modeled in the base runs. Because the spatial detail required for the FRAP-T6-B&W model is not altered for the other designs covered by the evaluation model, the study remains valid for all designs. The study remains applicable.

FRAP-T6-B&W Radial Fuel Segmentation Study

This study (BAW-10168, Appendix A, Section A.3.7) verified that the number of solution points selected for radial representation of the fuel pin used by the base FRAP-T6-B&W model was adequate. The study is dependent only on the basic aspects of the fuel design, which are consistent across the range of designs considered by the evaluation model. The study remains applicable.

BEACH Time Step Study

This study (BAW-10168, Revision 1; response to NRC question number 10) verified that the BEACH (RELAP5) time step controller governs the code solution sufficiently to assure converged results. Alternate system designs within the range of designs covered by the evaluation model will not change that result. Therefore, the study remains applicable.

5.2 Confirmable Sensitivity Studies

In addition to the generically applicable studies, some of the studies performed for the evaluation model are considered confirmable. These studies remain valid under most but not all circumstances. The following is a listing of such sensitivity studies with a discussion of why the conclusions of the study can be applied to the Trojan evaluation and a reference to the section in the evaluation model report where the study is documented.

RELAP5/MOD2-B&W Pump Degradation Study

This study (BAW-10168, Appendix A, Section A.3.3) established a most severe pump degradation multiplier by altering the pump effects on the core flow. The study can be applied to all plants which experience similar LOCA core flow histories during blowdown. The sensitivity study was performed for a standard Westinghouse 3411 Mwt four-loop plant and is directly applicable to the Trojan facility.

REFLOD3B Loop Noding Study

This study (BAW-10168, Appendix A, Section A.2.3) verified the noding detail used in the REFLOD3B code. It is applicable to plants with one-to-one correspondence of hot and cold legs, such

as the Trojan unit. A separate study is required only for severely altered loop designs, such as the B&W or Combustion Engineering 2-by-4 designs. Therefore, the study remains applicable.

Time-in-Life Study

The BWFC Evaluation Model position on the proper time in life to perform the LOCA evaluation is developed in Appendix B of the Evaluation Model Report, BAW-10168, and supported by the studies in Appendix A. The position is that "so long as no burnup condition exists within the allowed operating limits which will cause a cladding rupture to occur during blowdown, the beginning of life is the most severe LOCA evaluation condition."

The analyses presented in this report are done using TACO3-calculated fuel inputs. To establish BOL as the worst case, the possibility of a blowdown rupture must be precluded. It is evident that a rupture during blowdown does not occur for the BOL case in the analyses presented in this report. Confirmation that no blowdown rupture occurs for other burnup conditions has been established by the calculation of the burnup most likely to rupture during blowdown.

Figure 5-1 illustrates the variation in steady-state volume average fuel temperature for different pin powers and the hot channel pin pressure at power as functions of burnup for the Mark-BW fuel operating in Trojan within the LOCA Limits as developed by this report. Although the actual values of these variable are considered proprietary by BWFC, the trends of the variables with burnup are shown, and these are all that is required to establish the most likely rupture case. From Figure 5-1, the highest pin pressure occurs at burnups of 41,000 Mwd/MTu and above, and the volume average fuel temperature at 41,000 Mwd/MTu bounds the fuel temperatures for 20,000 Mwd/MTu and

above. From Figure 7-2, the allowed maximum local heating rate at 41,000 Mwd/MTu is the same as that allowed for lower burnups and higher than that allowed at burnups above 41,000 Mwd/MTu. Therefore, the combination of parameters most likely to produce a blowdown rupture for pin exposures between 20,000 Mwd/MTu and 60,000 Mwd/MTu -- highest initial fuel pellet energy, highest pin internal pressure, and highest local power -- occur at 41,000 Mwd/MTu.

For burnups below 20,000 Mwd/MTu, the initial fuel pellet energy is higher than at 41,000 Mwd/MTu, but the pin pressure is sufficiently low to preclude any possibility of a blowdown rupture. This is illustrated by the base runs in this report, which are evaluated at 0 Mwd/MTu. For these cases, at the closest approach to rupture during blowdown, the cladding temperature is more than 300 F below that required to induce rupture. At 10,000 Mwd/MTu, the initial pin pressure has increased by less than 15 percent of the difference between the 0 Mwd/MTu conditions and the 41,000 Mwd/MTu conditions. The volume average fuel temperature, on the other hand, has decreased by 50 percent of the difference in that parameter between the two burnups. With the substantial margins to rupture of the 0 Mwd/MTu case, the 10,000 Mwd/MTu conditions are also bounded by the conditions at 41,000 Mwd/MTu. Thus, demonstrating that the fuel at 41,000 Mwd/MTu will not incur a blowdown rupture also demonstrates that, when operated under the LOCA Limits, the Mark-BW fuel will not rupture during blowdown for any burnup up to 60,000 Mwd/MTu.

To establish the results for the 41,000 Mwd/MTu burnup an evaluation of the that case was run through the blowdown period. The cladding temperature peaked under 1600 F and was 99 F below the temperature required to rupture at the closest approach to rupture. Therefore, there is no occurrence of blowdown rupture for the Trojan plant when using the Mark-BW and the beginning of

life conditions, as demonstrated in Appendix B of BAW-10168, are the worst case for the LOCA evaluations. As a practical matter, the time-in-life actually selected for the TACO3 inputs for this report was 1 Mwd/MTu.

5.3 Break Location

The BWFC position on break location is developed in Appendix B of the Evaluation Model Report, BAW-10168. Substantial numbers of studies by BWFC and others have consistently shown that the suction piping and hot leg breaks are less severe than LOCA positioned in the pump discharge piping. This result is substantiated by geometric considerations associated with those breaks which assure enhanced ECCS performance. Therefore, the only accidents specifically evaluated for the Trojan plant are located in the reactor coolant pump discharge piping.

FIGURE 5-1. TACO3 FUEL TEMPERATURE AND INTERNAL PIN PRESSURE AS A FUNCTION OF BURNUP.

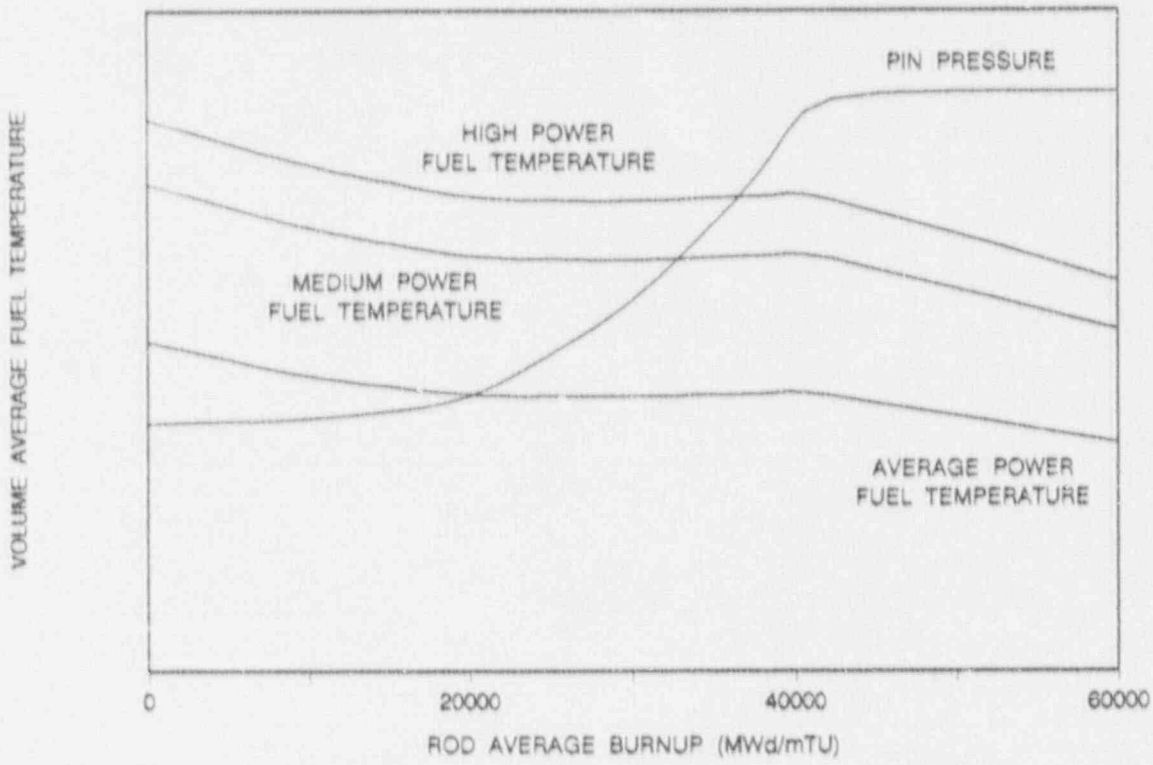

6. Plant-Specific Studies and Spectrum Analysis

Although a considerable portion of the analysis inputs and assumptions can be set by the evaluation model and its sensitivity studies, some parameters are dependent on plant-specific inputs and can only be established by individual plant studies. These studies and the spectrum analyses are performed to identify a worst case break to use in calculating the LOCA Limits. Figure 6-1 shows the order in which the plant-specific sensitivity studies and the spectrum analysis cases were performed. This chapter presents the results of the studies leading to the final configuration used in the LOCA Limits cases.

6.1 Base Case

The first step in performing a series of sensitivity studies is to establish a base case. For the studies presented in this chapter, the base case is a double-ended guillotine cold leg break, with a discharge coefficient of 1.0, located between the reactor coolant pump and the reactor vessel. Figures 6-2 through 6-14 present key parameters for this case. The results compare well to those documented in revision 0 of the evaluation model report, BAW-10168, which were for the same class of plant. The cases in BAW-10168 were run with a total allowed peaking factor of 2.32 while the current results are for a total peaking of 2.50. The increase in thermal pressure, however, is compensated for by the improvements in reflooding heat transfer made in revision 1 of the Evaluation Model.

6.2 Minimum ECCS Analysis

Prior to the break type or spectrum studies, a study is conducted to determine which condition for the ECCS is more severe, with or without a single failure. Under a single failure assumption,

only one train of pumped ECCS injection is available. With no failure, two full trains are available. Because the sizing of each individual train must be sufficient to mitigate an accident, the second train is redundant relative to providing adequate water for core cooling. In an analysis, nearly all the extra injection capacity will spill from the primary coolant system to the containment where it may interact with the atmosphere to reduce the containment pressure. As the lowering of the containment pressure causes a reduction in core reflooding rate, the evaluation of a fully functional ECCS may actually show a higher peak cladding temperature than would be predicted using the single failure assumption.

The calculations for the base case assumed no failure of the ECCS or supporting systems. This is normally referred to as the "maximum ECCS" case. To evaluate the assumption of a failure, a calculation was made under the condition that one of the diesel generators of the emergency power supply failed to operate, resulting in a loss of electrical power to half of the pumped ECC systems. This is generally referred to as a "minimum ECCS" case. Figures 6-15 through 6-25 present relevant parameters for the minimum ECCS case. These should be compared to the base case, Figures 6-2 through 6-14.

The extra ECC available in the maximum ECCS case has two effects during reflood: First, the ECCS water that is injected into the intact loops condenses more of the steam flowing through the loops and lowers the RCS pressure. Second, the ECCS water that is spilled into the containment mixes with the containment atmosphere and reduces its pressure. The reduced containment pressure in turn reduces the RCS pressure. The effect of reducing the RCS pressure is to increase the specific volume of the steam created during core reflooding. As a result, the steam is more difficult to vent through the system, and the core flooding rate decreases. A comparison of Figures 6-5 and 6-20

shows that the flooding rate for the Trojan plant is lower under the maximum ECCS condition. As there are no blowdown cooling benefits to compensate for the lower flooding rate, the cladding temperature is higher by 77 F as shown in Figures 6-9 and 6-22. The remainder of the evaluations will, therefore, proceed under the assumption of no failure of the ECCS systems or the supporting systems.

6.3 Break Type

The break spectrum analysis is performed to determine the worst case break size and the worst case break configuration. Chapter 5 of this report and Appendix B of the Evaluation Model Report, BAW-10168, discuss time-in-life and break location studies and show that the proper selection does not require a plant specific study. The differences between the split and the guillotine break and the range of break sizes cannot be generalized, however, and those studies were run for the Trojan evaluation. The break type study was performed first and followed by the break size study.

The guillotine break is modeled as a complete severance of the pipe, allowing separate discharges through the full area of the cold leg piping from both the reactor vessel and pump sides of the break location. No mixing of the flows from the two sides of the break is allowed. The split break assumes discharge from the cold leg piping through an area twice the size of the cold leg piping cross section. Although the flows from the two sides, RC pump and reactor vessel, must still pass through limiting pipe areas, they are allowed to mix at the break location. The blowdown rates and system flow splits are somewhat different for the two types of breaks, and that can lead to differences in cooling response.

Figures 6-26 through 6-33 present the results of the split type break case. These should be compared to Figures 6-2 through 6-14 which are for the reference guillotine case. Both are double-area breaks with C_d = 1.0 and located at the pump discharge. Key data from the split case are included with the spectrum studies in Table 6-1. As can be seen, the period of blowdown for the split break is shorter by less than one second. The split break, however, has a larger reverse flow through the core during blowdown resulting in lower fuel temperatures at the end-of-blowdown. At the end of blowdown the centerline fuel temperature at the location of peak power is 1347 F for the split break and 1508 F for the guillotine. With lower fuel temperatures at the start of refill and higher early flooding rates, rupture in the split case lags behind the guillotine. After rupture, but prior to the occurrence of peak cladding temperature (70 to 220 seconds), the flooding rate for the split case drops slightly below that for the guillotine. This results in less effective reflood heat transfer for the split. The temperature difference created during blowdown is thereby reduced somewhat, but the peak in cladding temperature remains lower for the split case by 41 F.

6.4 Break Spectrum Analysis

For the BWFC large break evaluation model, the break size study is interchangeable with a discharge coefficient study since the break flow is directly proportional to the product of the break area and the discharge coefficient. For the Trojan model, the discharge coefficient study was conducted for a guillotine break of twice the area of the cold leg piping located at the pump discharge with discharge coefficients of 1.0, 0.8, and 0.6. The base case, Figures 6-2 through 6-14, serves as the C_d of 1.0 case. Key parameters for the other two cases are shown grouped by case in Figures 6-34 through 6-49. Table 6-1 presents a comparison of the timing of events for the three cases.

There are no major differences among the sequences of events for the three cases that make up the discharge coefficient study; the peak cladding temperatures differ by only 5 F. As expected, blowdown is extended as the break flow is decreased. Core heat removal during blowdown is essentially the same for the 1.0 and 0.8 discharge coefficients cases while the 0.6 case cools slightly better. This is evident from the centerline fuel temperature at the location of peak power: 1508 F, 1516 F, and 1457 F for the C_d = 1.0, 0.8, and 0.6 cases, respectively. All three cases retain about 90 cubic feet of liquid in the reactor vessel at the end of blowdown, making the adiabatic heatup periods during lower head refilling nearly the same. The reflooding transients are almost identical for the three cases.

The small difference in the peak cladding temperatures between the C_d = 1.0 and the C_d = 0.8 cases is not surprising. Both experience similar blowdown cooling, refill times, and reflooding transients. Furthermore, the peak cladding temperature occurs in Node 14, at the center of the grid span above the peak power location. This elevation takes nearly 200 seconds during reflooding to reach its peak in cladding temperature. Because reflooding heat transfer changes slowly with time, the cladding temperature is mainly set by the need to remove the relatively fixed power being generated at that location. Because the powers are the same between the cases, the resultant peak cladding temperatures are the same. The argument is also true for the C_d = 0.6 case. Although the C_d = 0.6 case enters refill and reflooding with cooler fuel and cladding temperatures (by about 50 F), the reflooding heat transfer between 200 and 300 seconds is changing so slowly that the case continues to heat up until the temperature differential is sufficient to remove the power. With the power being nearly constant, this results in the C_d = 0.6 peaking somewhat later than do the other cases but at essentially the same temperature.

The conclusion for the spectrum study is that there is little difference among the results of the analyses and that a worst case defined strictly by peak cladding temperature would be hard to identify. The extra blowdown cooling for the C_d = 0.6 case is significant as it indicates that smaller discharge coefficients in the spectrum can be expected to attain lower temperatures. Between the C_d = 1.0 and the C_d = 0.8 cases there is no material difference in result at the location of peak cladding temperature (PCT for C_d = 1.0 is only 3 F higher than for C_d = 0.8). However, the temperature at locations removed from the location of PCT (see Table 6-1) are consistently slightly higher for the C_d = 1.0 case. Therefore, the C_d = 1.0 case was selected for the LOCA limits calculations.

TABLE 6-1 SPECTRUM AND BREAK TYPE COMPARISON

		Guillotines			Split
Item or Parameter	C_d =>	1.0	0.8	0.6	1.0
End of Blowdown, s		17.7	18.9	21.0	16.9
Liquid in Reactor Vessel at EOB, ft^3		90.5	98.1	83.3	74.7
Bottom-of-Core Recovery, s		29.4	30.4	32.6	28.6
Time of Rupture, s		45.0	46.7	54.0	50.8
Ruptured Node *		11	11	11	11
PCT at Rupture Node, F		1738	1725	1665	1628
Node Adjacent to Rupture *		12	12	12	12
PCT of Adjacent Node, F		1969	1958	1901	1863
PCT Node in Adjacent Grid Span *		14	14	14	14
PCT of Adjacent Grid Span, F		2047	2044	2042	2006
Pin PCT Node *		14	14	14	14
PCT of Pin PCT Node		2047	2044	2042	2006

* Refer to Figure 4-4 for noding arrangement

FIGURE 6-1. PLANT SPECIFIC STUDIES ANALYSIS DIAGRAM.

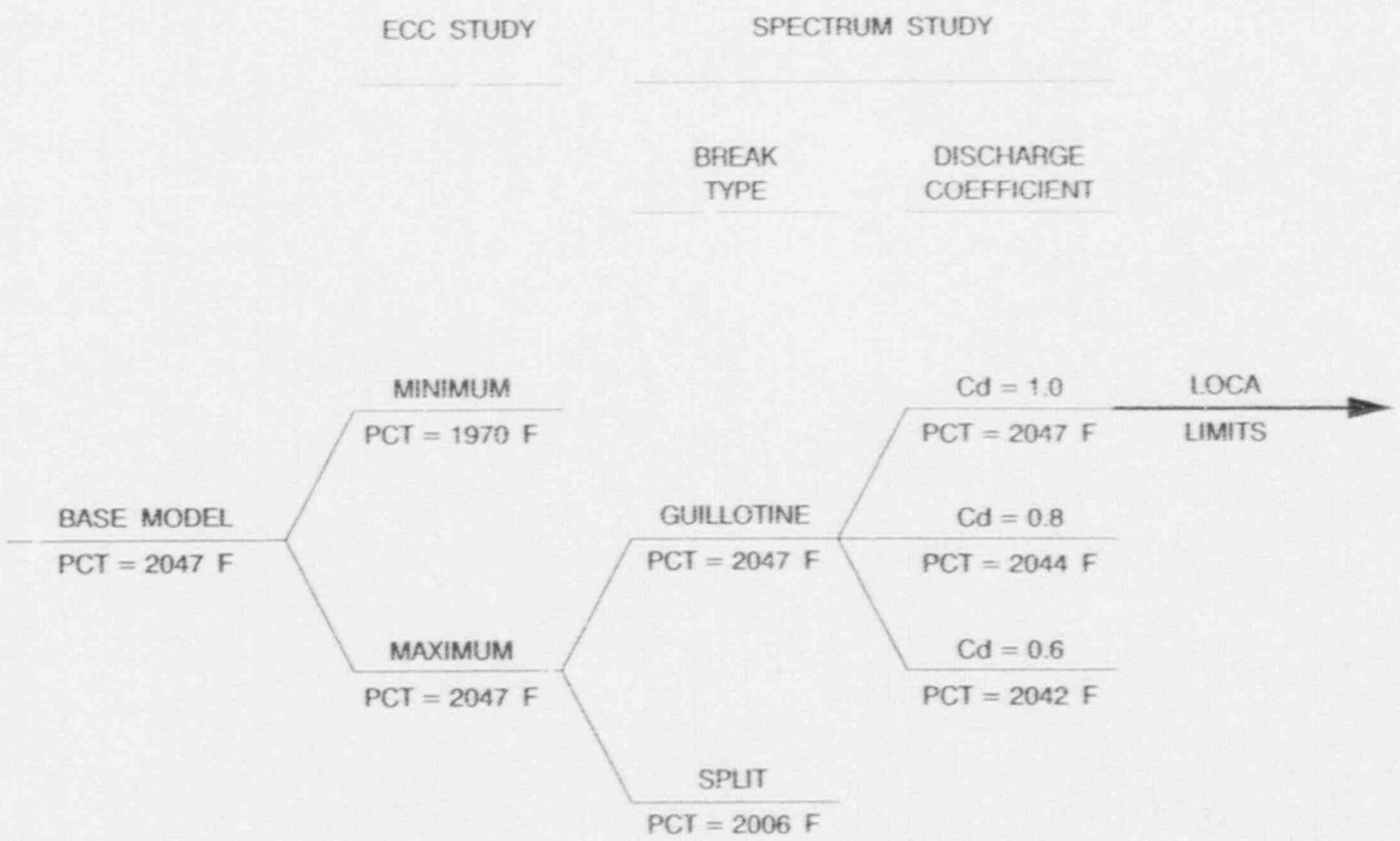

BASE MODEL: 2A/G @ PD Cd = 1.0

FIGURE 6-2. BASE CASE - DECLB, Cd = 1.0, MAX ECCS
SYSTEM PRESSURE DURING BLOWDOWN.

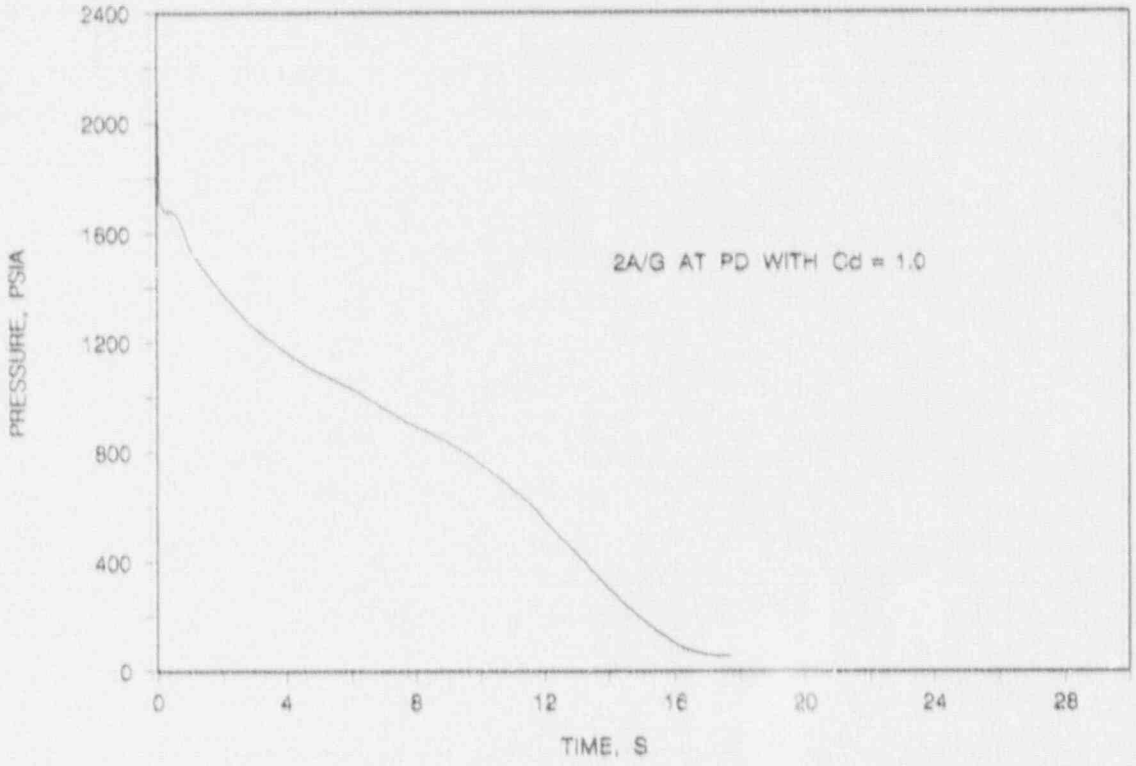

FIGURE 6-3. BASE CASE - DECLB, Cd = 1.0, MAX ECCS
MASS FLUX DURING BLOWDOWN AT PEAK POWER LOCATION.

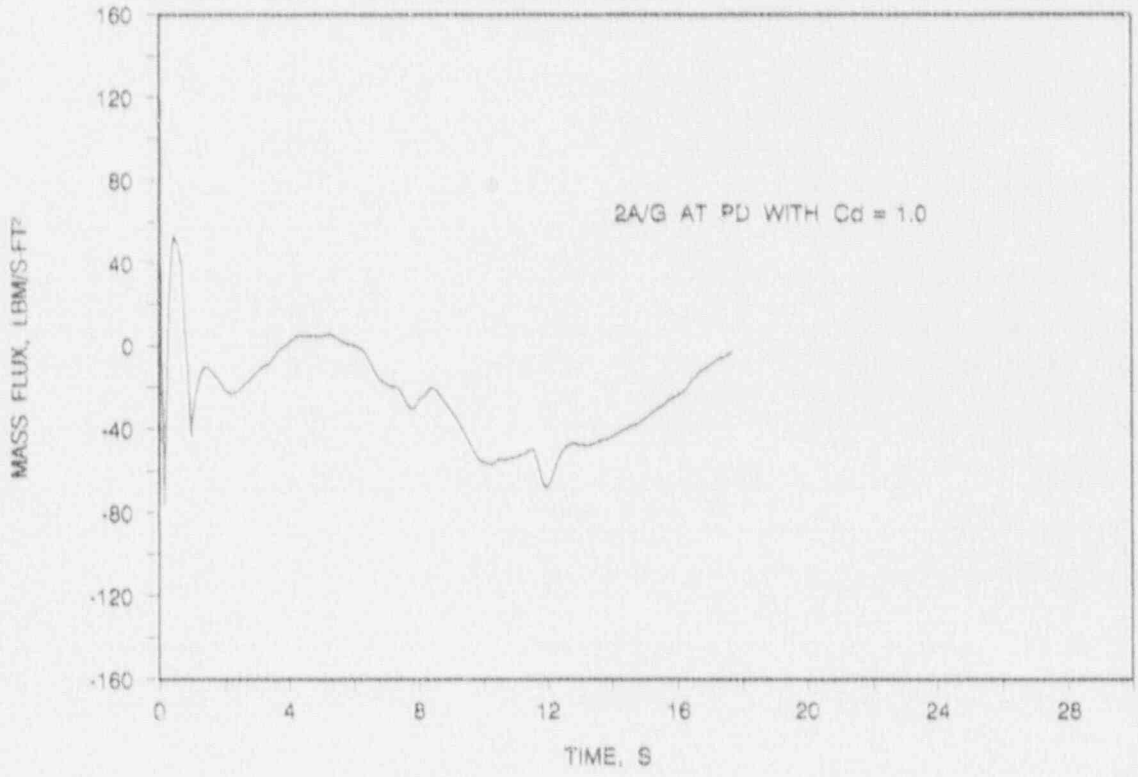

FIGURE 6-4. BASE CASE - DECLB, Cd = 1.0, MAX ECCS
MAXIMUM ECC PUMPED INJECTION CONTAINMENT PRESSURE.

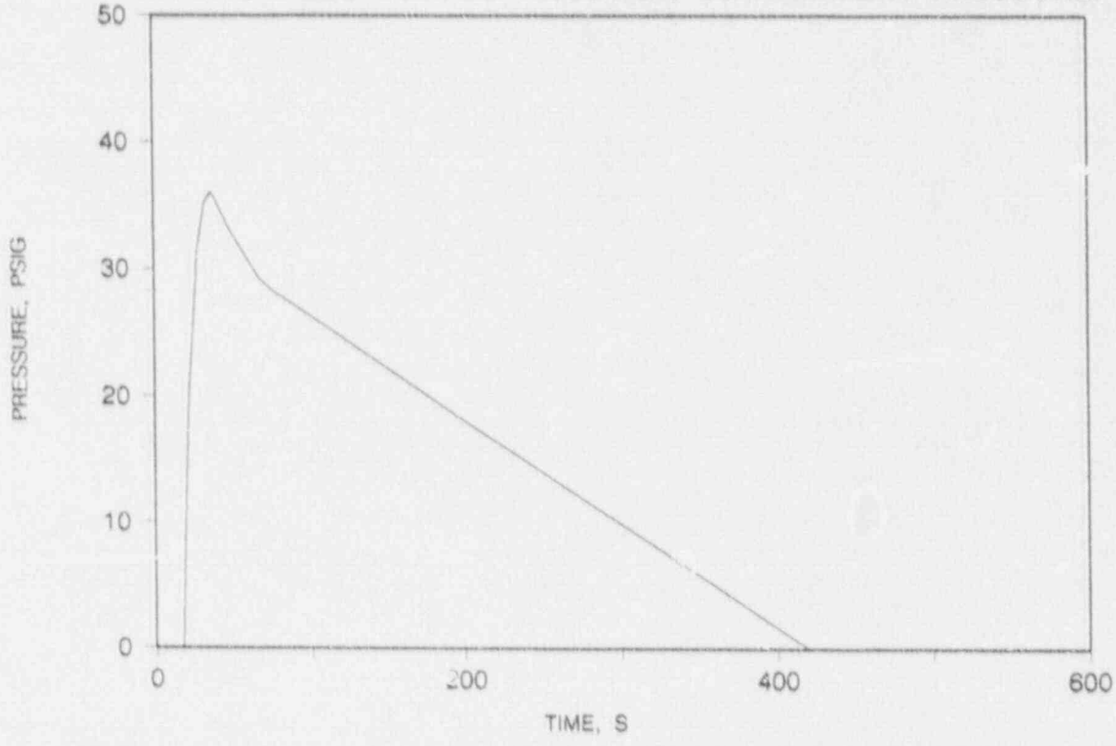

FIGURE 6-5. BASE CASE - DECLB, Cd = 1.0, MAX ECCS
REFLOODING RATE.

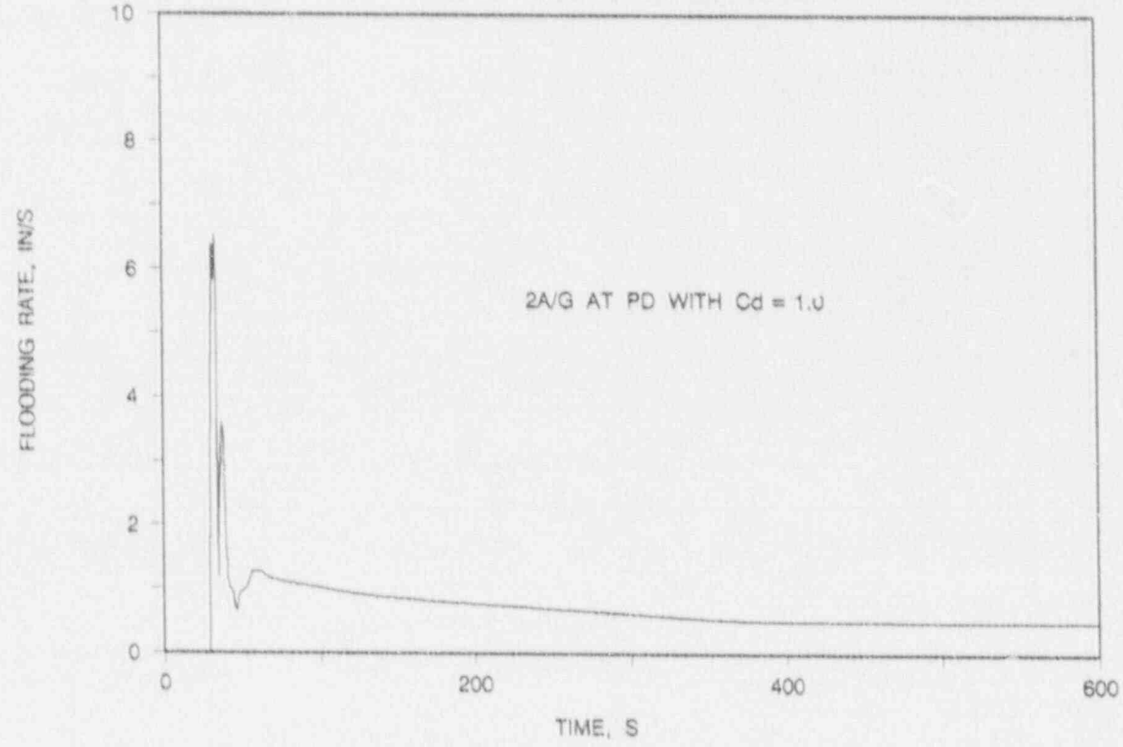

FIGURE 6-6. BASE CASE - DECLB, Cd = 1.0, MAX ECCS HEAT TRANSFER COEFFICIENT AT PCT LOCATION.

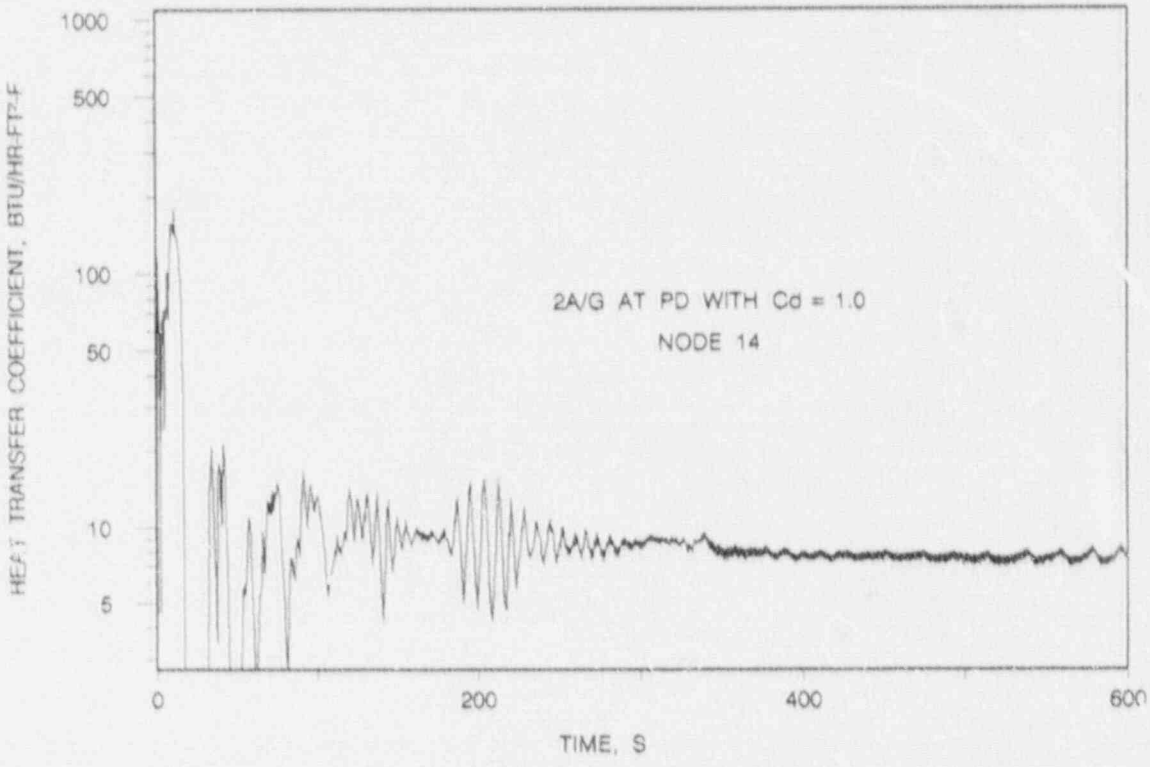

FIGURE 6-7. BASE CASE - DECLB, Cd = 1.0, MAX ECCS HEAT TRANSFER COEFFICIENT AT RUPTURE LOCATION.

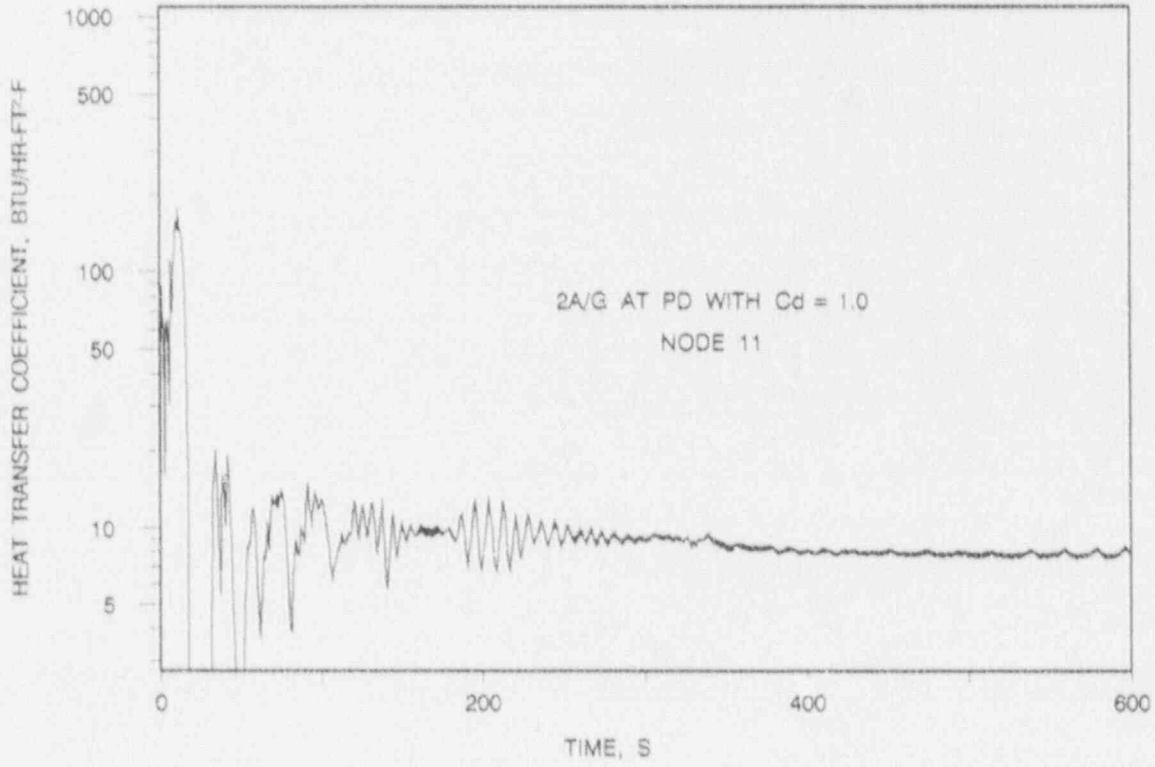

FIGURE 6-8. BASE CASE - DECLB, Cd = 1.0, MAX ECCS
HEAT TRANSFER COEFFICIENT ADJACENT TO RUPTURE LOCATION.

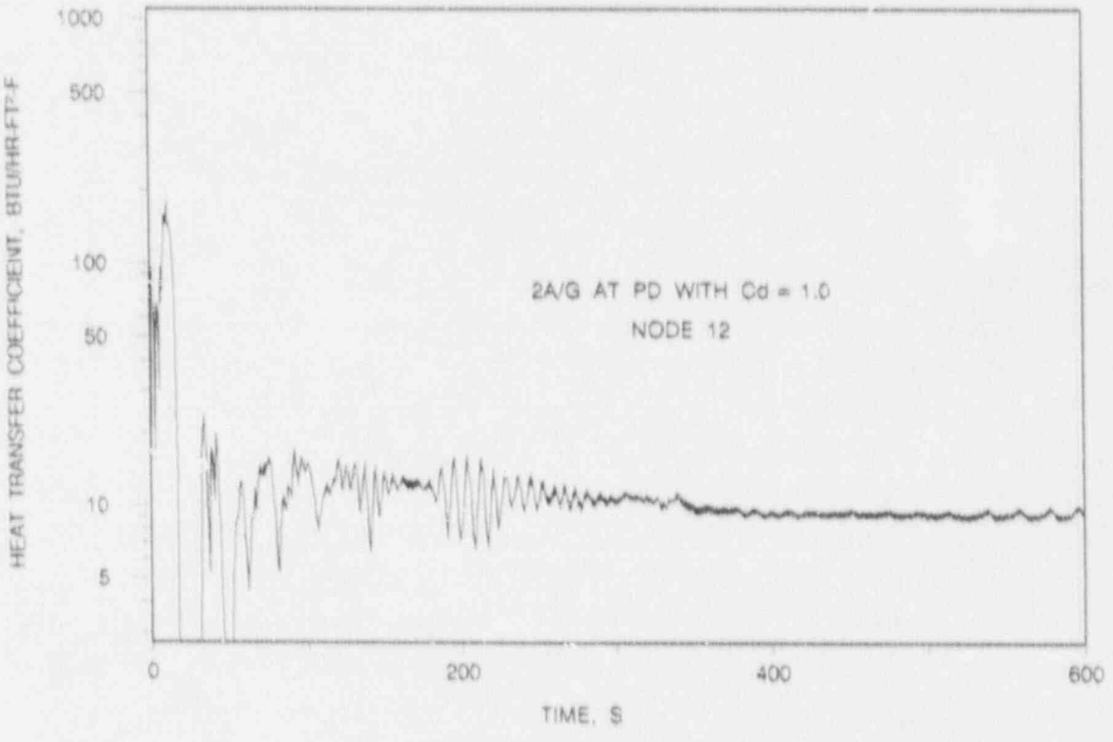

FIGURE 6-9. BASE CASE - DECLB, Cd = 1.0, MAX ECCS
PEAK CLADDING TEMPERATURE.

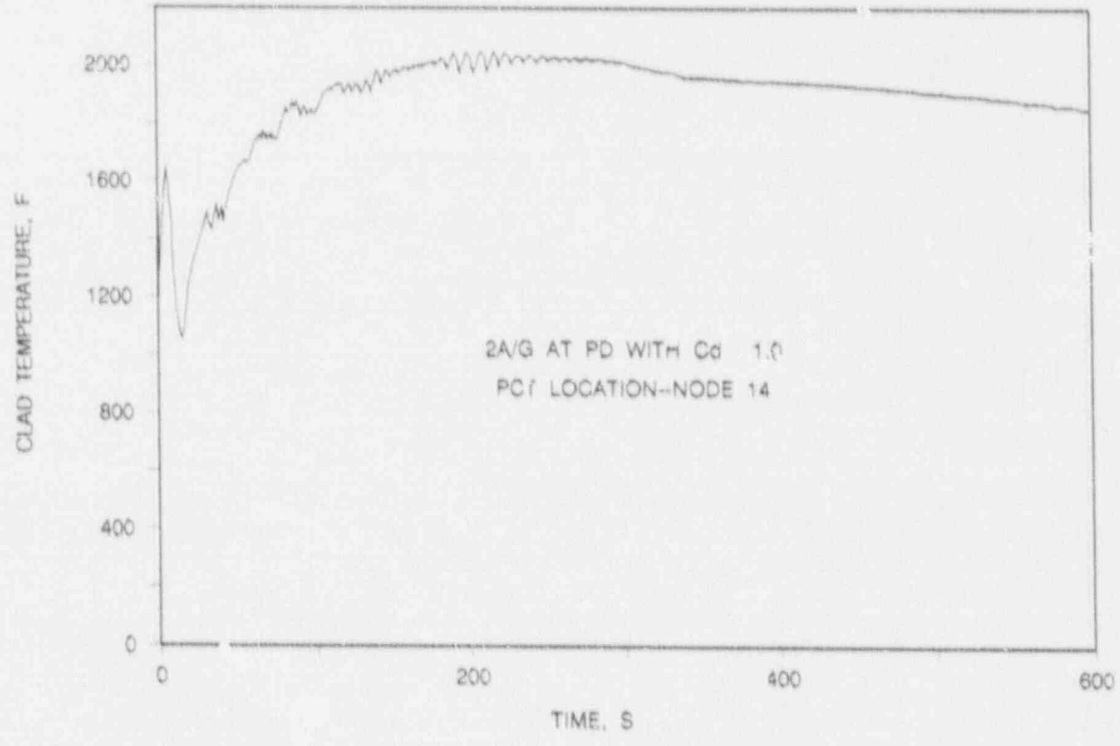

FIGURE 6-10. BASE CASE - DECLB, Cd = 1.0, MAX ECCS CLADDING TEMPERATURE AT RUPTURE LOCATION.

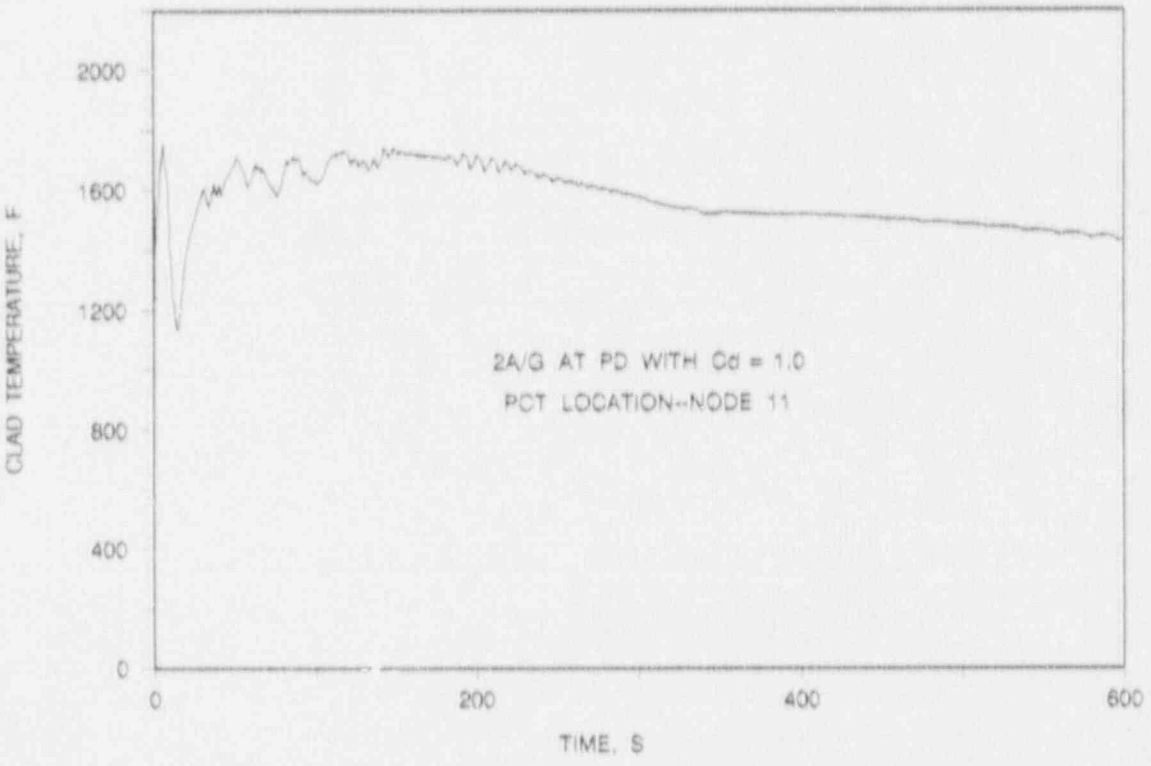

FIGURE 6-11. BASE CASE - DECLB, Cd = 1.0, MAX ECCS CLADDING TEMPERATURE ADJACENT TO RUPTURE LOCATION.

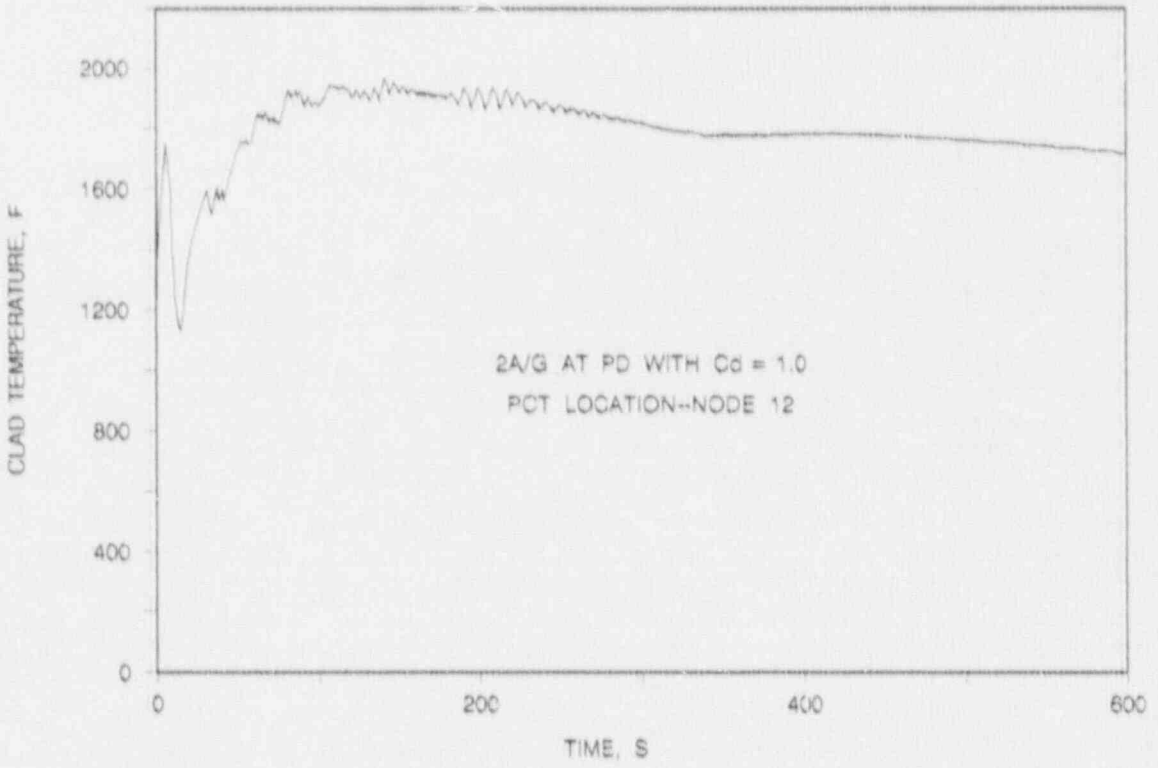

FIGURE 6-12a. BASE CASE - DECLB, Cd = 1.0, MAX ECCS FLUID TEMPERATURE AT PCT LOCATION.

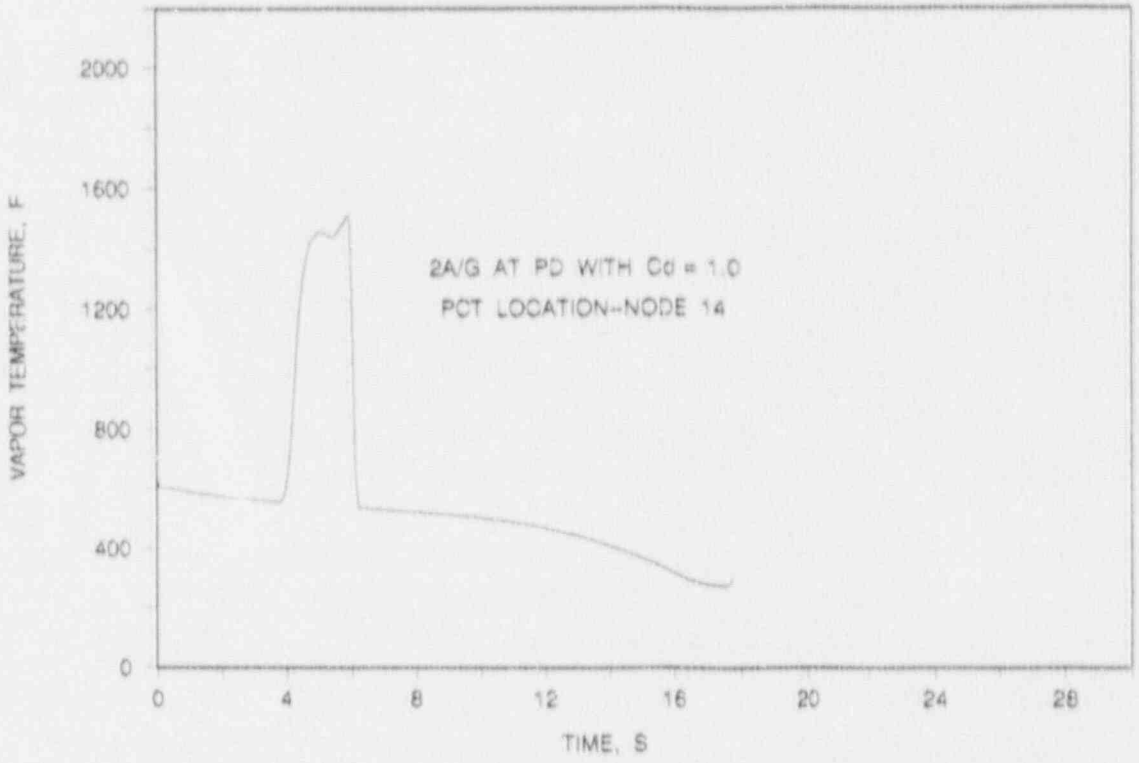

FIGURE 6-12b. BASE CASE - DECLB, Cd = 1.0, MAX ECCS FLUID TEMPERATURE AT PCT LOCATION.

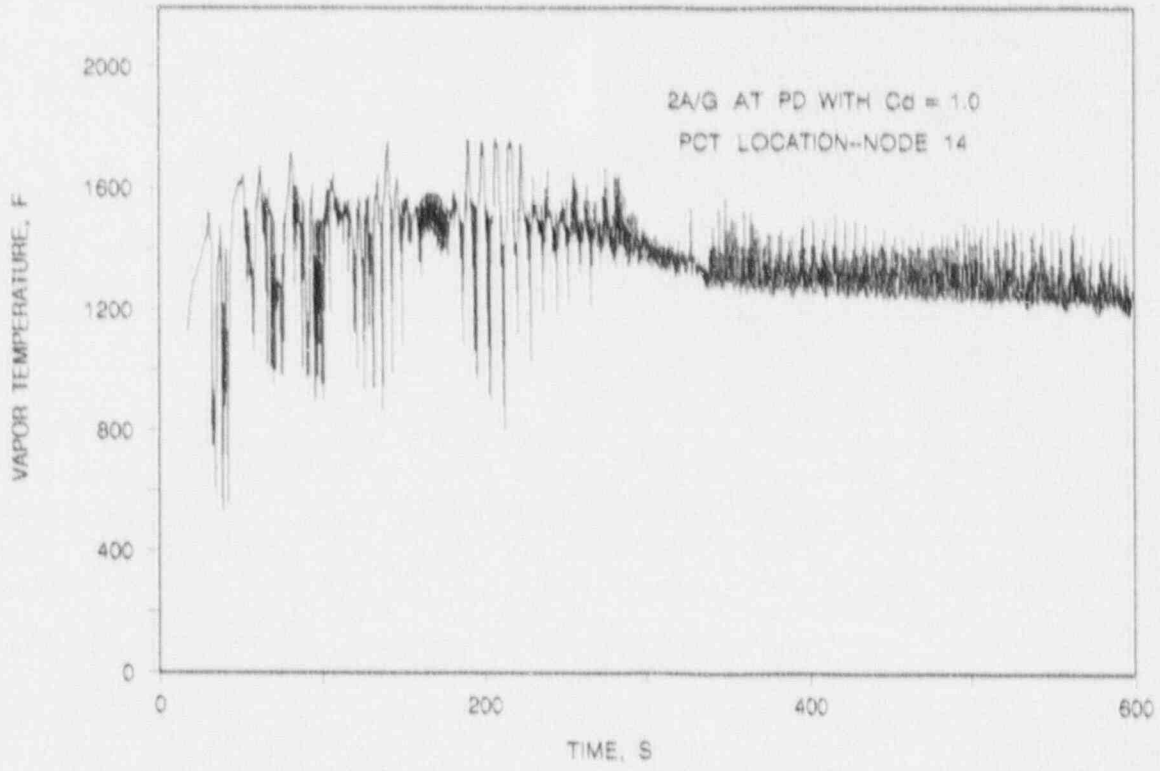

FIGURE 6-13a. BASE CASE - DECLB, Cd = 1.0, MAX ECCS FLUID TEMPERATURE AT RUPTURE LOCATION.

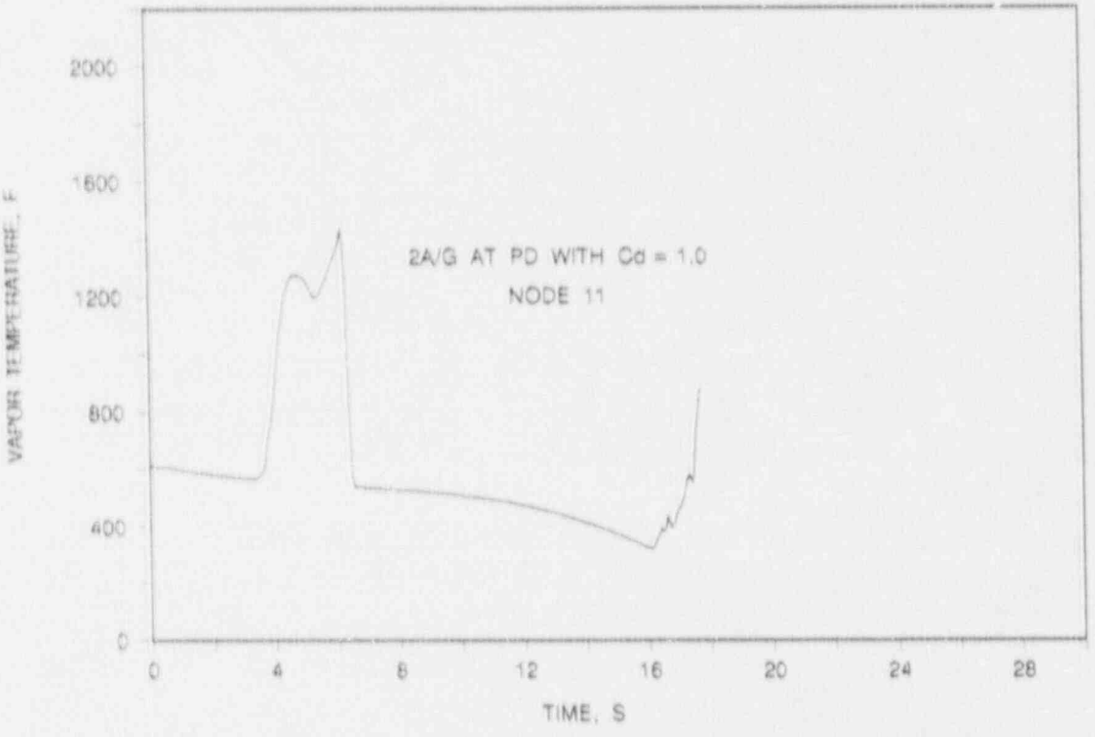

FIGURE 6-13b. BASE CASE - DECLB, Cd = 1.0, MAX ECCS FLUID TEMPERATURE AT RUPTURE LOCATION.

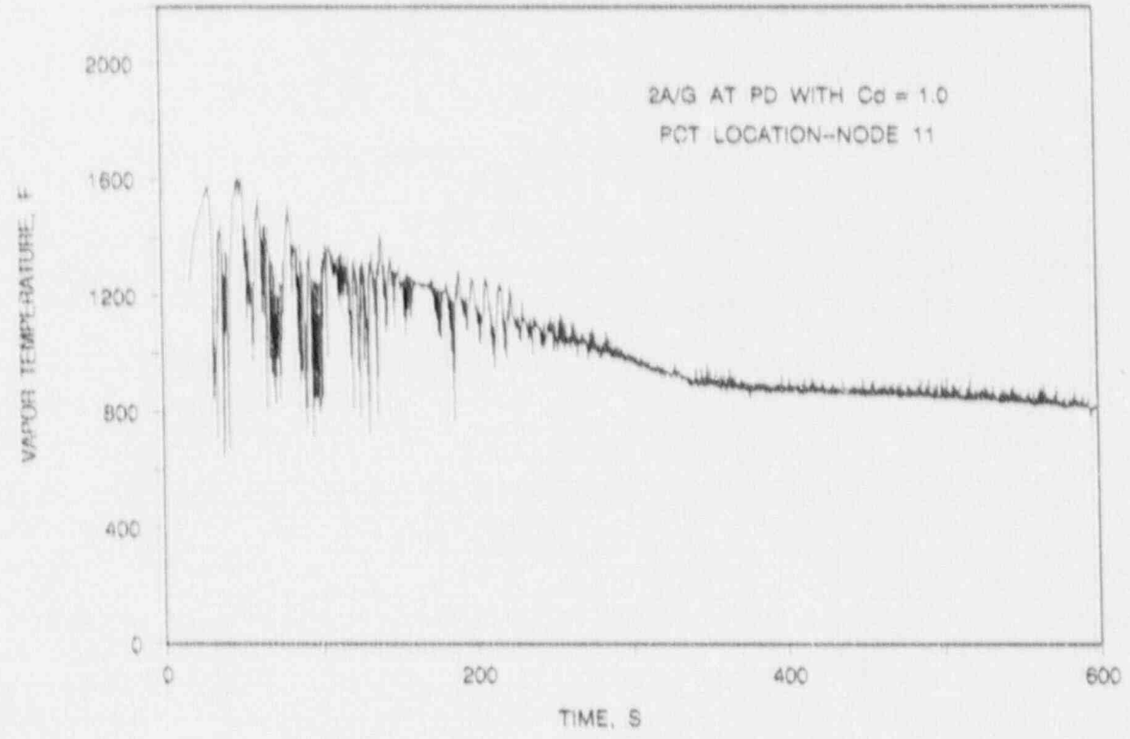

FIGURE 6-14a. BASE CASE - DECLB, Cd = 1.0, MAX ECCS FLUID TEMPERATURE ADJACENT TO RUPTURE LOCATION.

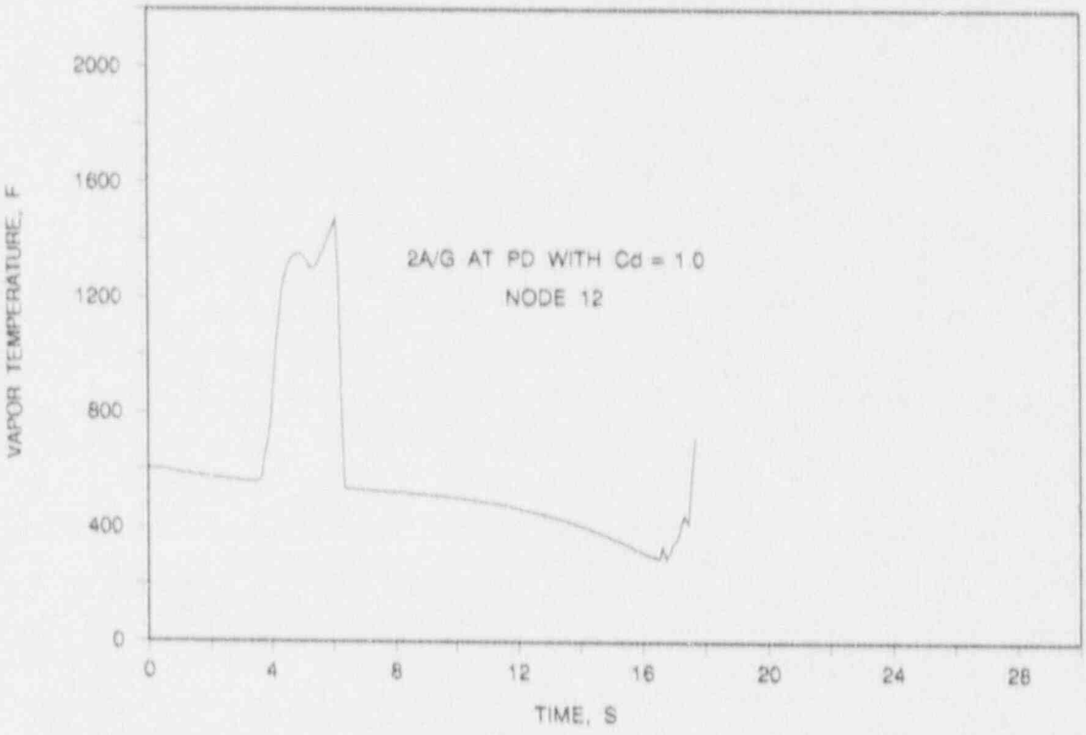

FIGURE 6-14b. BASE CASE - DECLB, Cd = 1.0, MAX ECCS FLUID TEMPERATURE ADJACENT TO RUPTURE LOCATION.

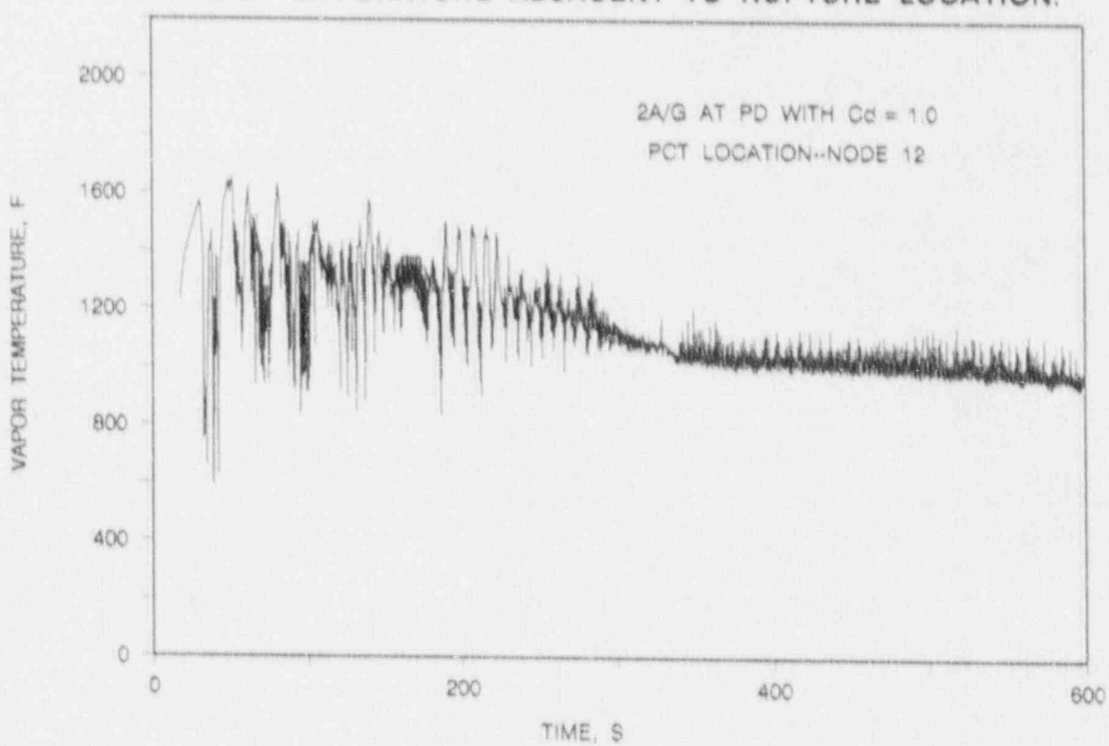

FIGURE 6-15. MINIMUM ECCS STUDY - DECLB, Cd = 1.0
MINIMUM ECC PUMPED INJECTION CONTAINMENT PRESSURE.

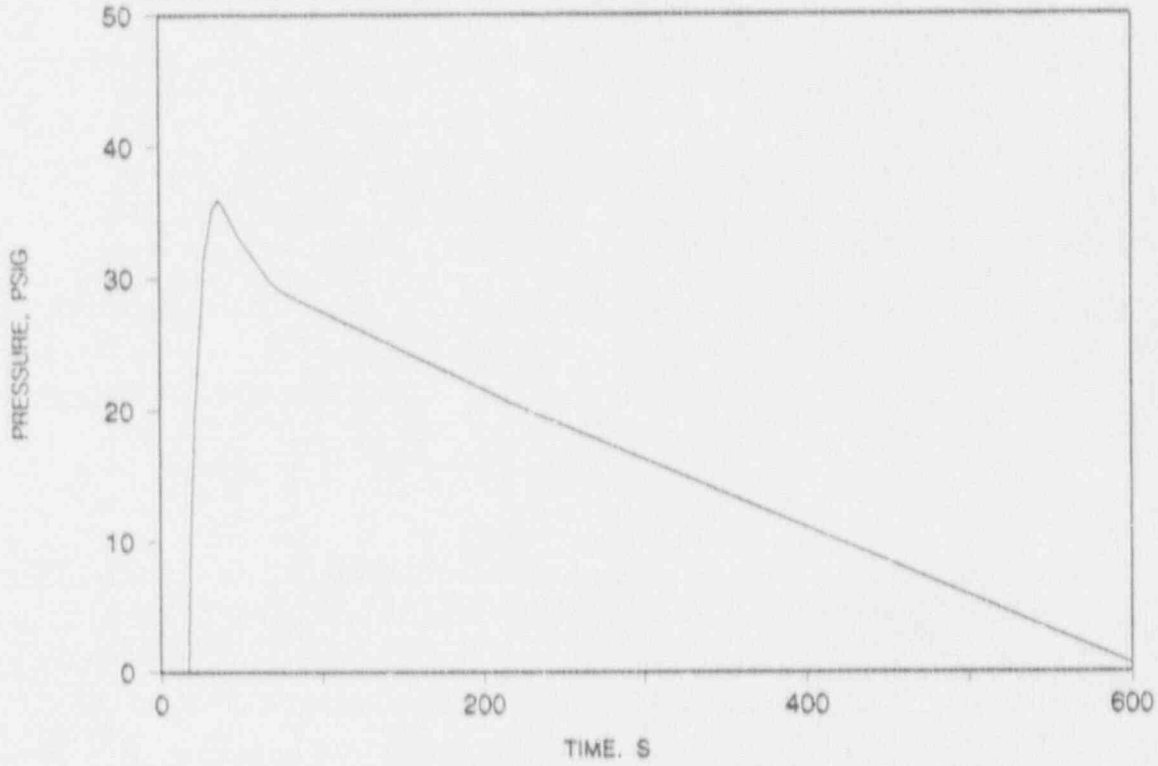

FIGURE 6-16. MINIMUM ECCS STUDY - DECLB, Cd = 1.0
PUMPED ECC INJECTION FLOW RATE.

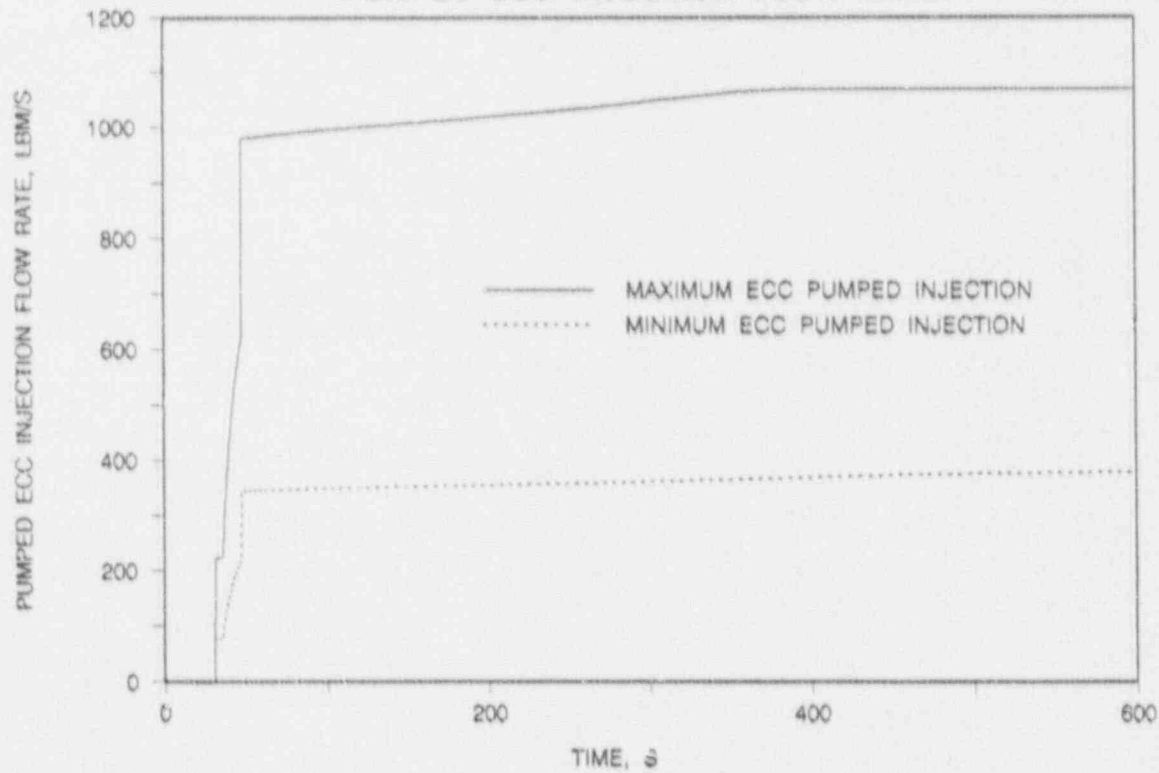

FIGURE 6-17. MINIMUM ECCS STUDY - DECLB, Cd = 1.0
DOWNCOMER WATER LEVEL.

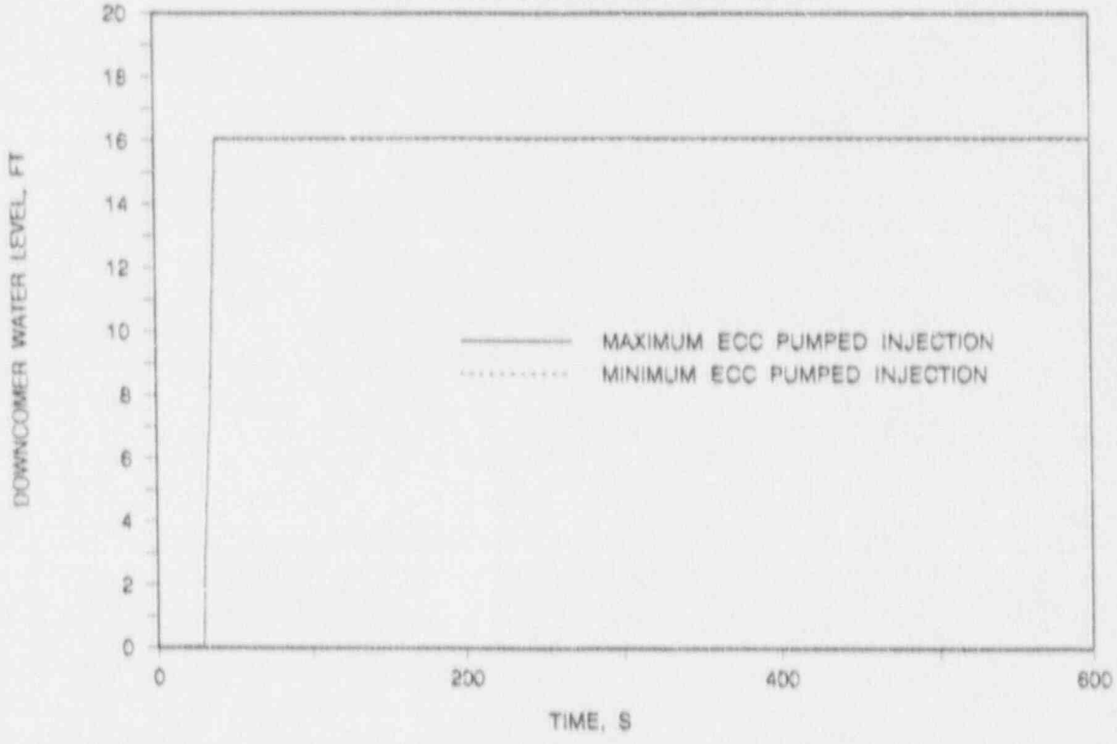

FIGURE 6-18. MINIMUM ECCS STUDY - DECLB, Cd = 1.0
SYSTEM PRESSURE DURING BLOWDOWN.

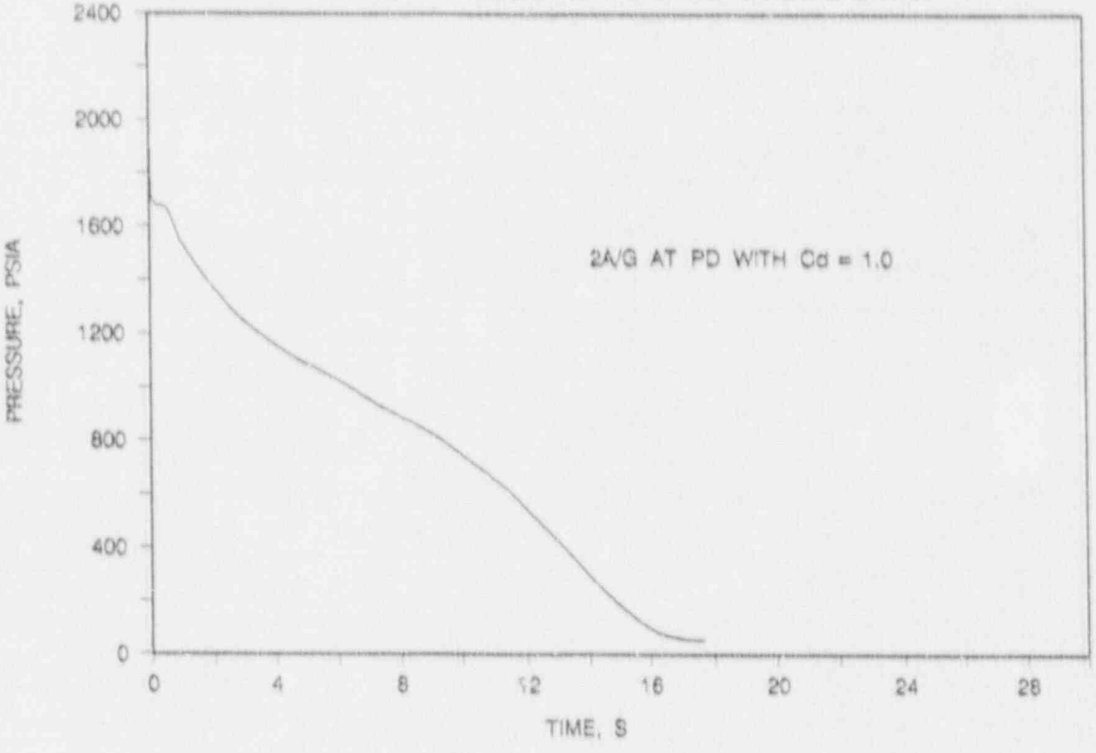

FIGURE 6-19. MINIMUM ECCS STUDY - DECLB, Cd = 1.0
MASS FLUX DURING BLOWDOWN AT PEAK POWER LOCATION.

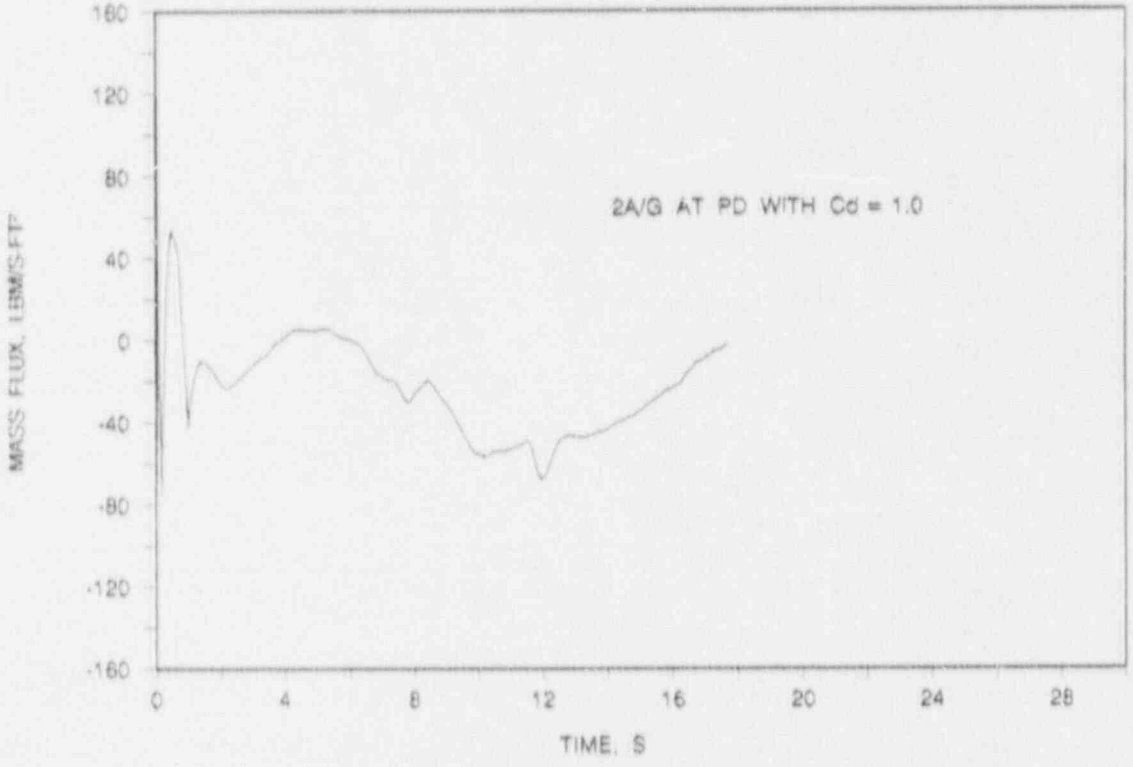

FIGURE 6-20. MINIMUM ECCS STUDY - DECLB, Cd = 1.0
REFLOODING RATE.

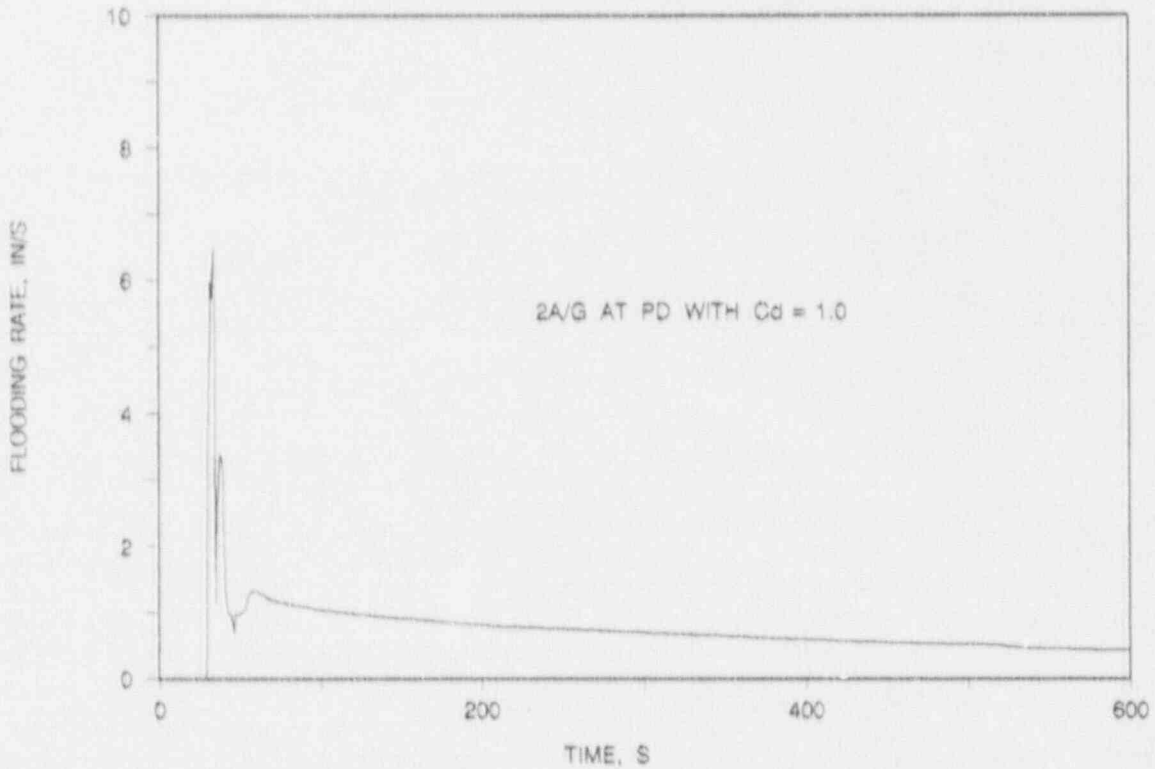

FIGURE 6-21. MINIMUM ECCS STUDY - DECLB, Cd = 1.0
HEAT TRANSFER COEFFICIENT AT PEAK POWER LOCATION.

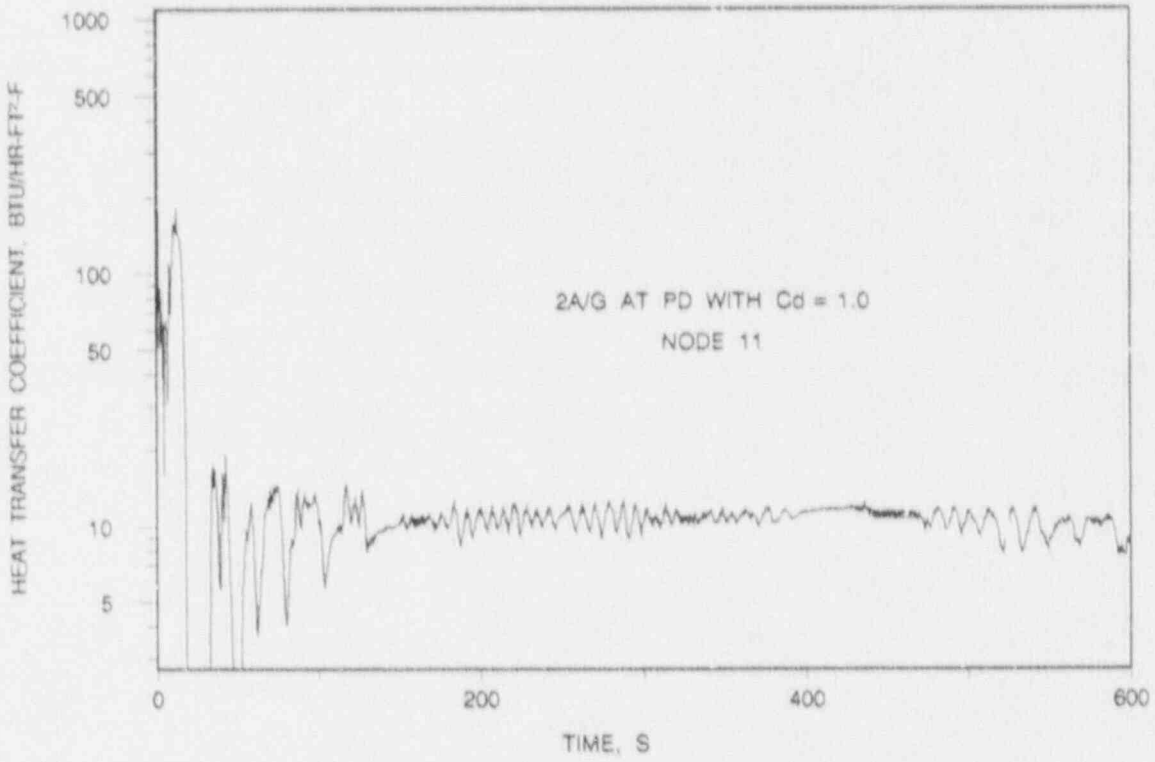

FIGURE 6-22. MINIMUM ECCS STUDY - DECLB, Cd = 1.0
PEAK CLADDING TEMPERATURE.

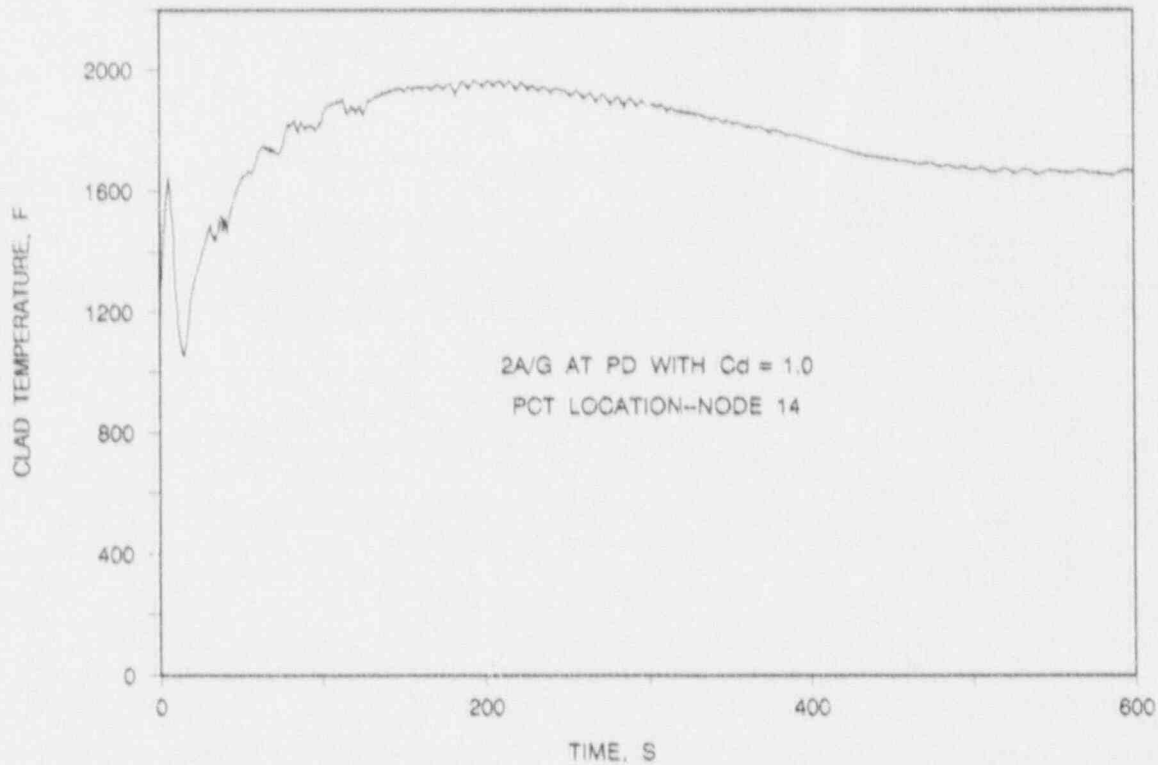

FIGURE 6-23. MINIMUM ECCS STUDY - DECLB, Cd = 1.0
CLADDING TEMPERATURE AT RUPTURE LOCATION.

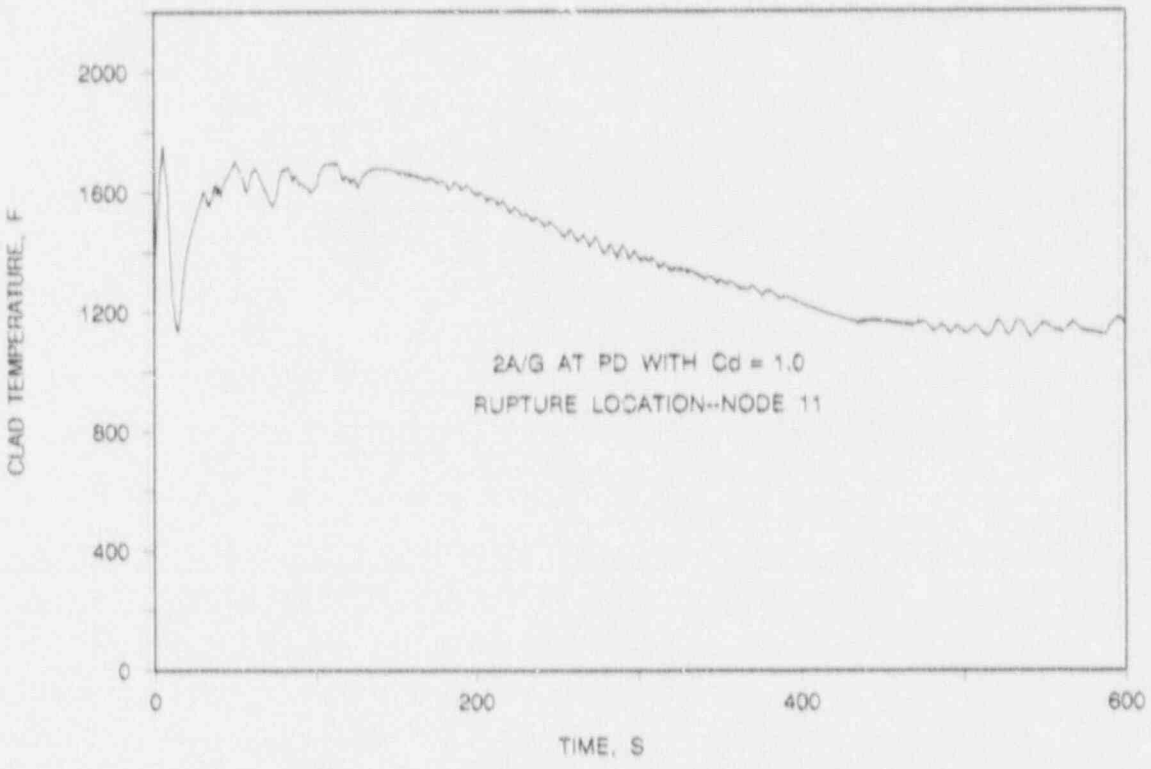

FIGURE 6-24. MINIMUM ECCS STUDY - DECLB, Cd = 1.0
CLADDING TEMPERATURE ADJACENT TO RUPTURE LOCATION.

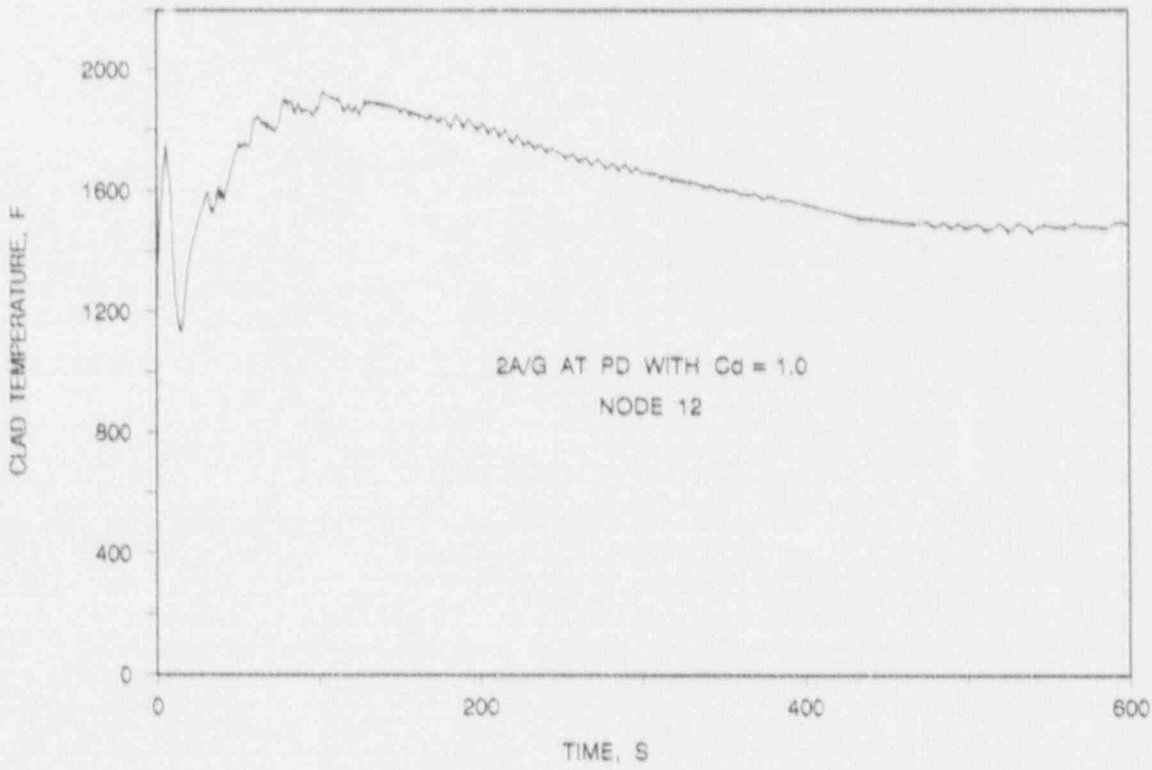

FIGURE 6-25a. MINIMUM ECCS STUDY - DECLB, Cd = 1.0
FLUID TEMPERATURE AT PCT LOCATION.

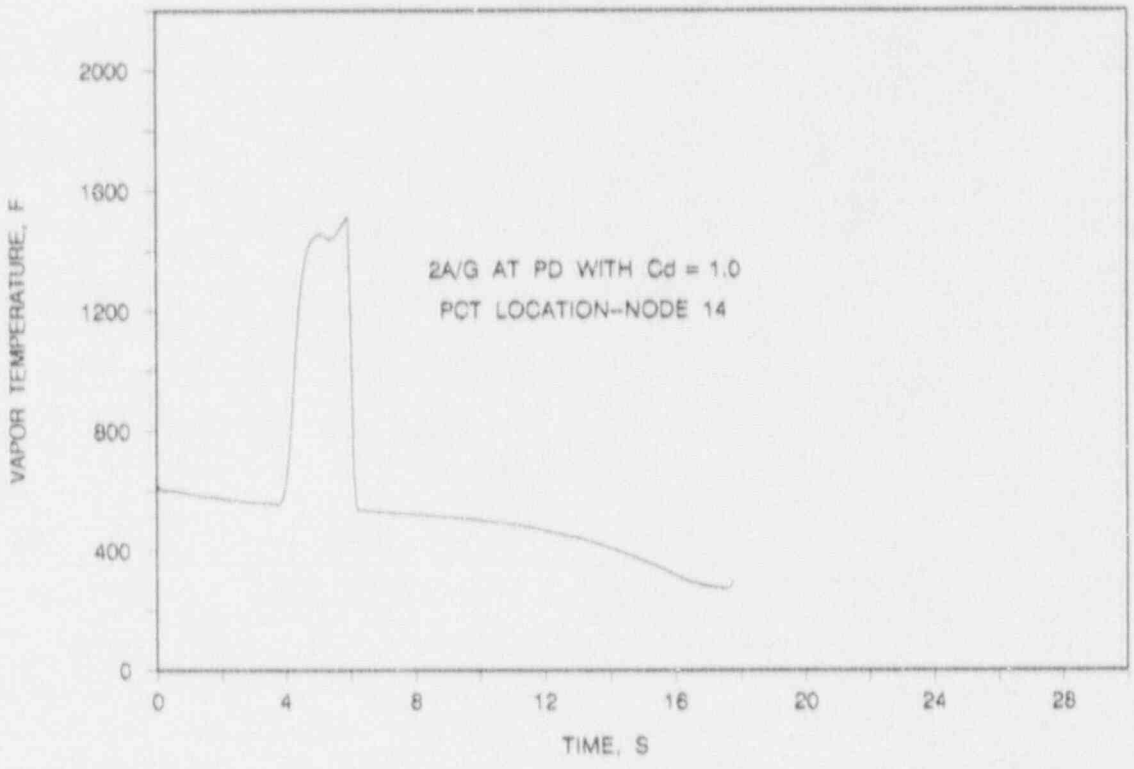

FIGURE 6-25b. MINIMUM ECCS STUDY - DECLB, Cd = 1.0
FLUID TEMPERATURE AT PCT LOCATION.

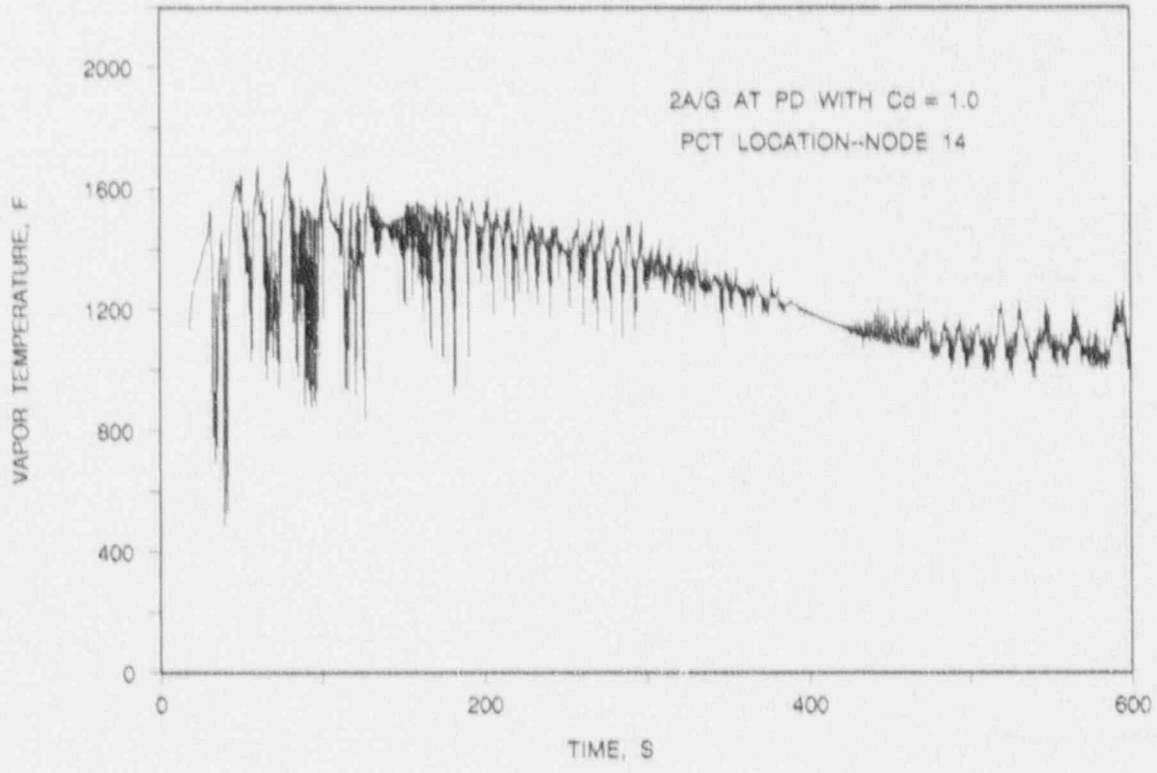

FIGURE 6-26. BREAK TYPE STUDY - SPLIT, Cd = 1.0
SYSTEM PRESSURE DURING BLOWDOWN.

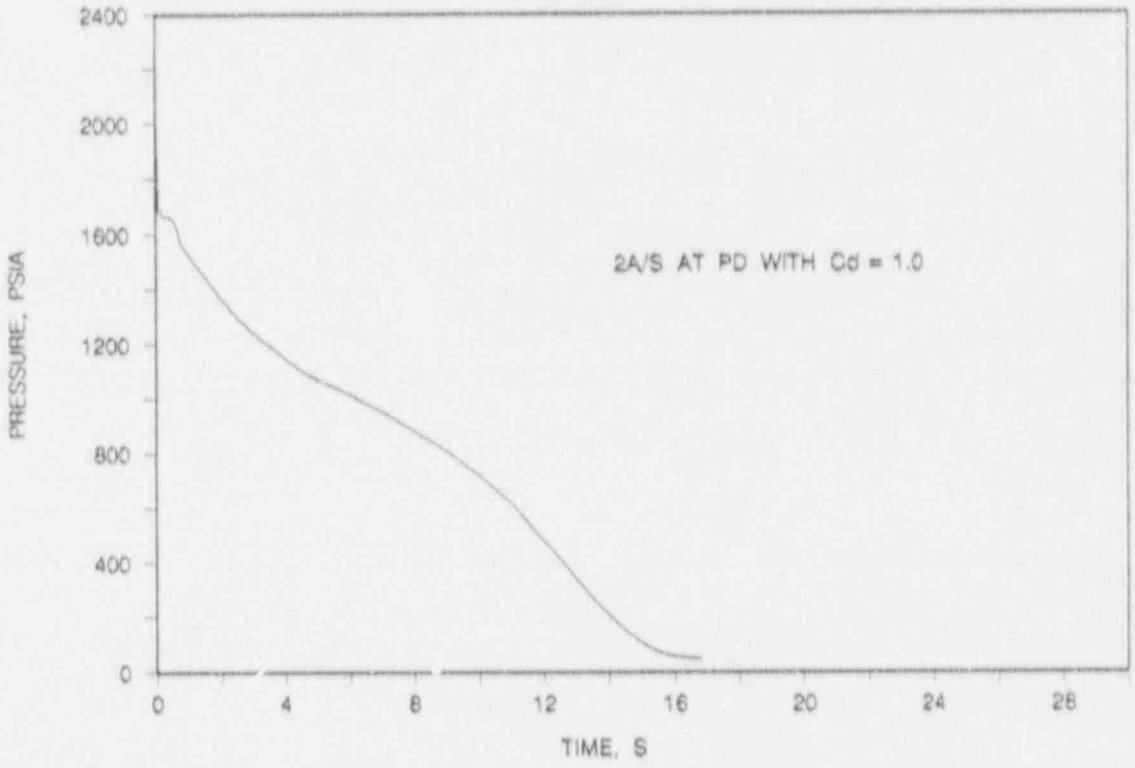

FIGURE 6-27. BREAK TYPE STUDY - SPLIT, Cd = 1.0
MASS FLUX DURING BLOWDOWN AT PEAK POWER LOCATION.

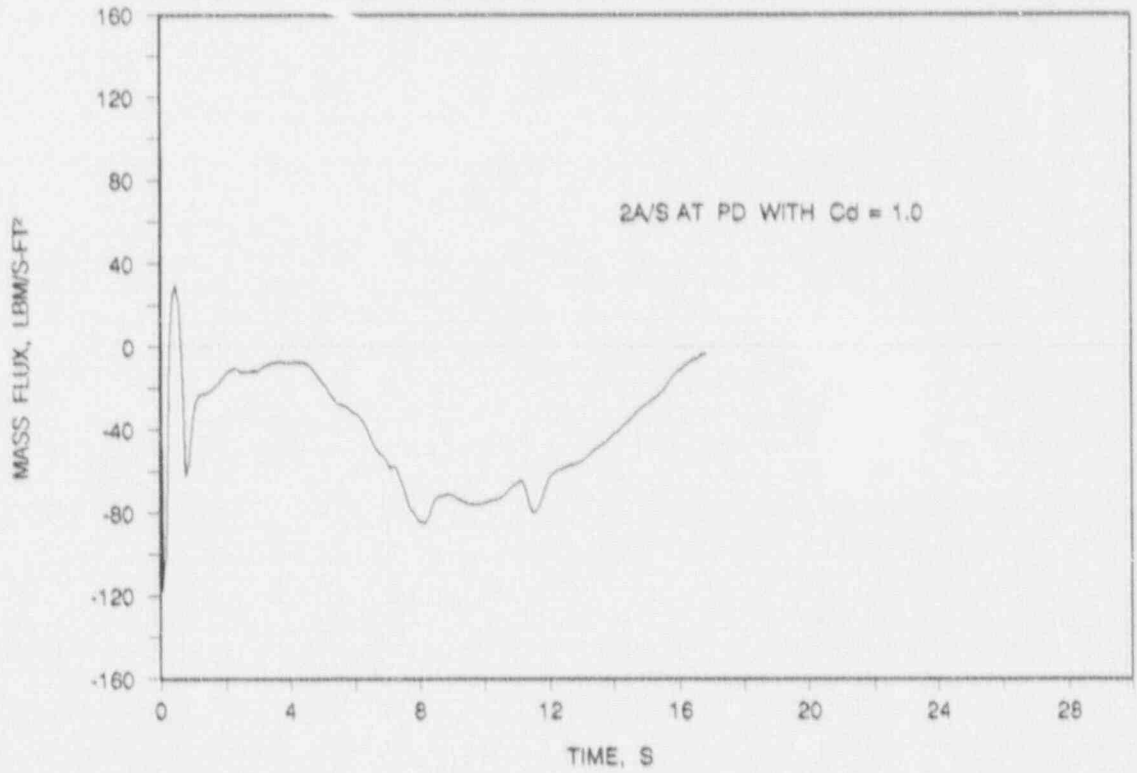

FIGURE 6-28. BREAK TYPE STUDY - SPLIT, Cd = 1.0
REFLOODING RATE.

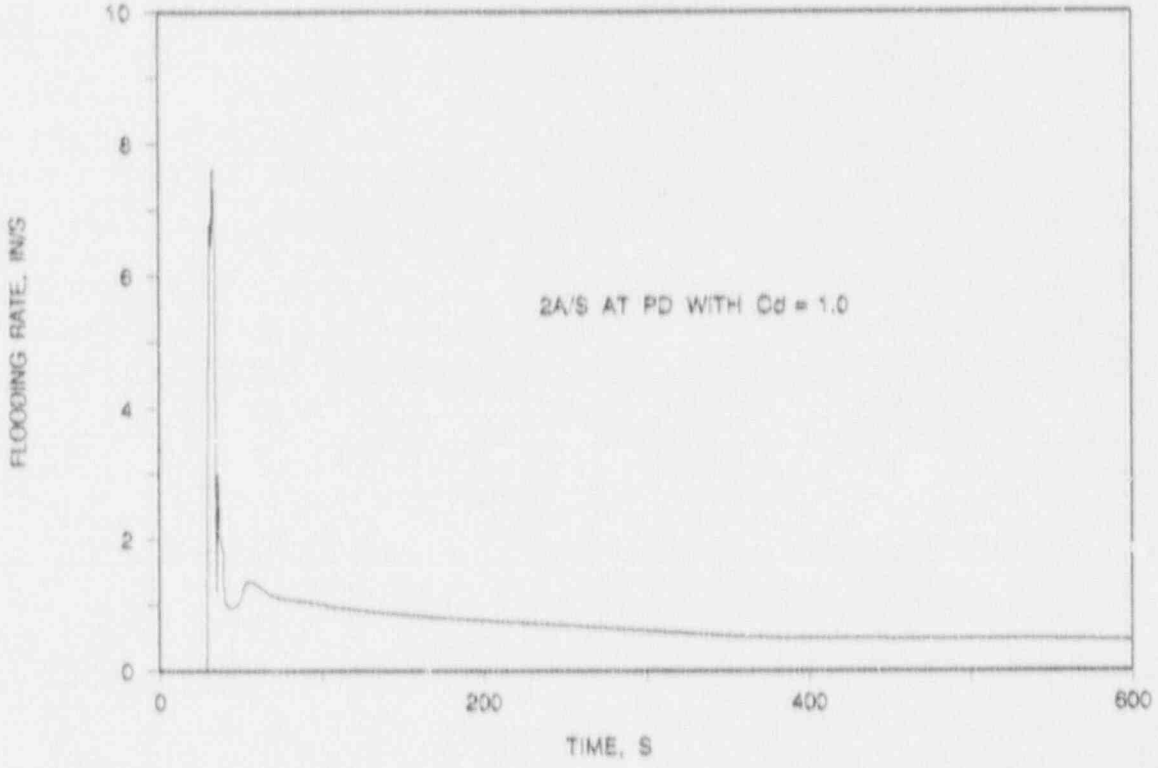

FIGURE 6-29. BREAK TYPE STUDY - SPLIT, Cd = 1.0
HEAT TRANSFER COEFFICIENT AT PEAK POWER LOCATION.

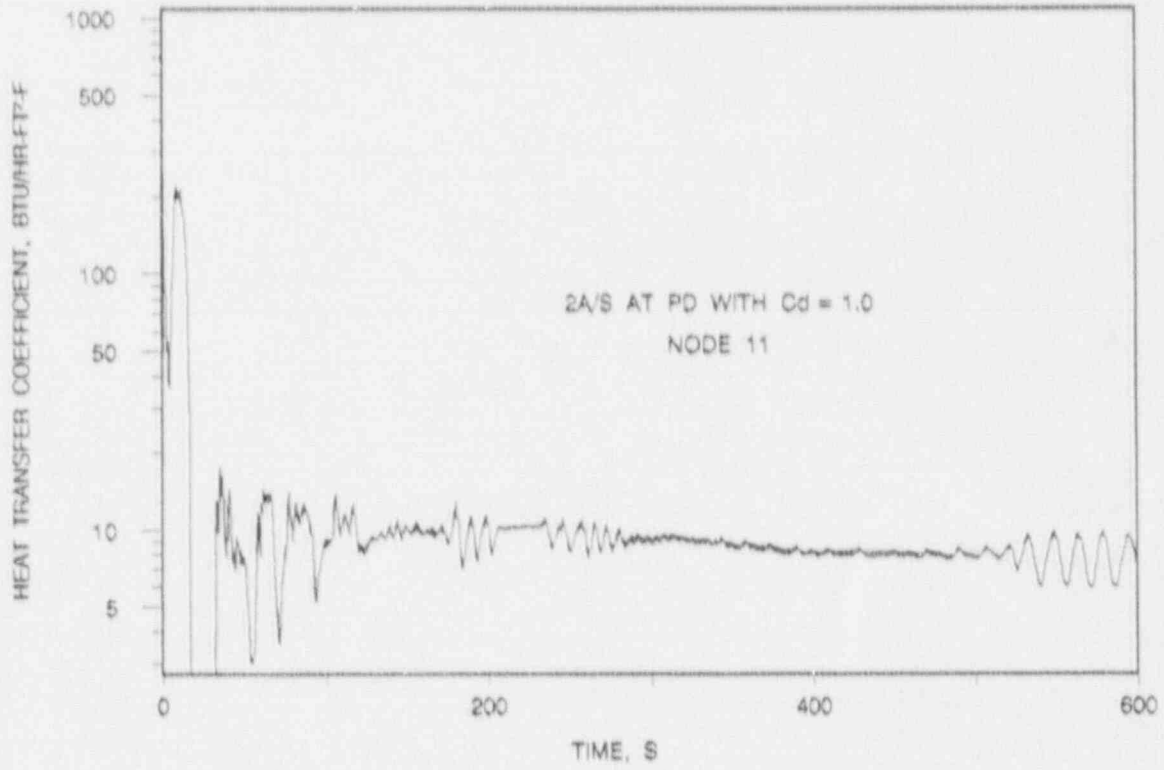

FIGURE 6-30. BREAK TYPE STUDY - SPLIT, Cd = 1.0
PEAK CLADDING TEMPERATURE.

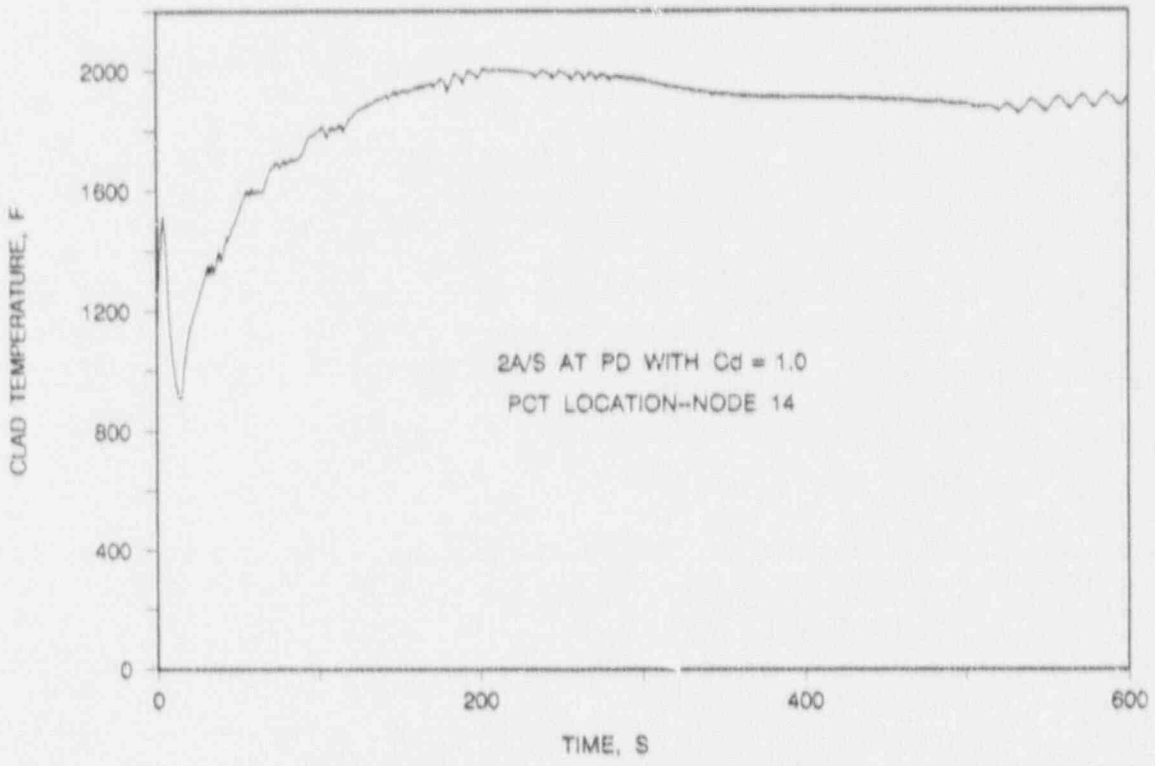

FIGURE 6-31. BREAK TYPE STUDY - SPLIT, Cd = 1.0
CLADDING TEMPERATURE AT RUPTURE LOCATION.

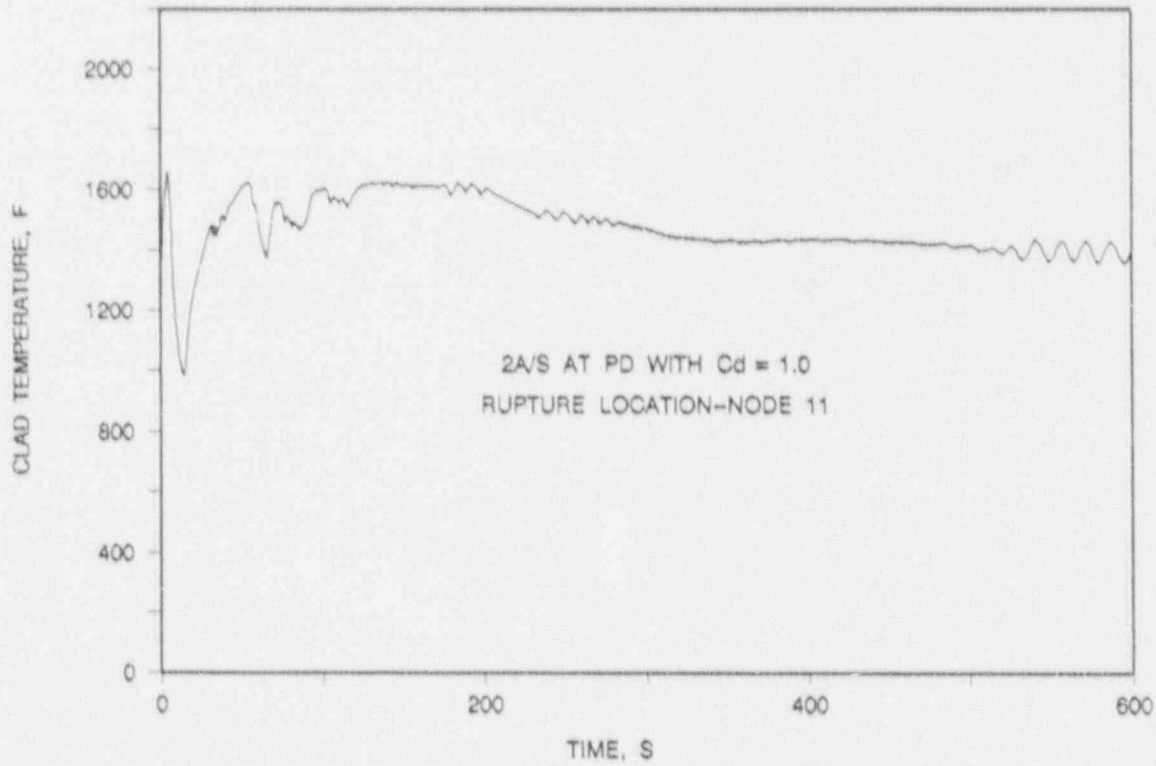

FIGURE 6-32. BREAK TYPE STUDY - SPLIT, Cd = 1.0
CLADDING TEMPERATURE ADJACENT TO RUPTURE LOCATION.

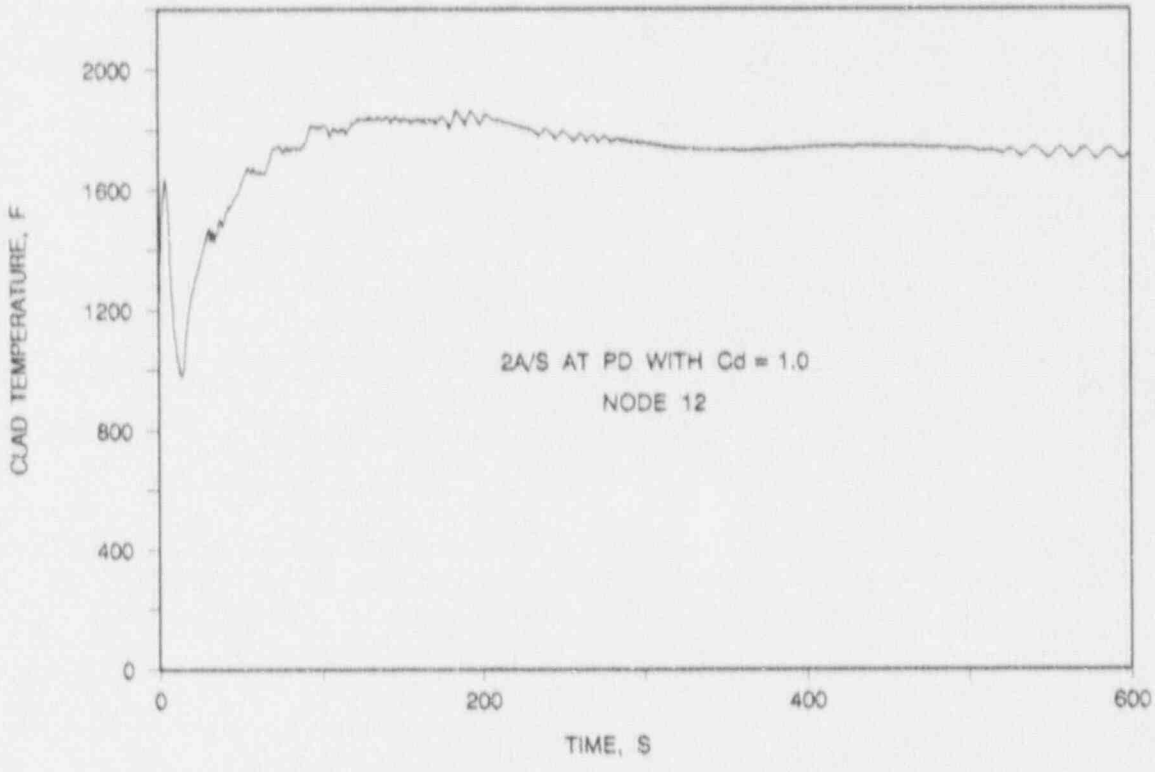

FIGURE 6-33a. BREAK TYPE STUDY - SPLIT, Cd = 1.0
FLUID TEMPERATURE AT PCT LOCATION.

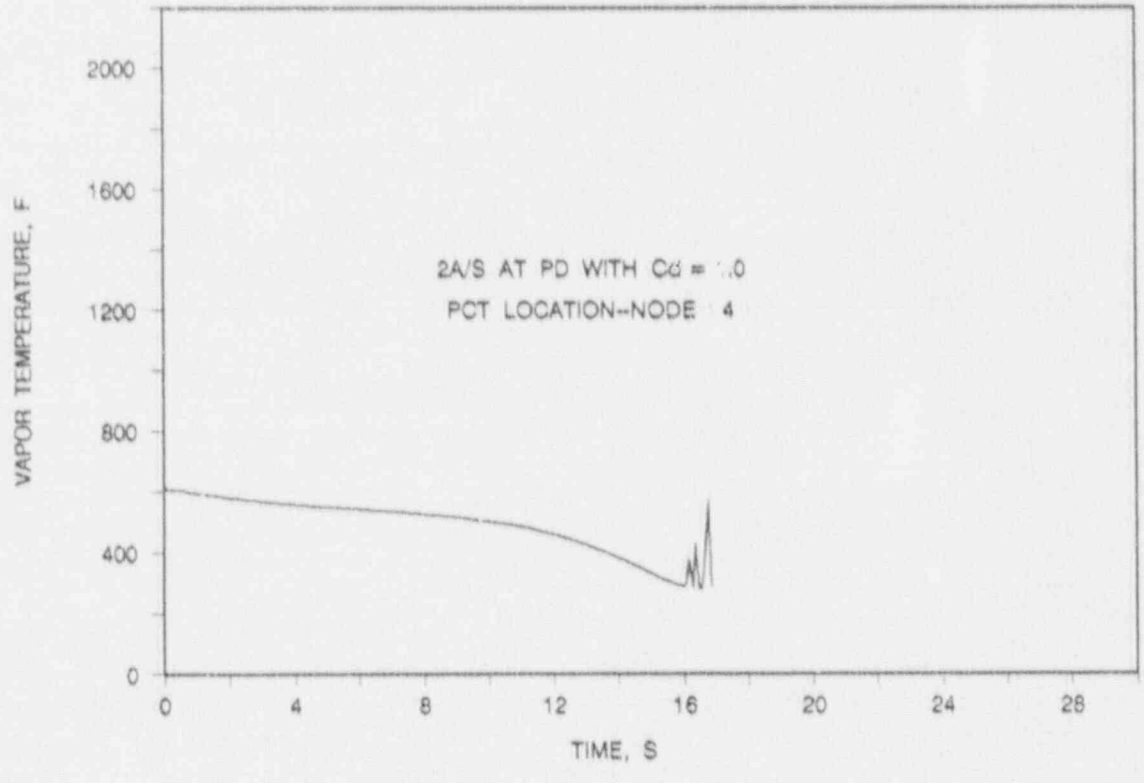

FIGURE 6-33b. BREAK TYPE STUDY - SPLIT, Cd = 1.0
FLUID TEMPERATURE AT PCT LOCATION.

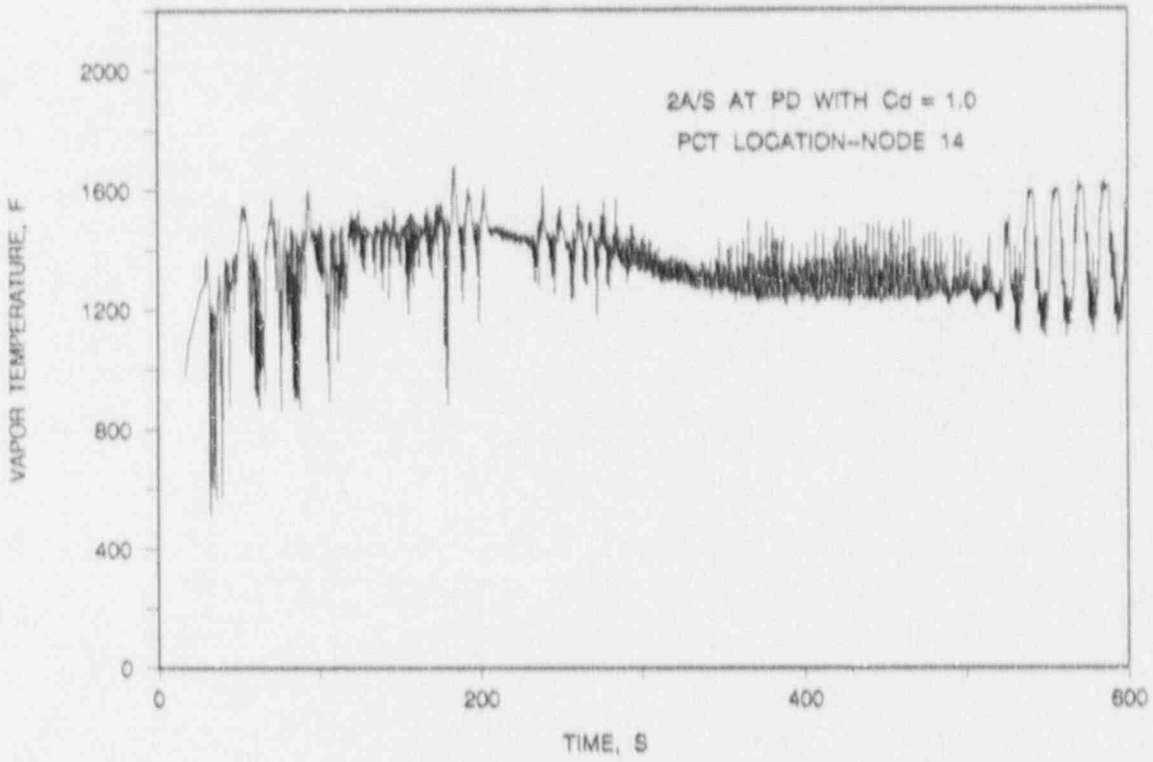

FIGURE 6-34. DISCHARGE COEFFICIENT STUDY - DECLB, Cd = 0.8
SYSTEM PRESSURE DURING BLOWDOWN.

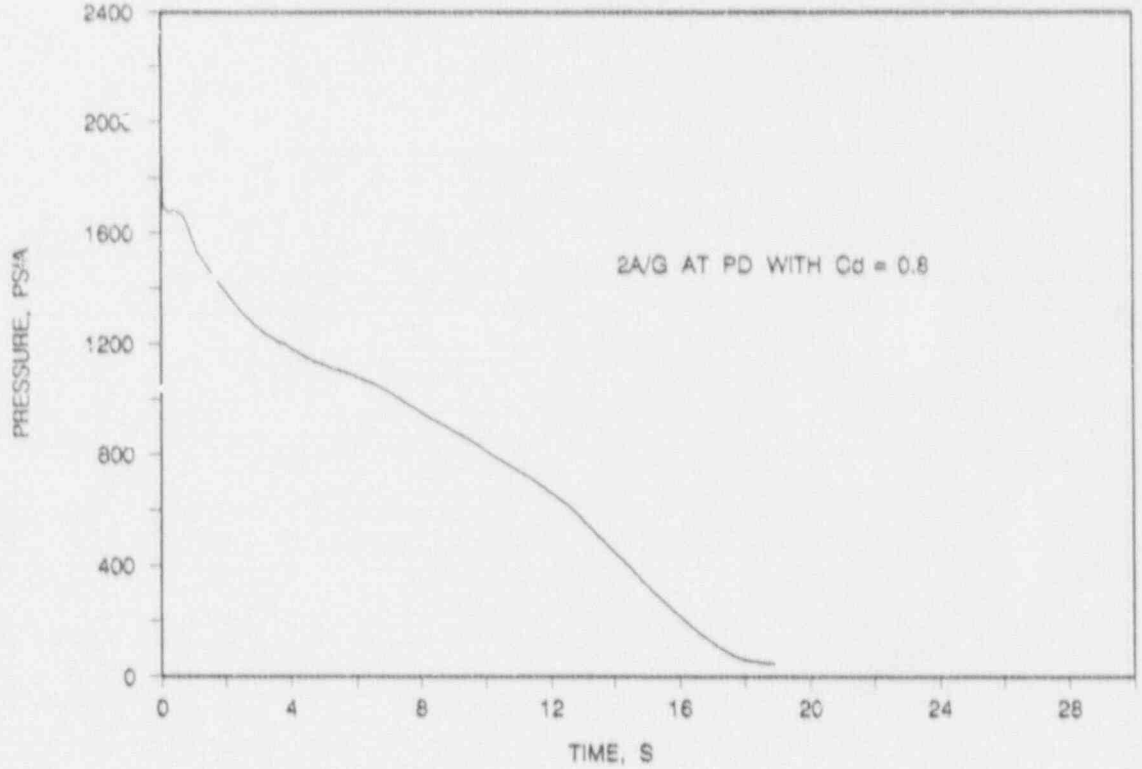

FIGURE 6-35. DISCHARGE COEFFICIENT STUDY - DECLB, Cd = 0.8
MASS FLUX DURING BLOWDOWN AT PEAK POWER LOCATION.

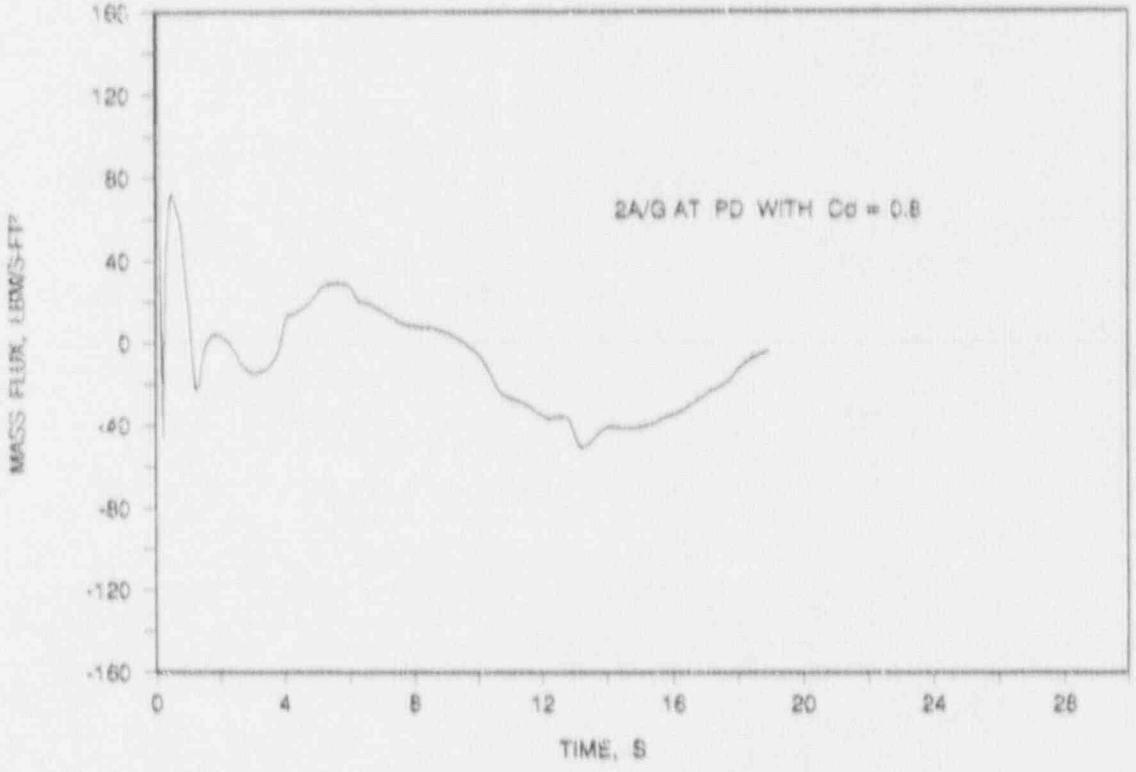

FIGURE 6-36. DISCHARGE COEFFICIENT STUDY - DECLB, Cd = 0.8
REFLOODING RATE.

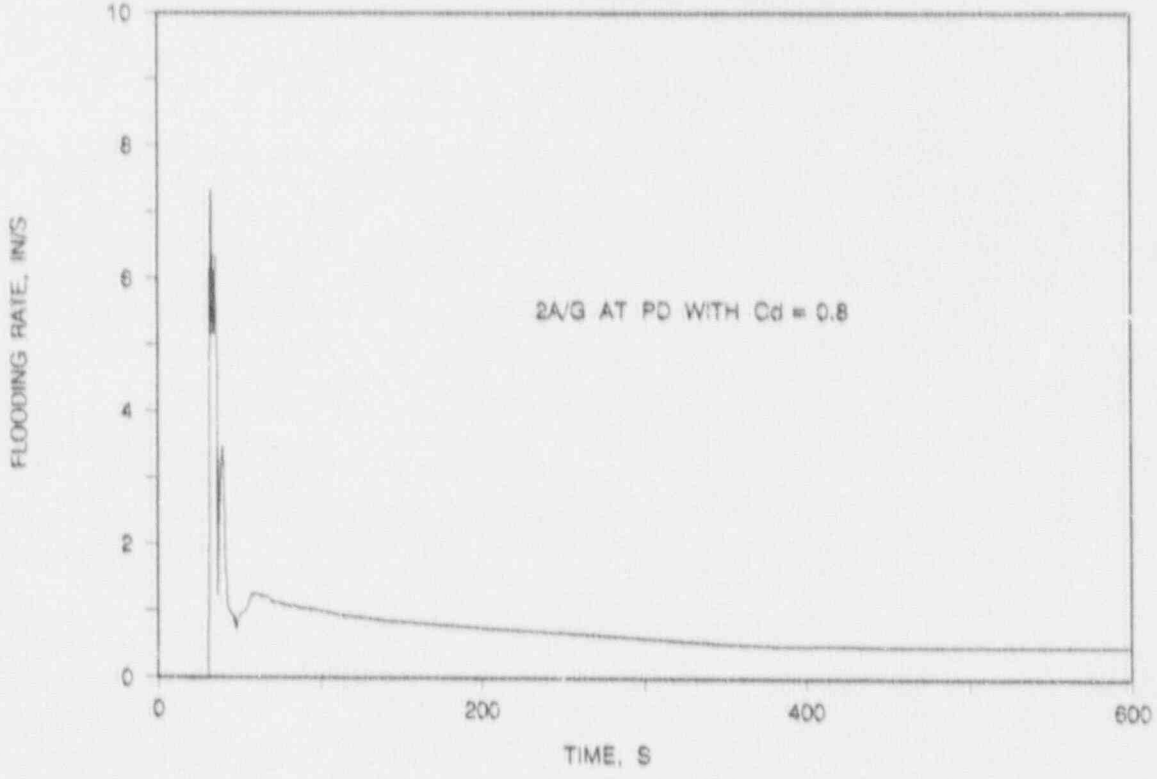

FIGURE 6-37. DISCHARGE COEFFICIENT STUDY - DECLB, Cd = 0.8
HEAT TRANSFER COEFFICIENT AT PEAK POWER LOCATION.

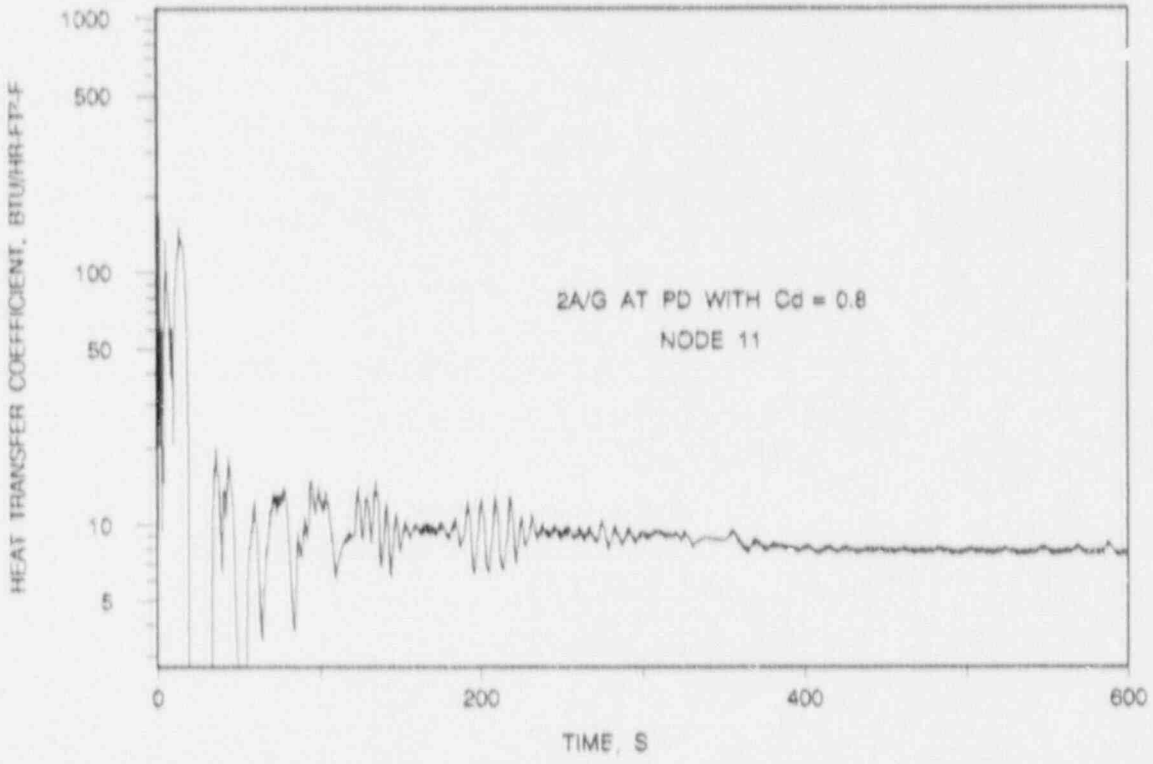

FIGURE 6-38. DISCHARGE COEFFICIENT STUDY - DECLB, Cd = 0.8
PEAK CLADDING TEMPERATURE.

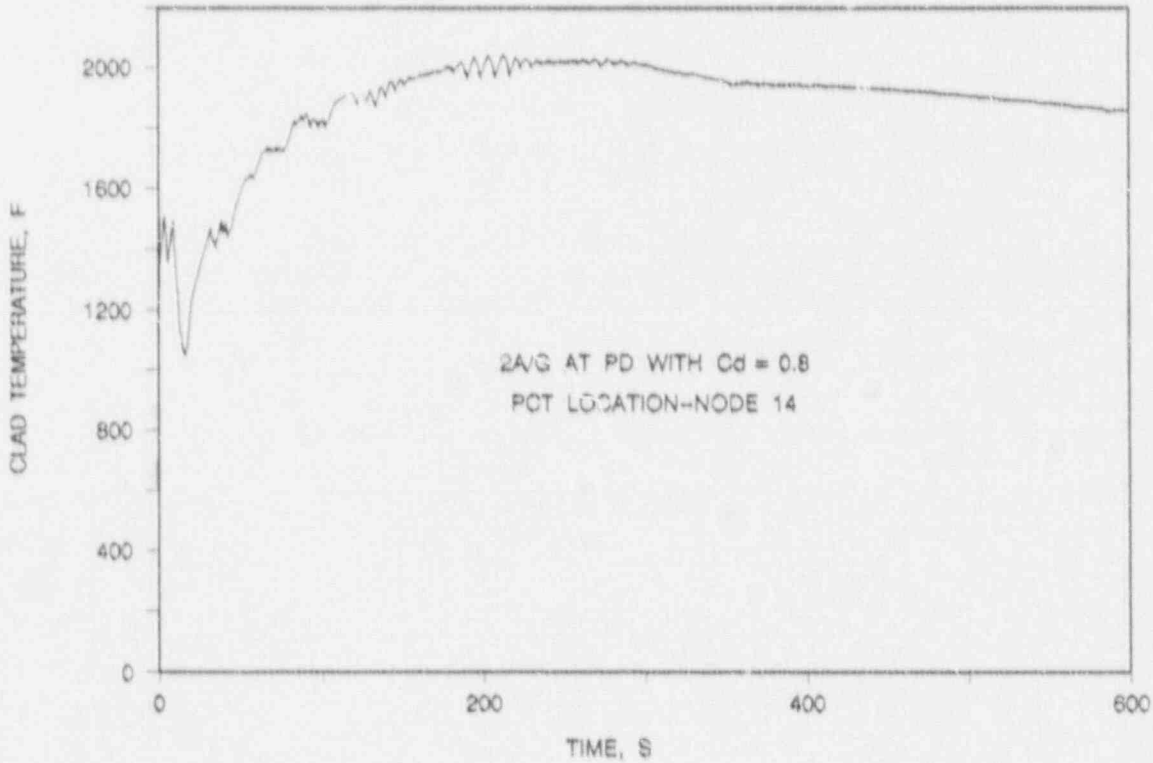

FIGURE 6-39. DISCHARGE COEFFICIENT STUDY - DECLB, Cd = 0.8
CLADDING TEMPERATURE AT RUPTURE LOCATION.

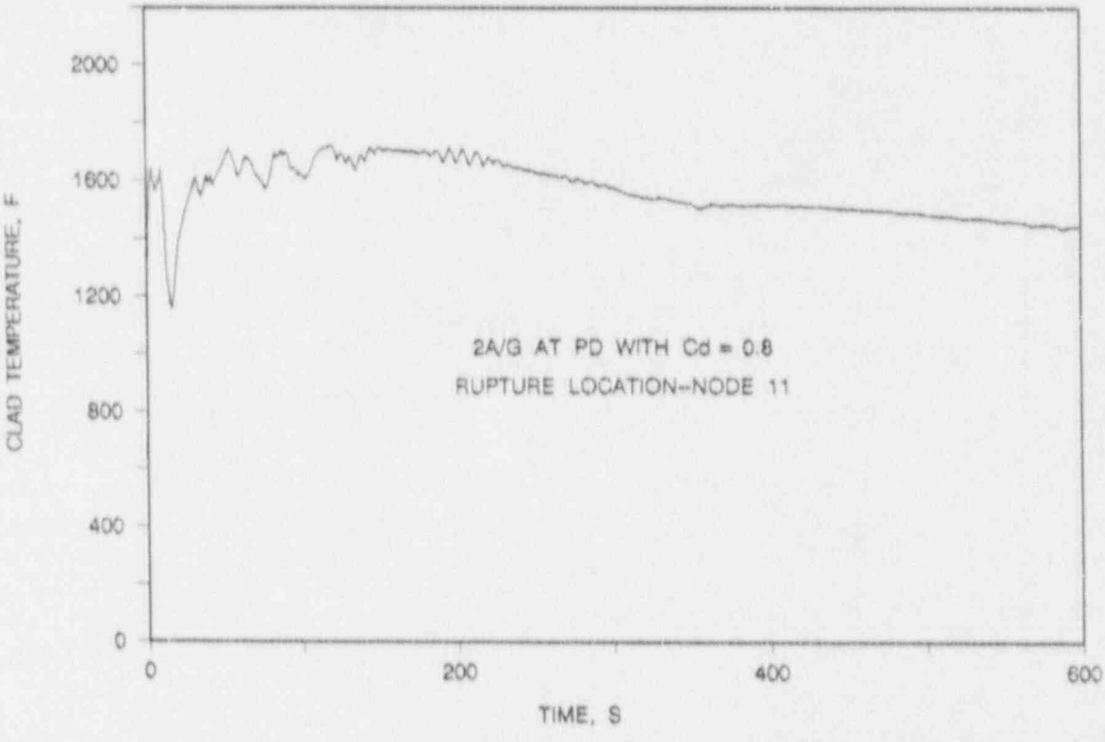

FIGURE 6-40. DISCHARGE COEFFICIENT STUDY - DECLB, Cd = 0.8
CLADDING TEMPERATURE ADJACENT TO RUPTURE LOCATION.

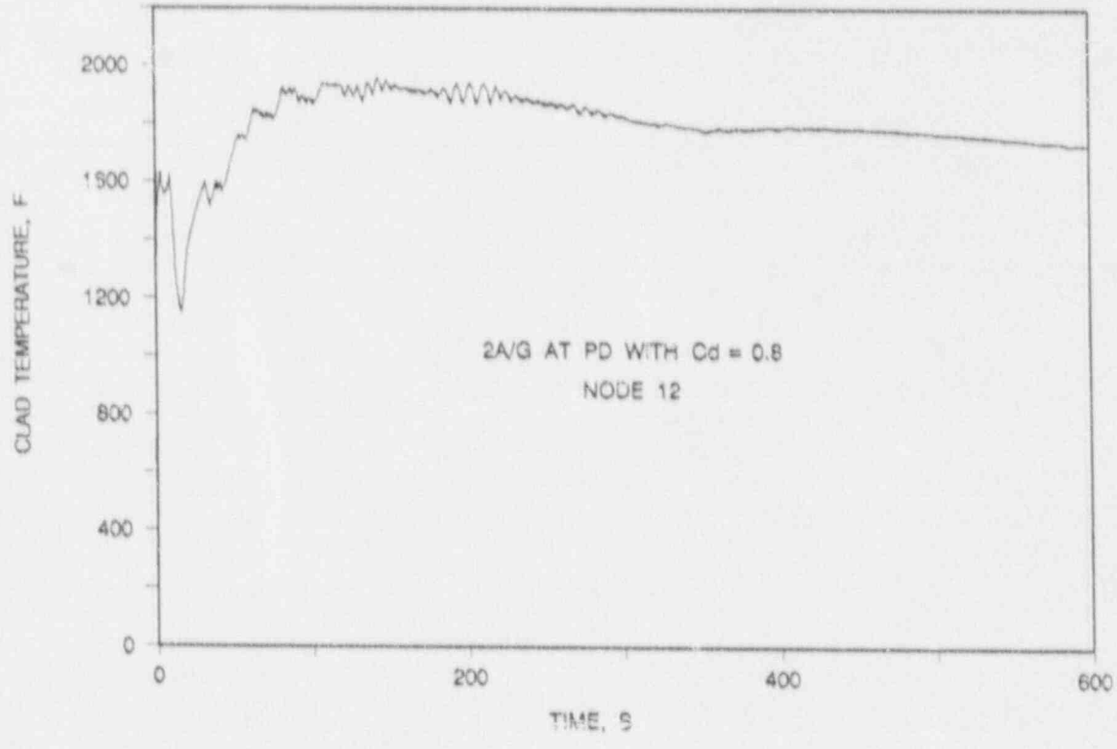

FIGURE 6-41a. DISCHARGE COEFFICIENT STUDY - DECLB, Cd = 0.8
FLUID TEMPERATURE AT PCT LOCATION.

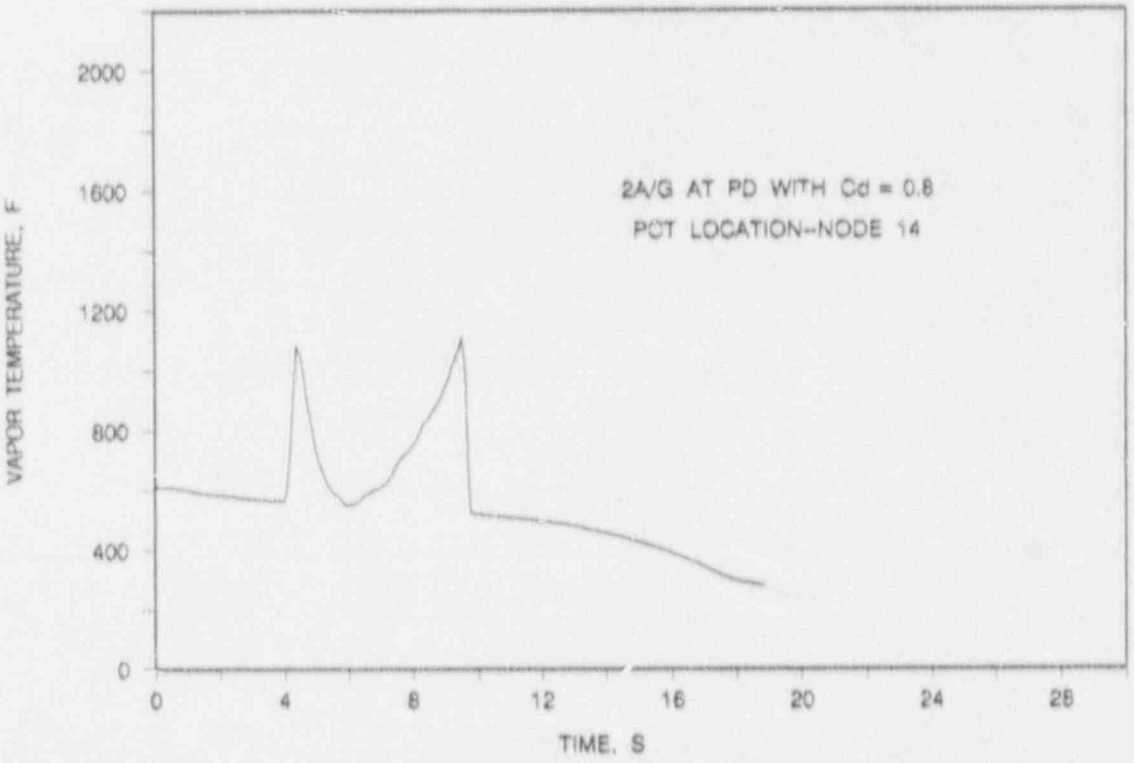

FIGURE 6-41b. DISCHARGE COEFFICIENT STUDY - DECLB, Cd = 0.8
FLUID TEMPERATURE AT PCT LOCATION.

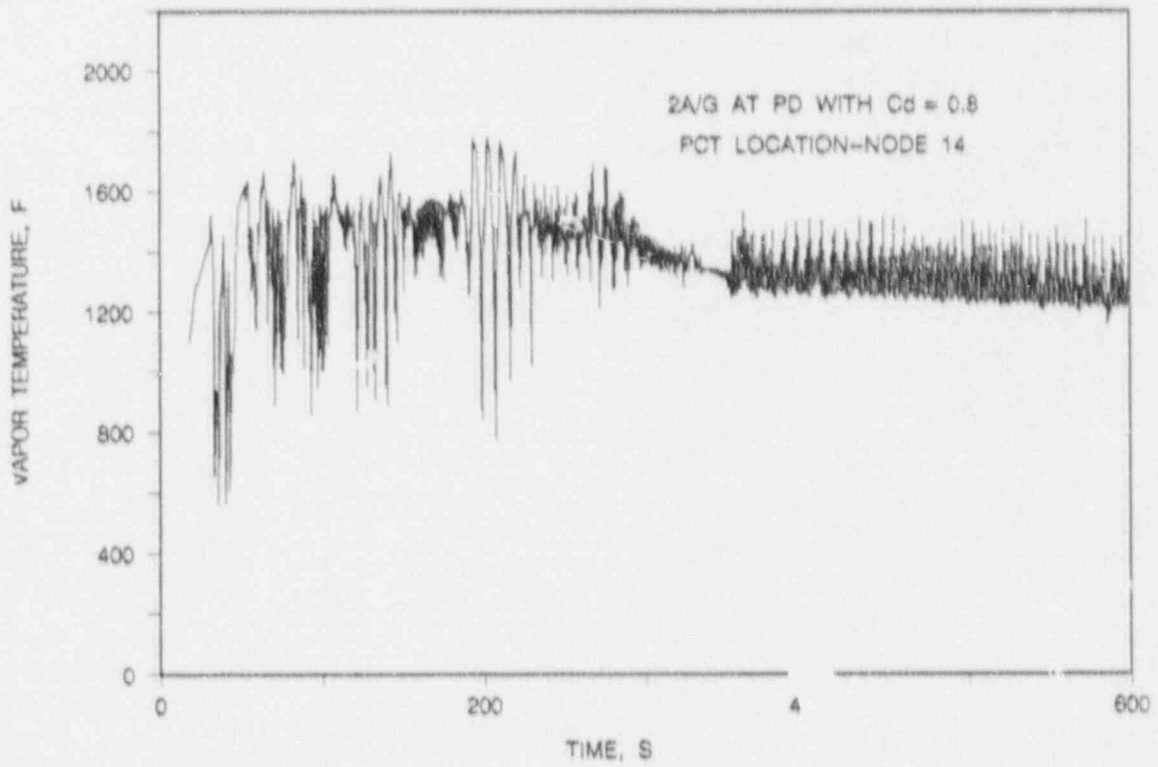

FIGURE 6-42. DISCHARGE COEFFICIENT STUDY - DECLB, Cd = 0.6
SYSTEM PRESSURE DURING BLOWDOWN.

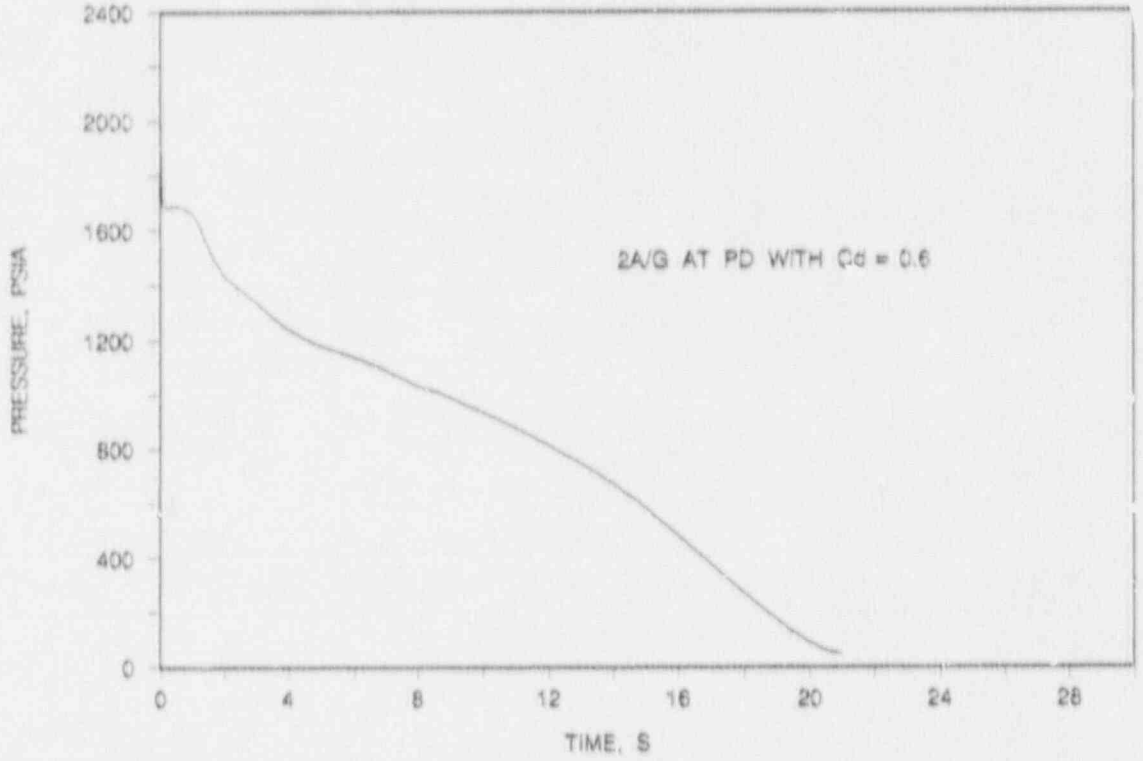

FIGURE 6-43. DISCHARGE COEFFICIENT STUDY - DECLB, Cd = 0.6
MASS FLUX DURING BLOWDOWN AT PEAK POWER LOCATION.

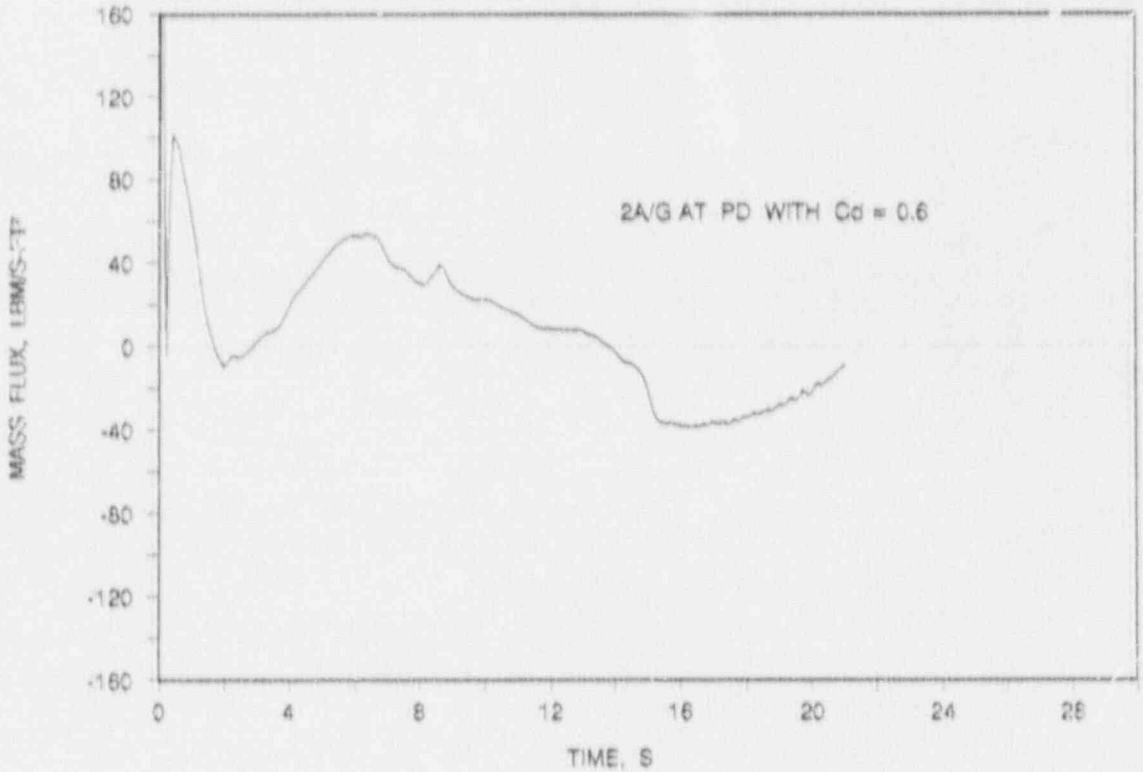

FIGURE 6-44. DISCHARGE COEFFICIENT STUDY - DECLB, Cd = 0.6 REFLOODING RATE.

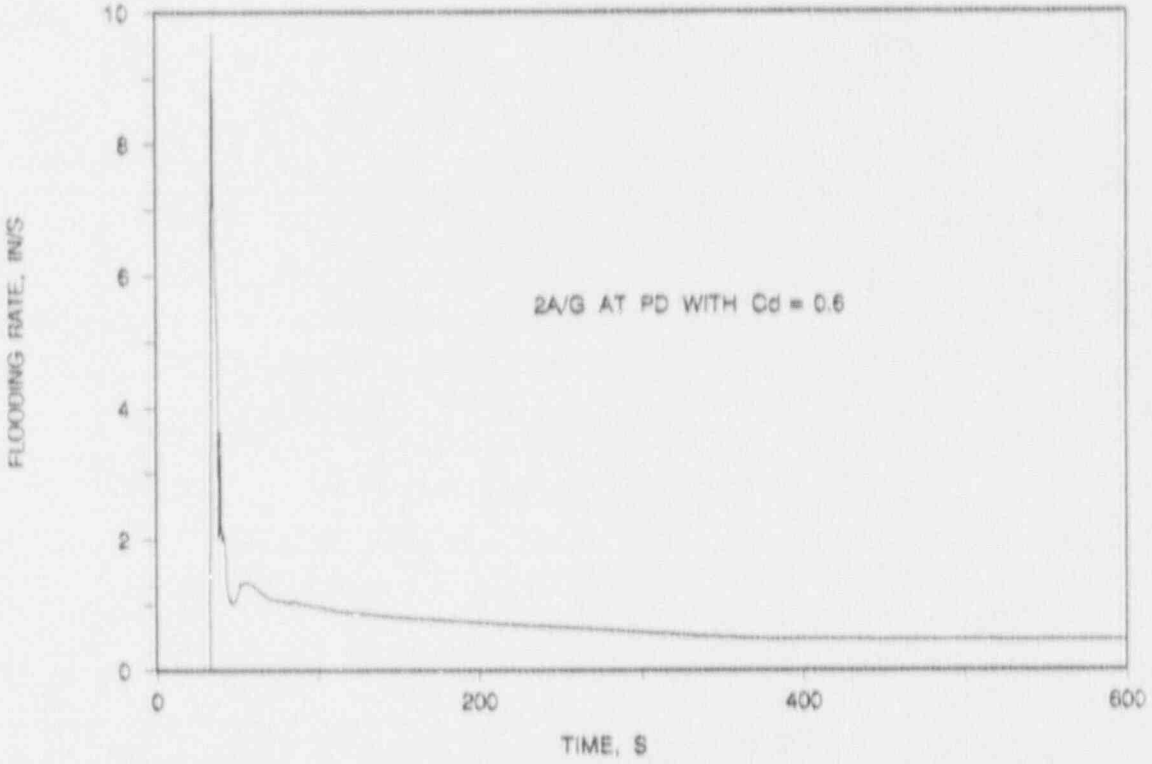

FIGURE 6-45. DISCHARGE COEFFICIENT STUDY - DECLB, Cd = 0.6 HEAT TRANSFER COEFFICIENT AT PEAK POWER LOCATION.

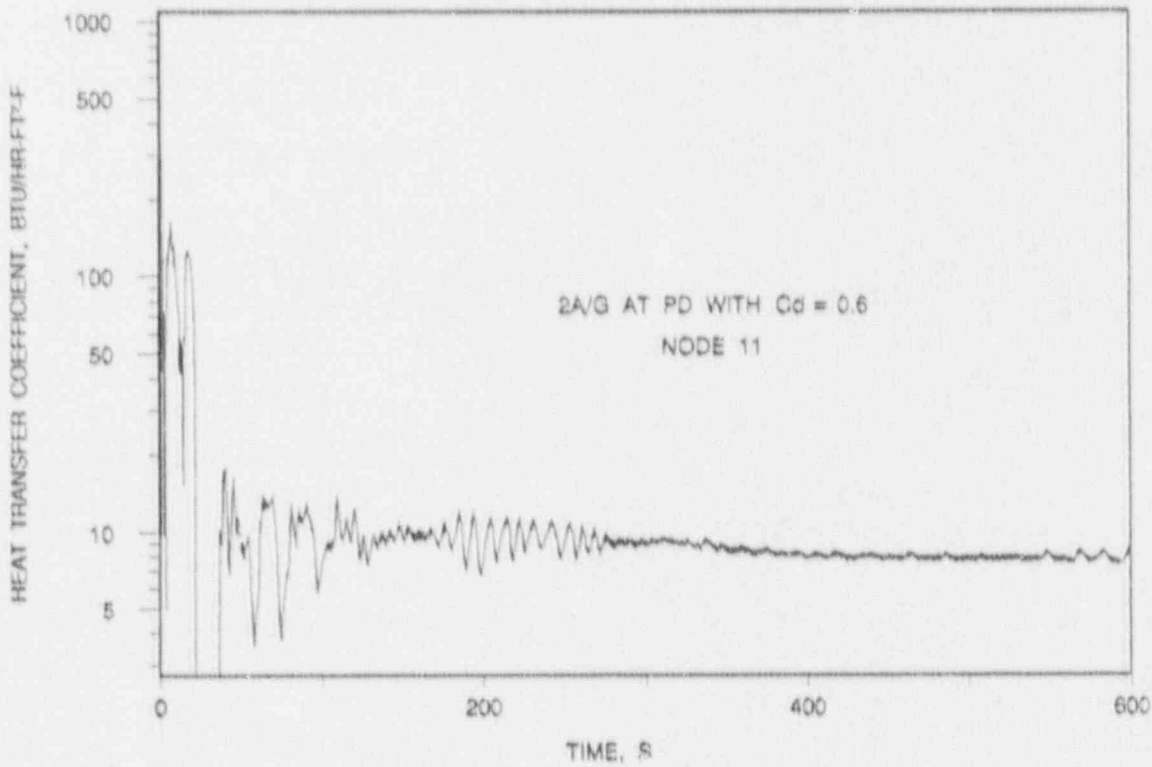

FIGURE 6-46. DISCHARGE COEFFICIENT STUDY - DECLB, Cd = 0.6
PEAK CLADDING TEMPERATURE.

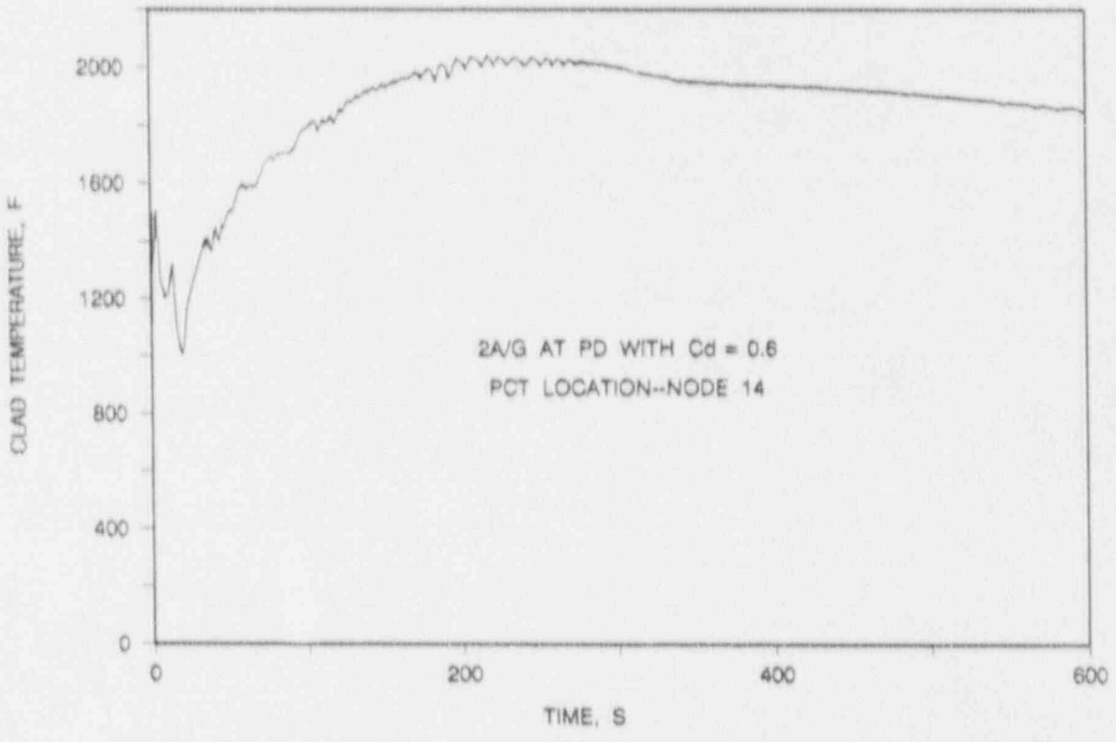

FIGURE 6-47. DISCHARGE COEFFICIENT STUDY - DECLB, Cd = 0.6
CLADDING TEMPERATURE AT RUPTURE LOCATION.

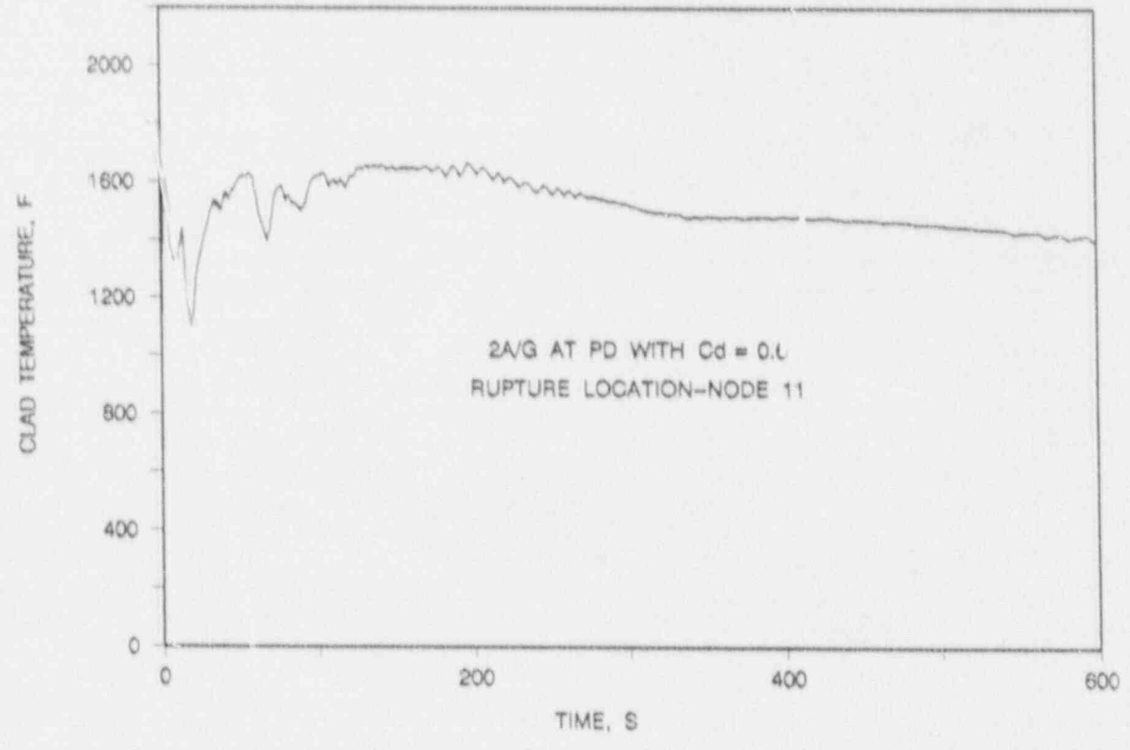

FIGURE 6-48. DISCHARGE COEFFICIENT STUDY - DECLB, Cd = 0.6
CLADDING TEMPERATURE ADJACENT TO RUPTURE LOCATION.

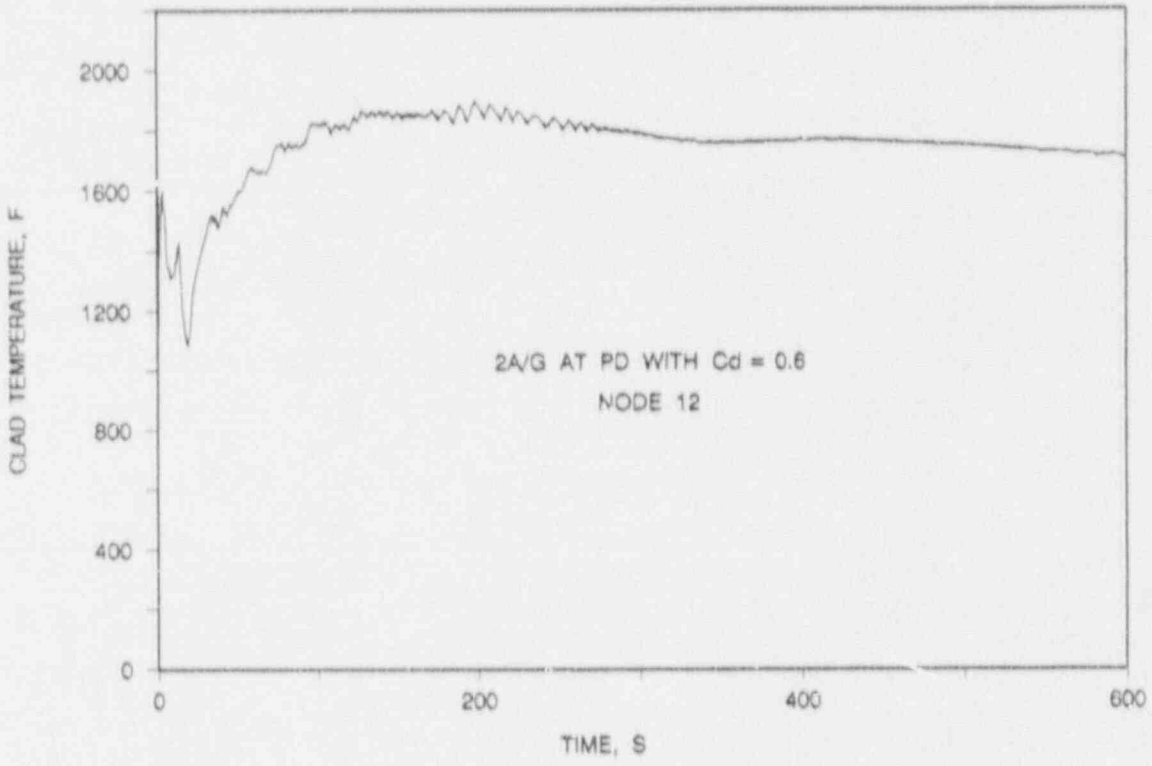

FIGURE 6-49a. DISCHARGE COEFFICIENT STUDY - DECLB, Cd = 0.6
FLUID TEMPERATURE AT PCT LOCATION.

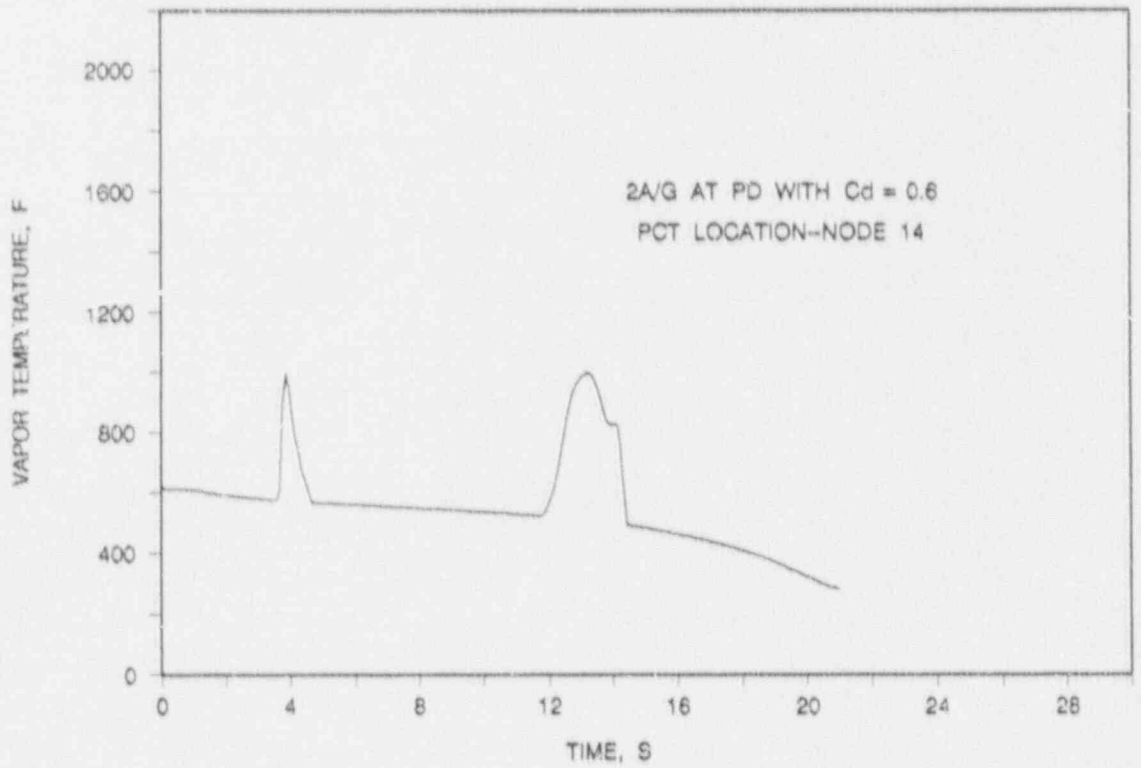

FIGURE 6-49b. DISCHARGE COEFFICIENT STUDY - DECLB, Cd = 0.6
FLUID TEMPERATURE AT PCT LOCATION.

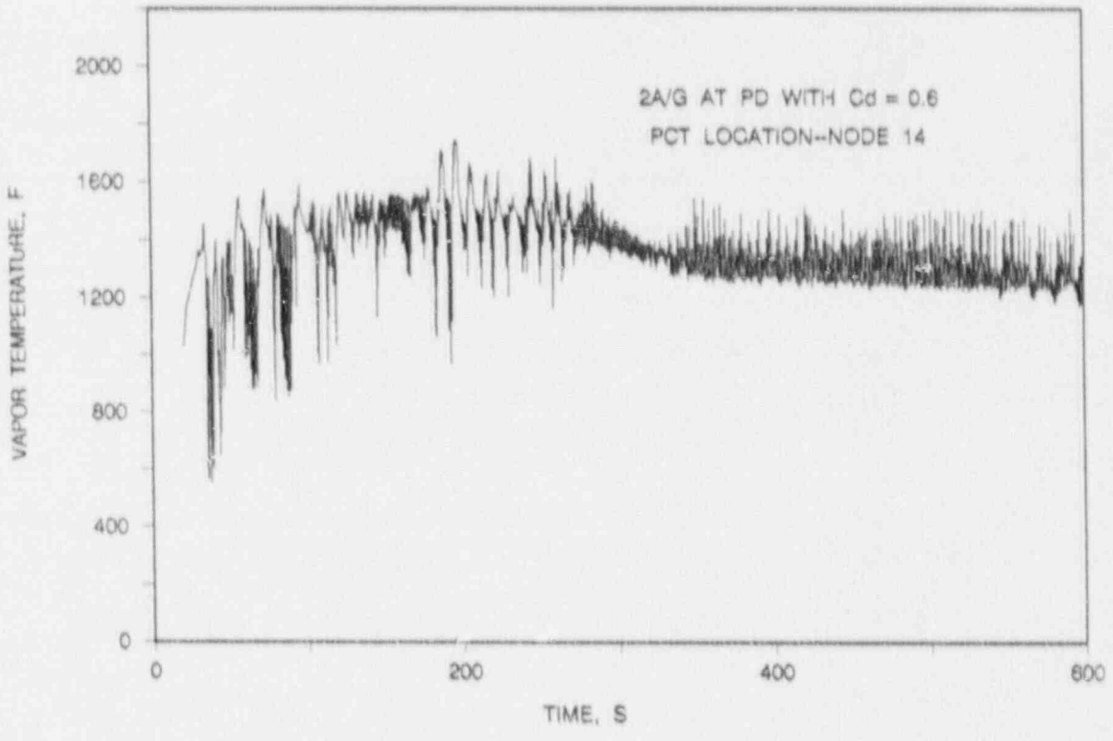

7. LOCA Limits

The LOCA evaluation is completed with a set of analyses done to show compliance with 10 CFR 50.46 for the core power and peaking that will be taken as the limiting LOCA conditions for core operation, that is, the LOCA limits. The term limit is applied because these cases are run at the limit of allowable local power operation. Actually, these LOCA evaluations serve as the bases for the allowable local power. As such, the LOCA limits calculations comprise the cases that are used to demonstrate compliance of the reload fuel cycles and peaking limits to the criteria of 10 CFR 50.46. Five runs are made at differing axial elevations such that a curve of allowable peak linear heat rates as a function of elevation in the core can be constructed or, in this case, confirmed. This curve becomes a part of the plant technical specifications, and plant operation is controlled such that the local peaking and power do not exceed the allowable values.

7.1 LOCA Limits Dependencies

The absolute LOCA limits to power and peaking for each elevation in the core can be determined through repeated calculations at each elevation, with successively higher local power levels, until the analysis shows one or more of the applicable acceptance criteria to be exceeded. The highest linear heat rate for which the criteria are not exceeded is the absolute LOCA limit for a particular elevation. The more practical approach, the one adopted for this report, assumes a set of peaking limits at a given power level that have been determined to be acceptable for fuel cycle design and plant operations purposes. The LOCA limits analyses are then done to confirm that the assumed limits will meet the applicable criteria.

Figure 7-1 shows the axial power and peaking selected and confirmed as applicable to the Trojan plant for operation with Mark-BW fuel.

With the axial power ar peaking dependency established, LOCA calculations are performed with the core power level and total peaking initialized at different positions on the curve to demonstrate that these peaking limitations assure compliance with 10 CFR 50.46. Should the results not comply, the allowed peaking is reduced, and the analysis is repeated until acceptable results can be obtained. Likewise, if the results show large margins of compliance, the peaking may be increased to provide additional operational flexibility. For these analyses, neither of these steps was taken.

An additional condition assumed in these analyses is that the allowable peaking will be dependent on fuel assembly burnup in accordance with Figure 7-2. This limitation is made necessary because, at burnups above 41,000 Mwd/MTu, the initial fuel enthalpy and internal pressure can become a more severe combination than at beginning-of-life. By assuring that the local heating rates will be limited to those shown in Figure 7-2, the reduction in power compensates for the increases in fuel temperature and pin pressure such that beginning-of-life conditions remain the most severe (This is discussed in greater detail in Section 5.2.). Therefore, Figure 7-2 is a limit of operation for the Mark-BW fuel. The limit is checked during the fuel cycle design process. However, at the high burnup at which the limit is imposed there should be no restrictions on core operation, because the highly depleted fuel is unlikely to reach the limit within the operational envelopes of the plant Technical Specifications.

7.2 LOCA Limits Results

To validate Figure 7-1, five separate LOCA c culations were performed. Power peaks were run centered at the middle of the second through the sixth grid spans. Figure 7-3 shows the axial power shapes evaluated. For all cases, the radial power peaking was 1.67. The combination of the axial peaking of Figure 7-3 and a

1.67 radial yields the total peaking at the corresponding elevation shown in Figure 7-1.

The results of the calculations are tabulated in Table 7-1 and shown in Figures 7-4 through 7-23. The figures comprise five sets with four figures in each set. The four figures of each set show (1) the mass flux at the elevation of peak power, (2) the cladding temperature for three different locations on the pin, (3) the heat transfer coefficient at the location of highest cladding temperature, and (4) the distribution of cladding oxidation along the pin. Only one mass flux plot is provided for each case because the axial variations in mass flux are not strong.

To demonstrate the cladding temperature results, three curves are presented for each case. Temperature histories are shown for the rupture location, for the node adjacent to the rupture, and for the high temperature node in an adjacent grid span. For power distributions peaked toward the middle of the core, the rupture location is almost certain to correspond to the location of peak power. Near the time of rupture, the portion of the pin immediately above the rupture site will be at nearly the same temperature. Following rupture, the burst location cools quickly as the cladding pulls away from the fuel, and the area for heat transfer is increased. Due to axial heat conduction in the cladding and the effect of the rupture on flow conditions, the cooling in the node just above the rupture is substantially improved. This means that although one of the nodes in the adjacent grid span is at a lower power, it can develop as the location of the highest cladding temperature.

The heat transfer coefficient (HTC) is shown for the peak cladding temperature location. HTC variations with elevation are as expected (see Figures 6-6 through 6-8), such that the HTC from one elevation reasonably characterizes the other elevations. The last figure in each set shows the local oxide thickness as a function of

elevation for the fuel pin. Each figure shows total oxidation including that assumed prior to the start of the accident. Oxidation up to the time the cladding falls below 1000 F or the elevation has been quenched, as measured by REFLOOD3B, is included. The large variations of the resultant curve reflect the relatively lower cladding oxidation in the vicinity of the grid and rupture locations.

2.9-ft Peak Power Case

In this case, the axial power shape is peaked well below the core midplane, and the cladding temperature responses differ accordingly from those calculated in the 4-, 6-, and 8-ft cases. The peak power locations on the rod are cooled rapidly during reflood and have not reached temperatures sufficient to cause a rupture by the time of temperature turnaround. Therefore, the rupture occurs in Node 8, the center node of the grid span above the location of peak power. This region of the core is also cooled rapidly, and the peak cladding temperature occurs in the grid span above the ruptured location. Although the power at the midplane is about 80 percent of that at the peak power location, the central node in the mid-core grid span produces the highest cladding temperature, 1894 F. The highest local oxidation, 3.4 percent, occurs at the ruptured location. The whole core oxidation calculated for this LOCA is 0.43 percent.

4.6-ft Peak Power Case

With the power peaked at 4.6 feet, the cladding temperature responses resemble closely those obtained for the other two mid-core peaks. The rupture occurs at the location of peak power. The node above the rupture experiences increased cooling post-rupture, and the peak cladding temperature occurs in the downstream grid span (Node 11). The temperature at this location is about 200 F above the temperatures near the rupture location. The highest

local oxidation, 4.8 percent, also occurs at the mid-core elevation. The whole core oxidation during this LOCA is 0.63 percent.

6.3-ft Peak Power Case

This case is the same as the worst case evaluated in Chapter 6 and is repeated here for completeness of this chapter. For a peak power situated at the core midplane, the cladding temperature response corresponds to that described in the previous paragraph. The rupture is at the location of peak power. For this case, the post-rupture cooling above the rupture, although less effective than in the 4.6-ft case, also cools the adjacent node sufficiently such that the peak cladding temperature occurs in the downstream grid span (Node 14). As shown in Figure 7-9, the temperature, 2047 F, is only slightly higher, by about 80 F, than in the node adjacent to the rupture. The highest local oxidation in this case, 6.8 percent, occurs for the peak cladding temperature node. The whole core oxidation is 0.79 percent.

8.0-ft Peak Power Case

With the power peaked toward the outlet, the grid span that will produce high cladding temperatures lies below the location of peak power. The rupture occurs at the location of peak power and the peak cladding temperature, 1993 F, is predicted to occur in the grid span below the peak power location. The power shape for this case causes the node adjacent to the rupture location (Node 15) and the node at which the peak cladding temperature occurs (Node 12) to have about the same power. Rupture-induced cooling effects do not substantially improve the heat transfer in the node downstream of the rupture. Thus, there is nearly the same reflood heat transfer at Nodes 15 and 12, and both locations achieve a peak temperature of 1993 F. Node 12 is listed as the location of PCT because it is

higher by a few tenths of a degree. The highest local oxidation is 5.3 percent, and the whole core oxidation is 0.74 percent.

9.7-ft Peak Power Case

In accordance with the axial dependency of power peaking shown in Figure 7-1, this case is run at a slightly lower total peaking than the other four cases. The location of peak power is in Node 17, which is also the rupture location. With the reduction in peaking and the severe outlet shape, the power in Node 15 is only slightly less than that in Node 17. Node 15 is at the end of a grid span and experiences little, if any, grid effects. Hence, the peak cladding temperature of 2119 F occurs at this location. Because the power drops off sharply above Node 17, and rupture effects provide some cooling, the temperature in Node 18 peaks at 1960 F about 60 F below the PCT. The peak local oxidation is 7.4 percent and the whole core oxidation is 0.84 percent.

7.3 Compliance to 10 CFR 50.46

The LOCA limits calculations directly demonstrate compliance to two of the criteria of 10 CFR 50.46 and serve as the basis for demonstrating compliance with two others. As shown in the figures and in Table 7-1, the highest peak cladding temperature, 2119 F, and the highest local oxidation, 7.4 percent, are below the 2200 F and 17 percent criteria. Chapter 8 documents compliance with the whole core oxidation limit based on the local oxidations calculated for these evaluations, and Chapter 9 documents that the core geometry remains amenable to cooling based on the deformations predicted for the LOCA limits studies.

FIGURE 7-3. LOCA LIMIT STUDY - AXIAL POWER SHAPES.

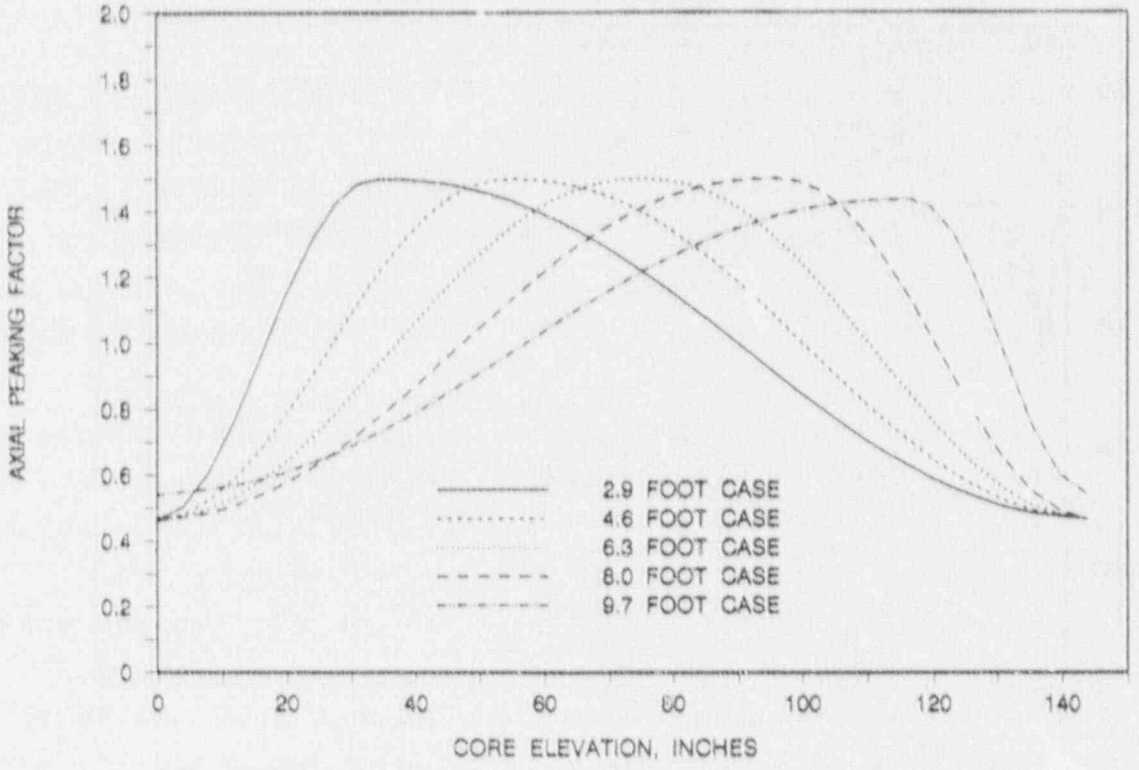

FIGURE 7-4. LOCA LIMITS STUDY - 2.9 FOOT CASE
MASS FLUX DURING BLOWDOWN AT PEAK POWER LOCATION.

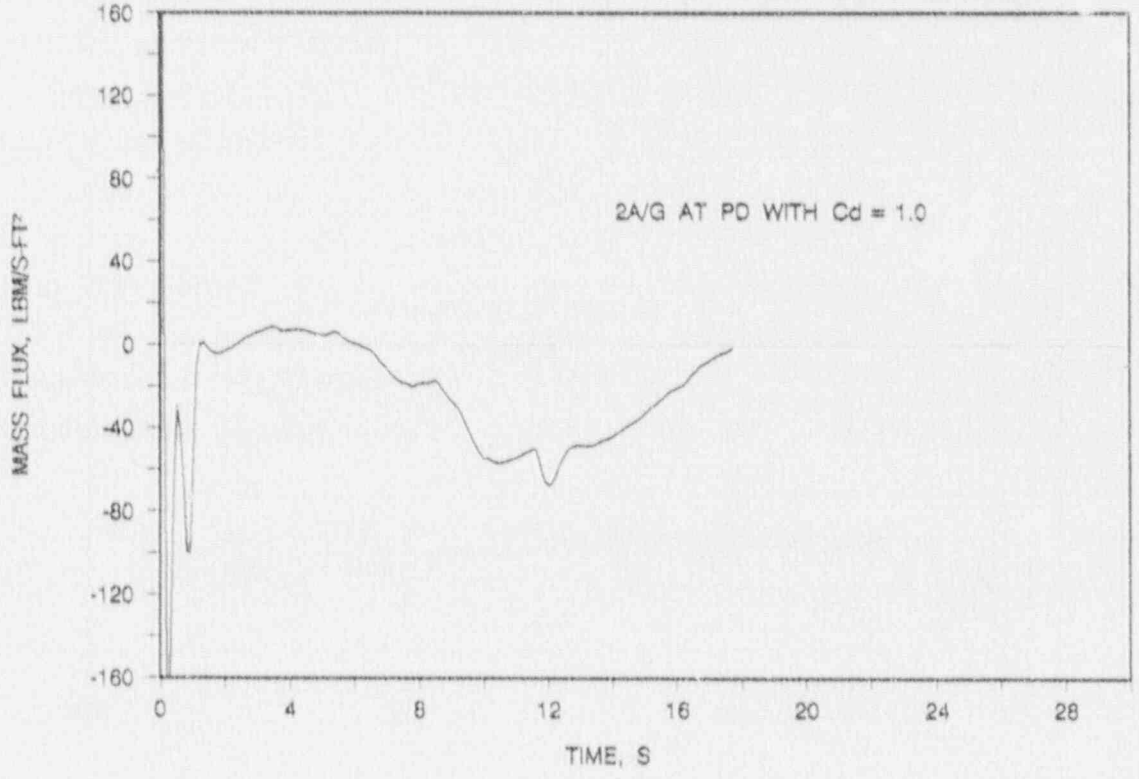

FIGURE 7-1. AXIAL DEPENDENCE OF ALLOWED TOTAL PEAKING FACTOR LARGE BREAK LOCA MARK-BW.

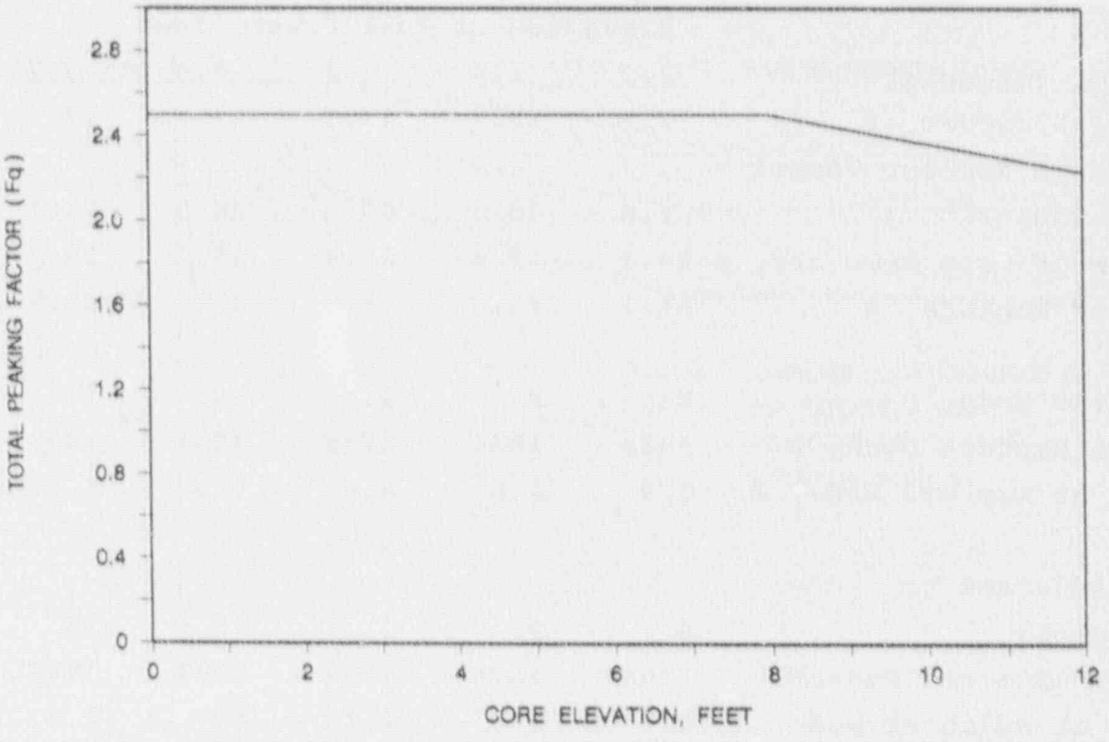

FIGURE 7-2. NORMALIZED LOCAL POWER BURNUP DEPENDENCY FACTOR.

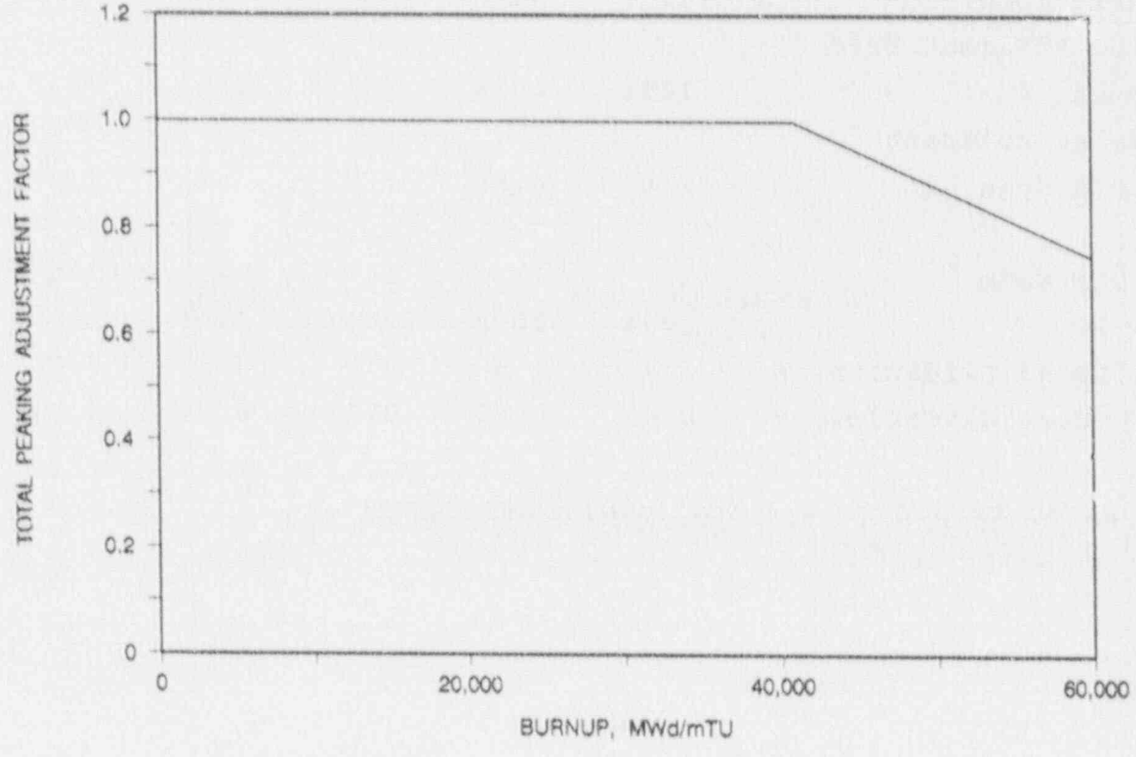

Table 7-1 LOCA Limits Results

Item or Parameter	Elevation of Peak Power, Feet 2.9	4.6	6.3	8.0	9.7
End-of-Blowdown, s	17.7	17.7	17.7	17.7	17.7
Liquid in Reactor Vessel at EOB, ft^3	91.6	90.5	90.5	94.5	93.7
Bottom-of-Core Recovery, s	29.4	29.4	29.4	29.3	29.3
Time of Rupture, s	51.7	44.0	45.0	43.2	48.9
Ruptured Node *	8	8	11	14	17
PCT at Rupture Node, F	1632	1644	1738	1854	1837
Oxide at Rupture Node, %	1.9	1.6	4.6	5.3	6.8
Node Adjacent to Rupture *	9	9	12	15	18
PCT of Adjacent Node, F	1764	1839	1969	1993	1960
Oxide at Adjacent Node, %	1.7	1.9	4.4	5.3	5.5
Node in Adjacent Grid Span *	11	11	14	12	15
PCT of Adjacent Grid Span, F	1894	2028	2047	1993	2119
Oxide at Adjacent Grid Span, %	3.4	4.8	6.8	3.7	7.4
Pin PCT Node *	11	11	14	12	15
PCT, F	1894	2028	2047	1993	2119
Peak Local Oxidation, %	3.4	4.8	6.8	5.3	7.4
Whole-Core Oxidation, %	0.43	0.63	0.79	0.74	0.84

* Refer to Figure 4-4 for noding arrangement

FIGURE 7-1. AXIAL DEPENDENCE OF ALLOWED TOTAL PEAKING FACTOR LARGE BREAK LOCA MARK-BW.

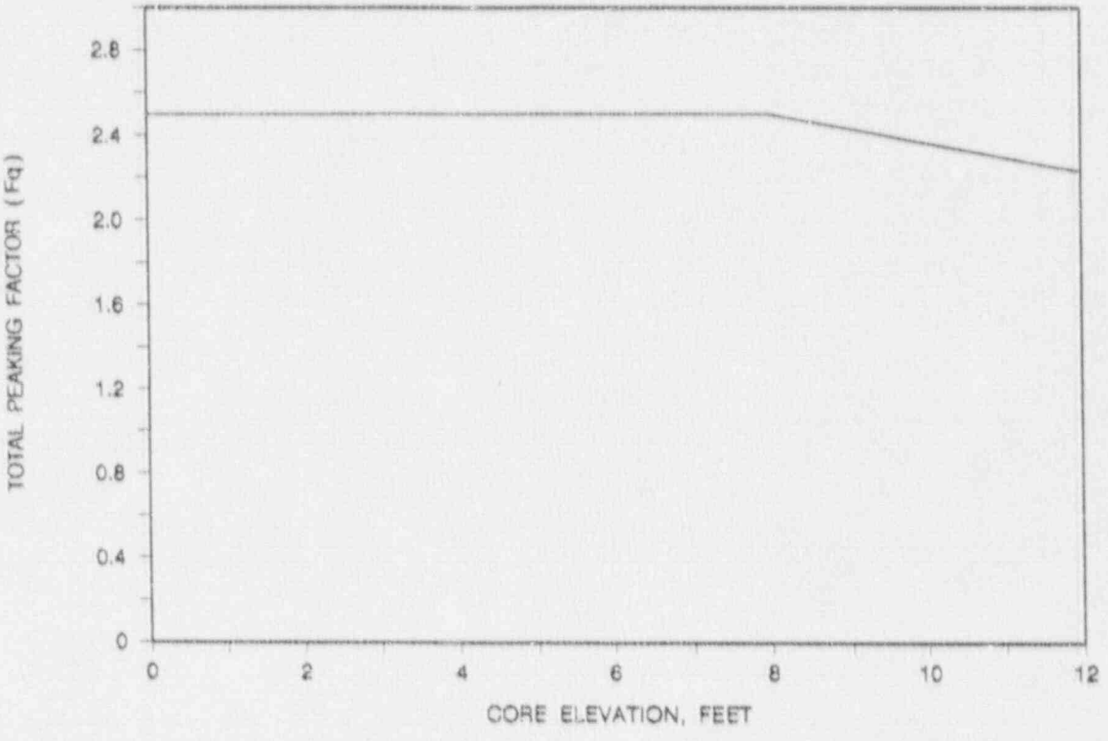

FIGURE 7-2. NORMALIZED LOCAL POWER BURNUP DEPENDENCY FACTOR.

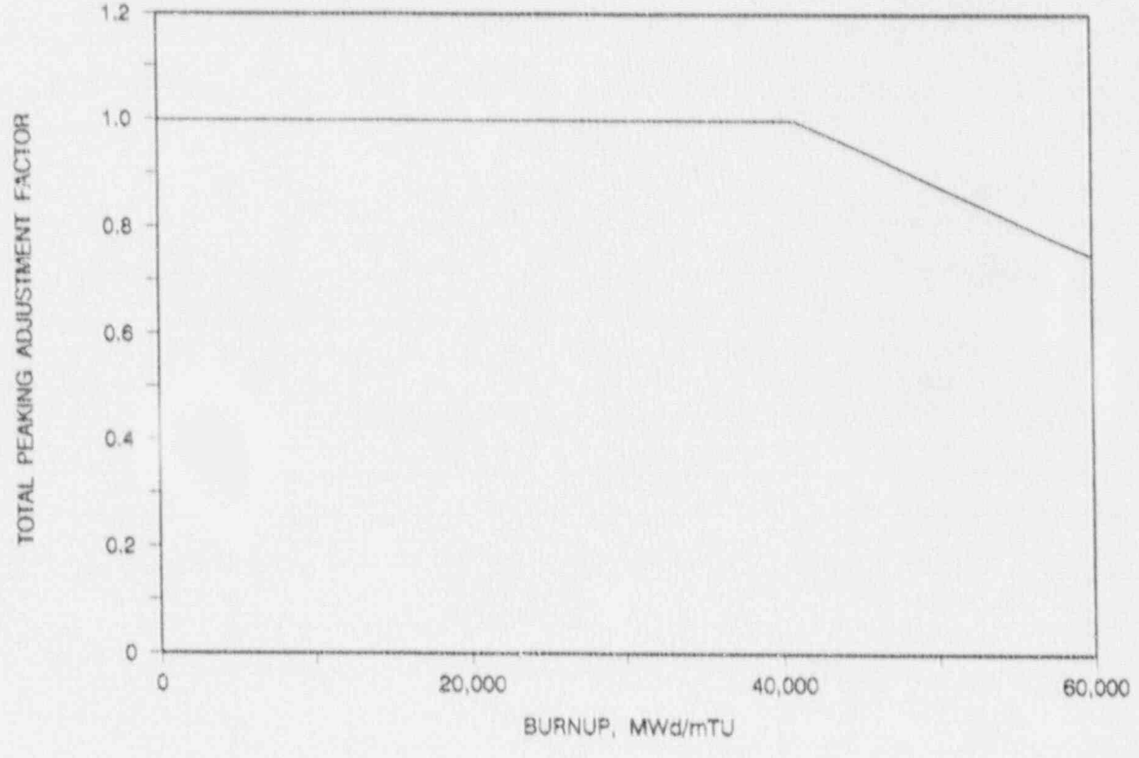

FIGURE 7-3. LOCA LIMIT STUDY - AXIAL POWER SHAPES.

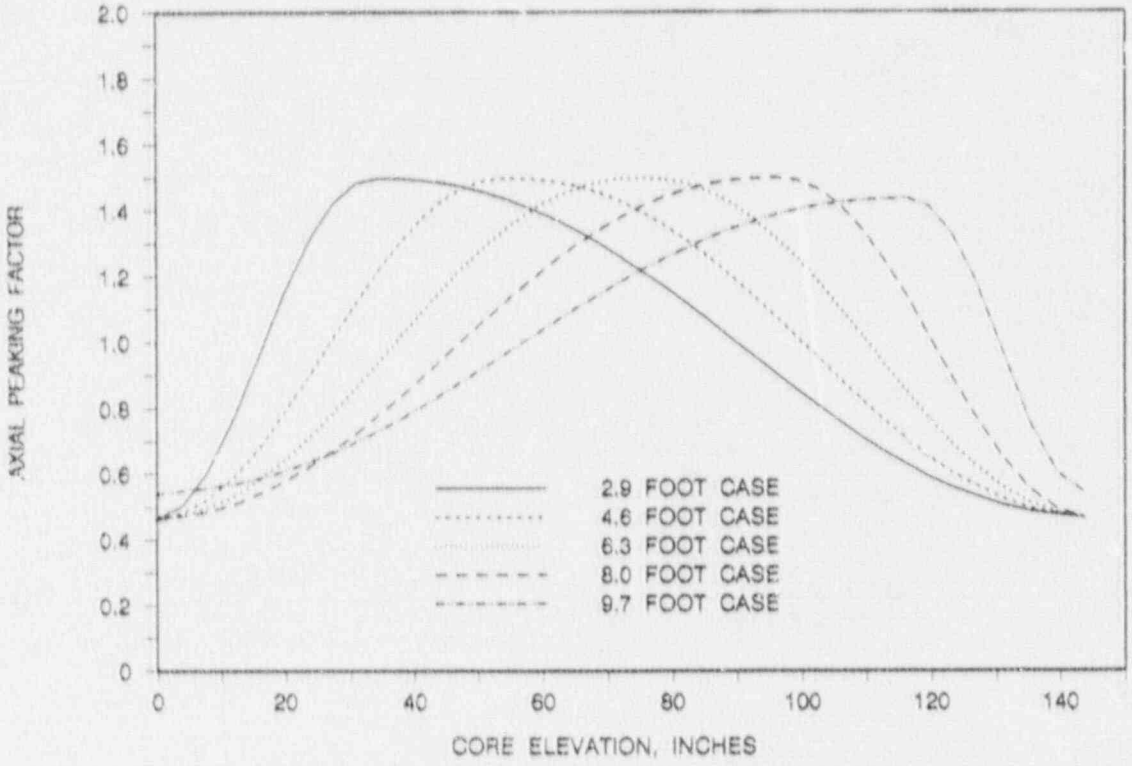

FIGURE 7-4. LOCA LIMITS STUDY - 2.9 FOOT CASE
MASS FLUX DURING BLOWDOWN AT PEAK POWER LOCATION.

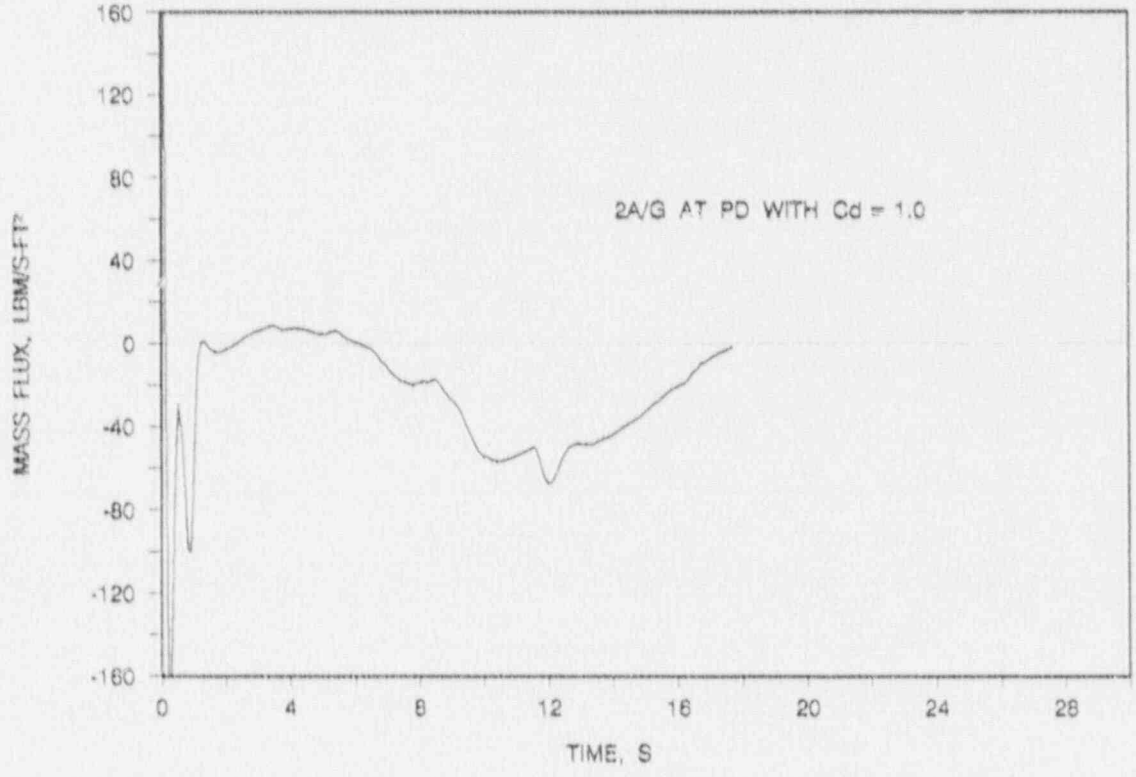

FIGURE 7-5. LOCA LIMITS STUDY - 2.9 FOOT CASE
CLADDING TEMPERATURES.

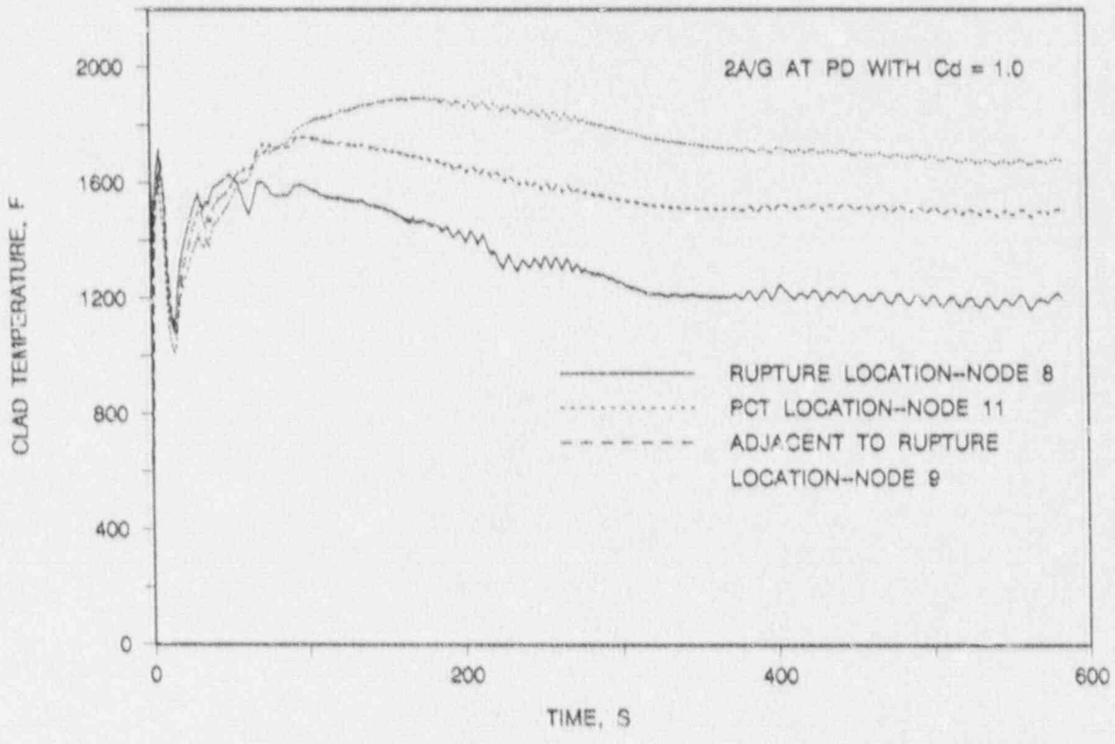

FIGURE 7-6. LOCA LIMITS STUDY - 2.9 FOOT CASE
HEAT TRANSFER COEFFICIENT AT PCT LOCATION.

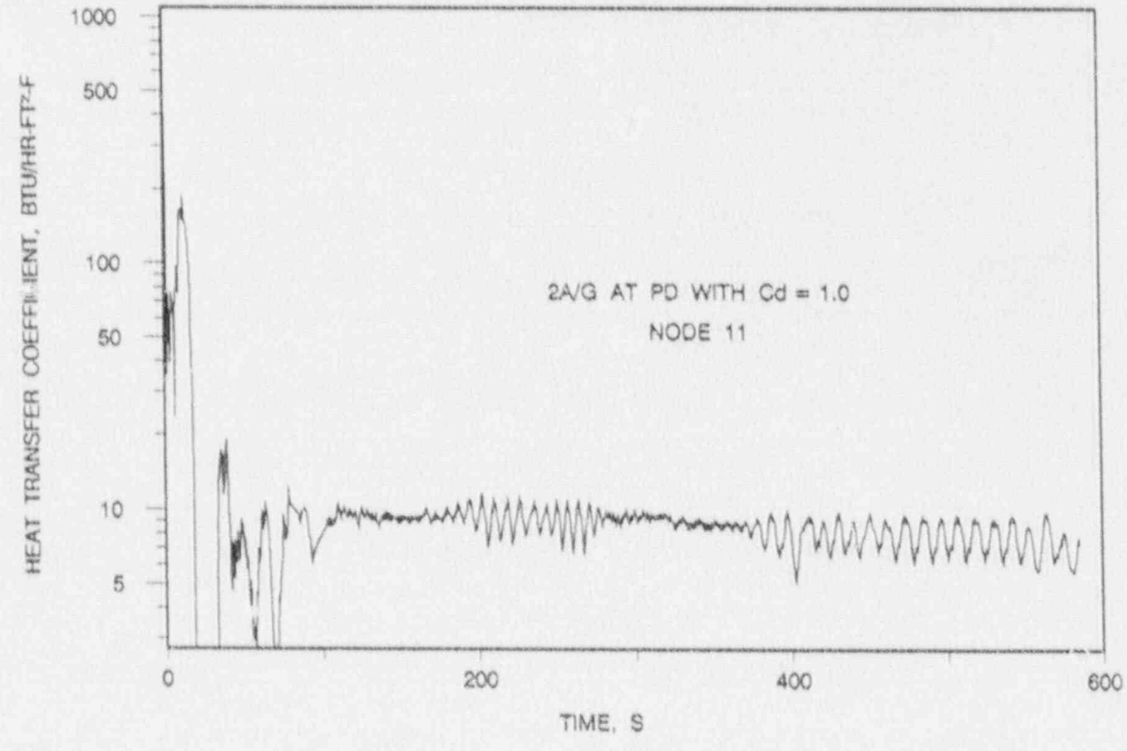

FIGURE 7-7. LOCA LIMITS STUDY - 2.9 FOOT CASE
LOCAL OXIDATION.

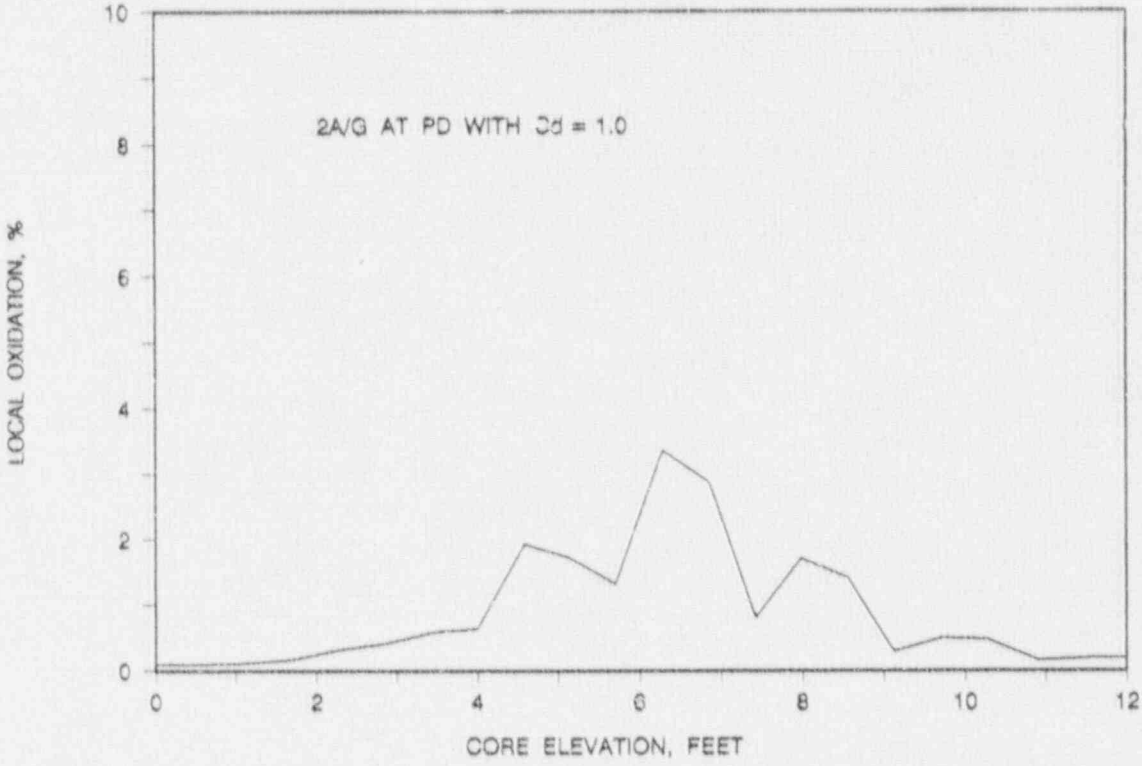

FIGURE 7-8. LOCA LIMITS STUDY - 4.6 FOOT CASE
MASS FLUX DURING BLOWDOWN AT PEAK POWER LOCATION.

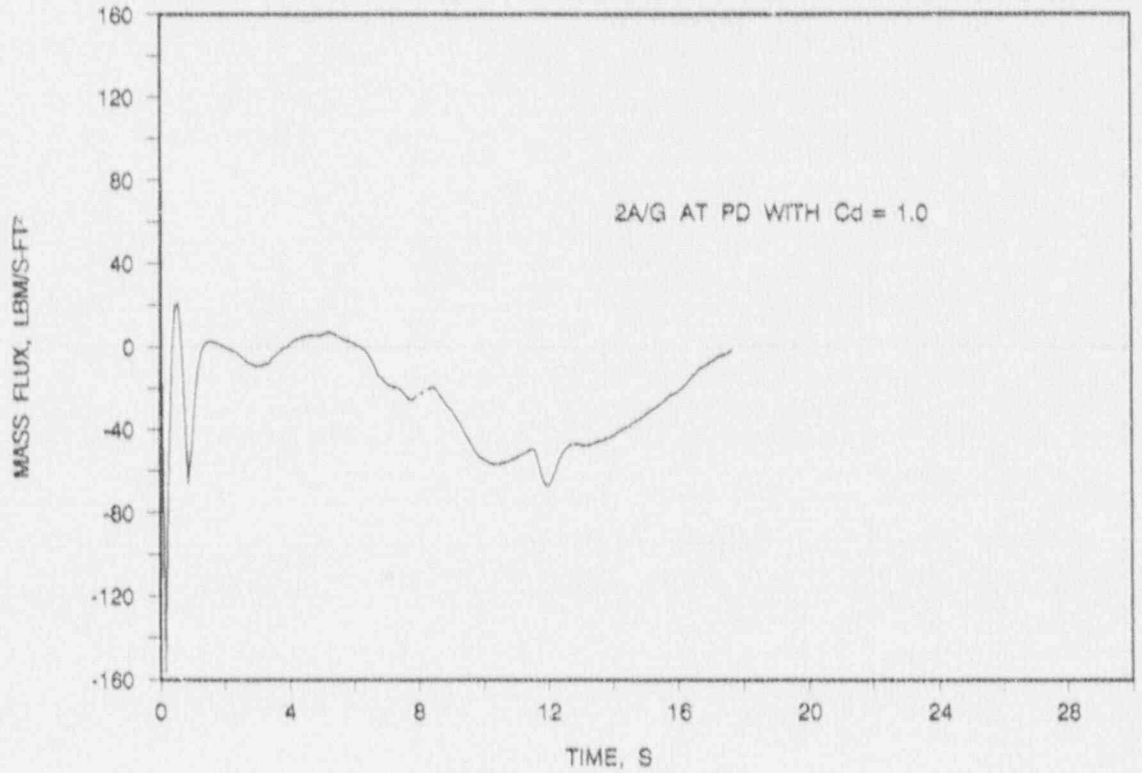

FIGURE 7-9. LOCA LIMITS STUDY - 4.6 FOOT CASE CLADDING TEMPERATURES.

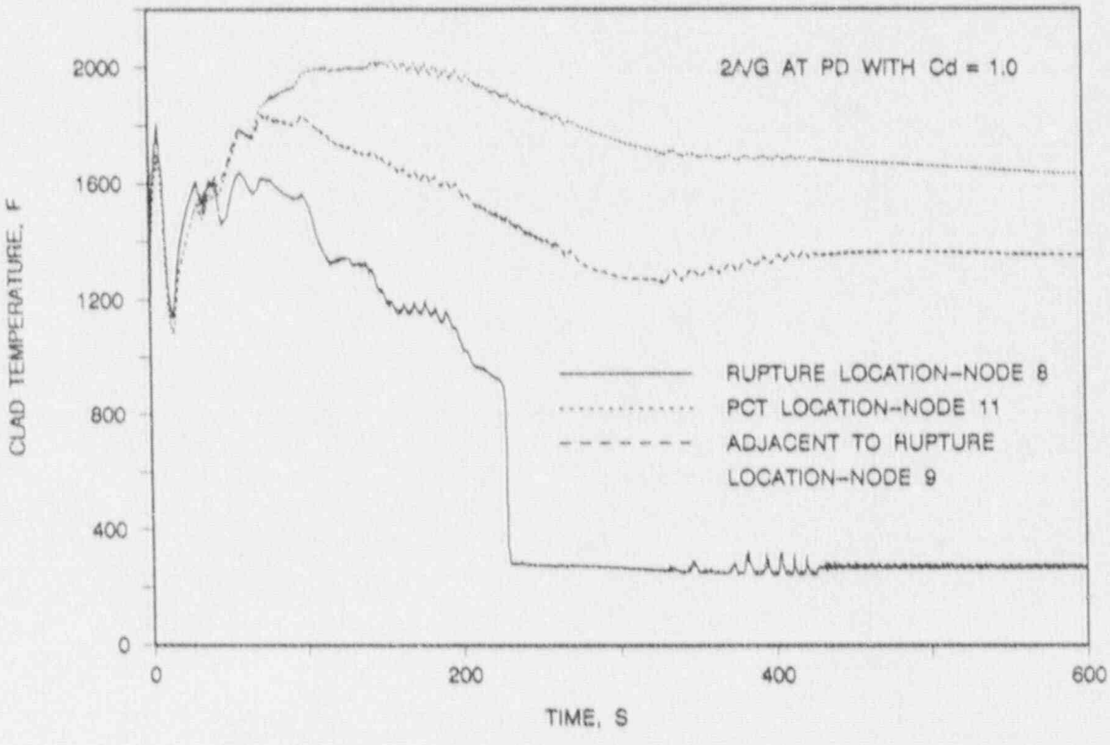

FIGURE 7-10. LOCA LIMITS STUDY - 4.6 FOOT CASE HEAT TRANSFER COEFFICIENT AT PCT LOCATION.

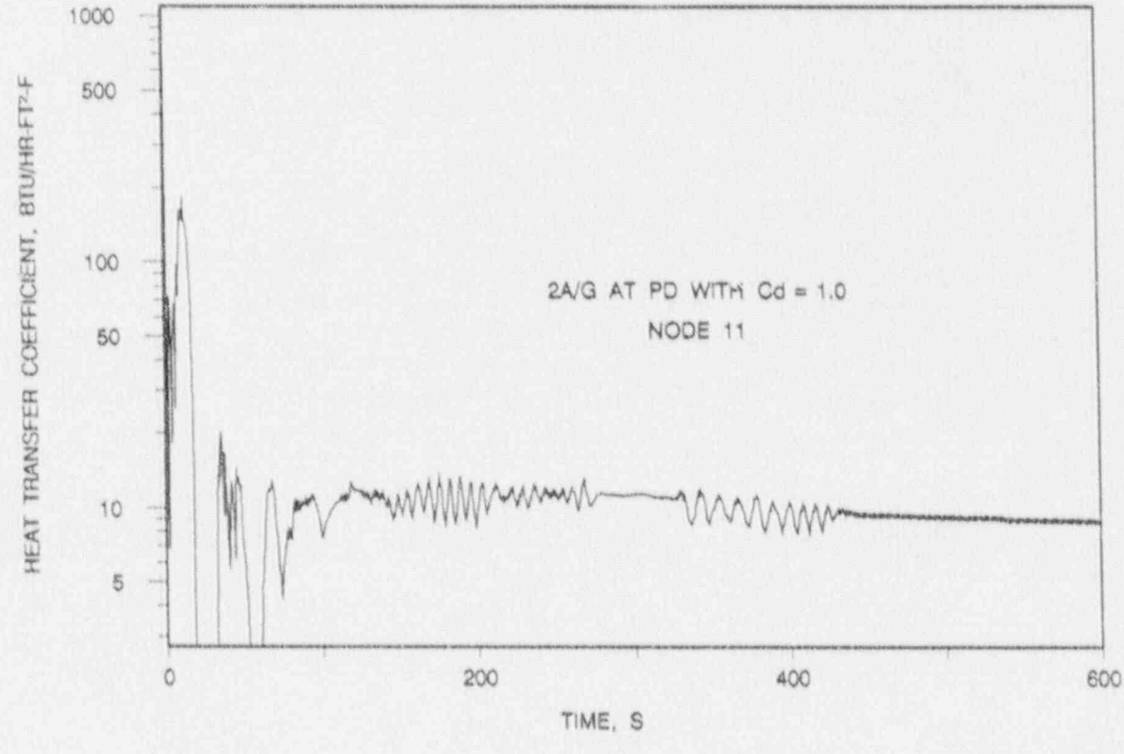

FIGURE 7-11. LOCA LIMITS STUDY - 4.6 FOOT CASE
LOCAL OXIDATION.

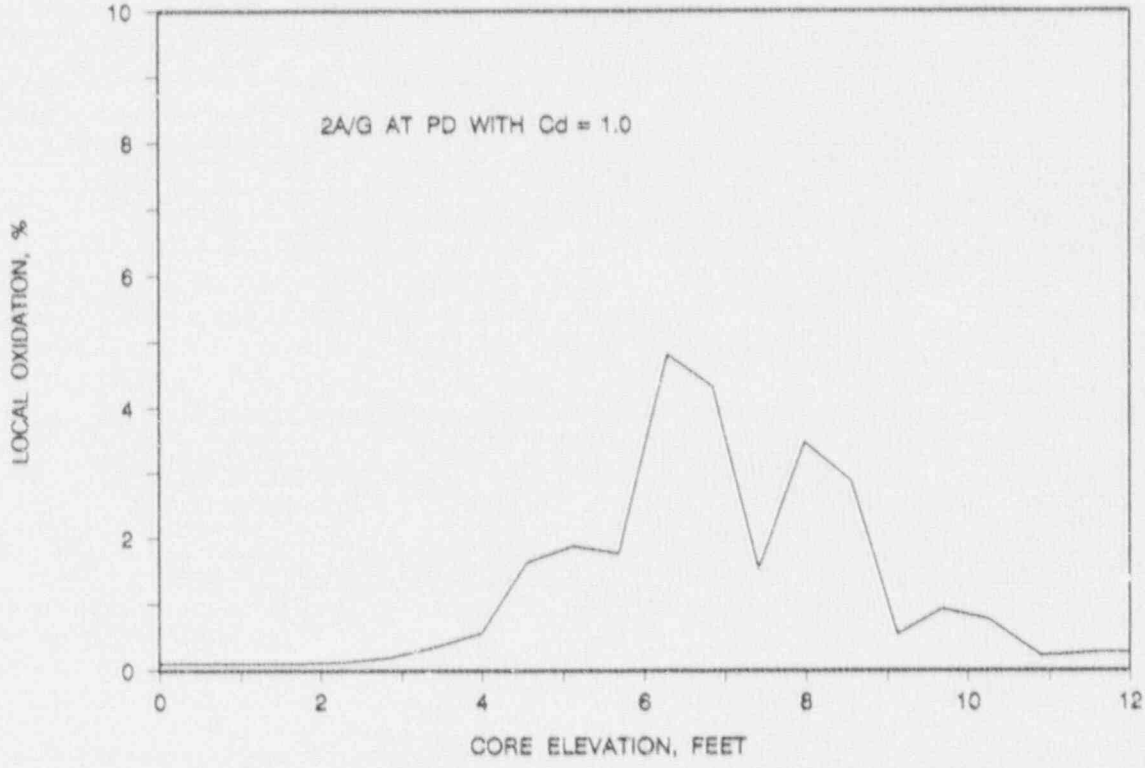

FIGURE 7-12. LOCA LIMITS STUDY - 6.3 FOOT CASE
MASS FLUX DURING BLOWDOWN AT PEAK POWER LOCATION.

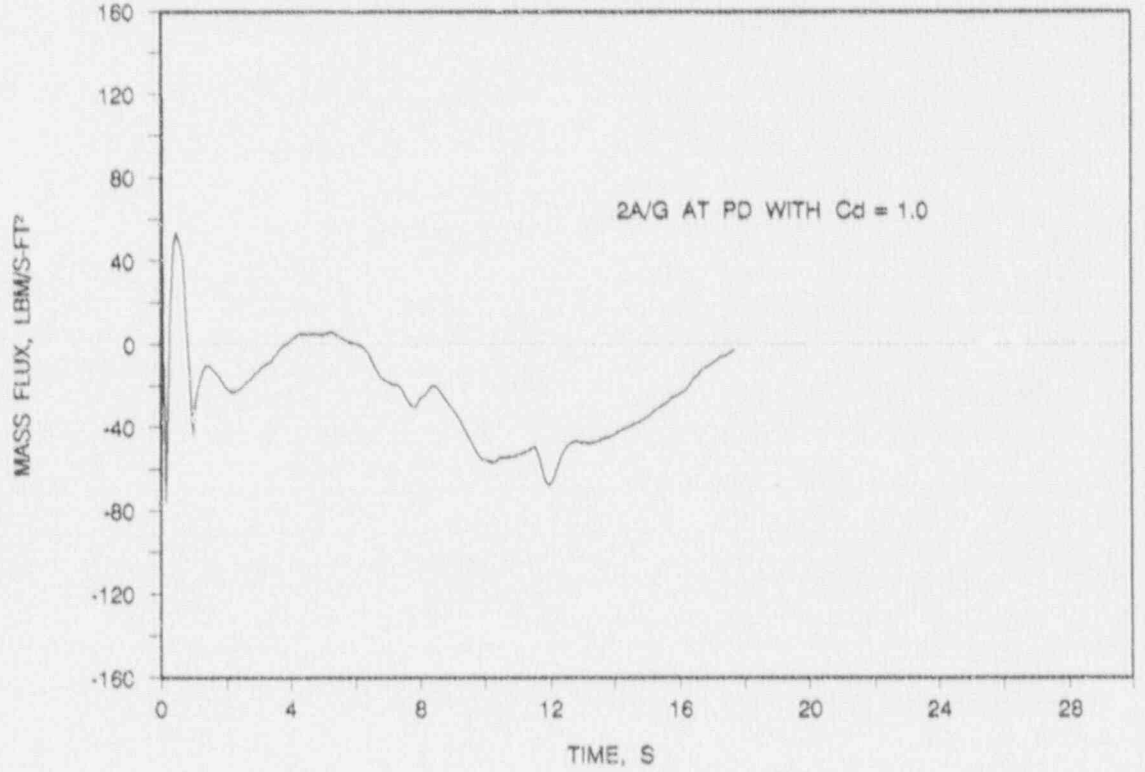

FIGURE 7-13. LOCA LIMITS STUDY - 6.3 FOOT CASE
CLADDING TEMPERATURES.

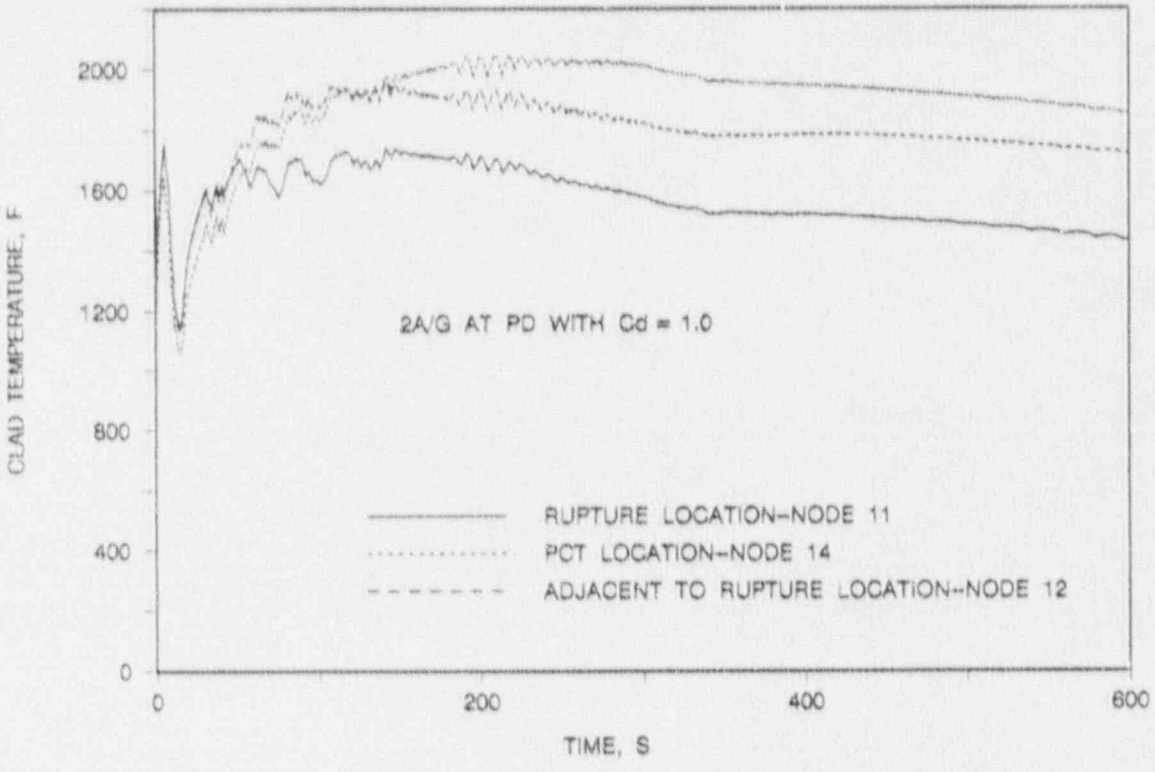

FIGURE 7-14. LOCA LIMITS STUDY - 6.3 FOOT CASE
HEAT TRANSFER COEFFICIENT AT PCT LOCATION.

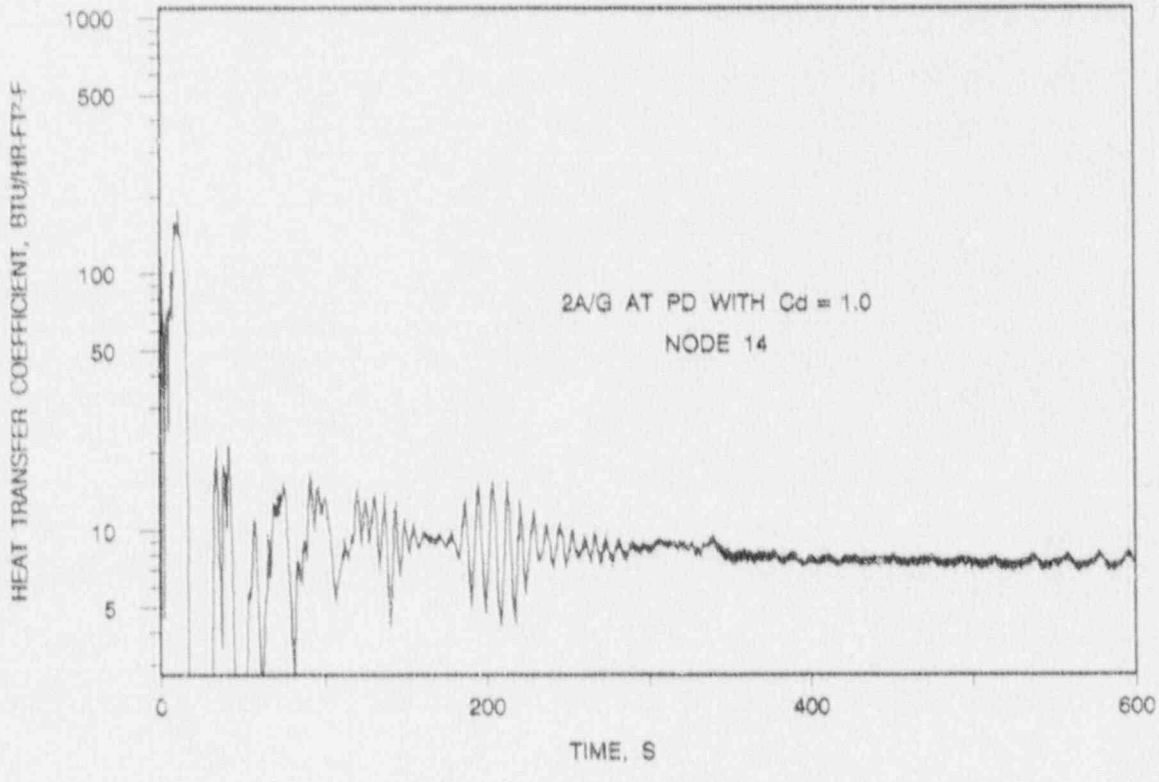

FIGURE 7-15. LOCA LIMITS STUDY - 6.3 FOOT CASE
LOCAL OXIDATION.

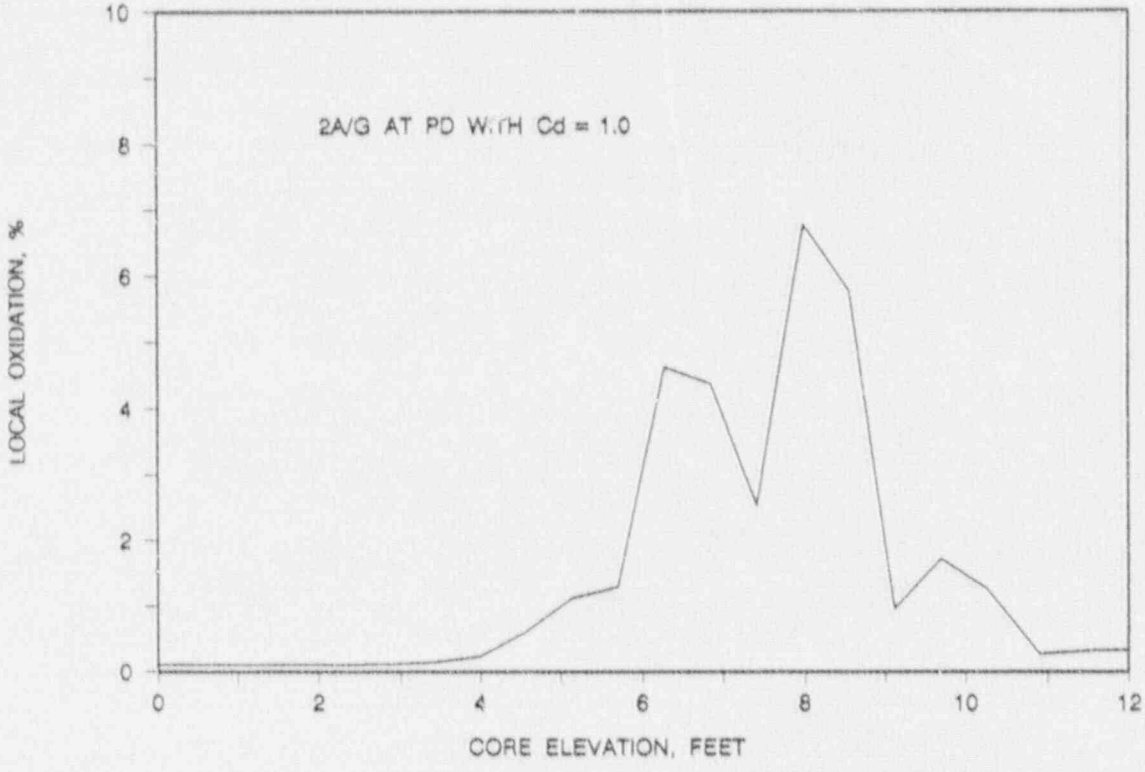

FIGURE 7-16. LOCA LIMITS STUDY - 8.0 FOOT CASE
MASS FLUX DURING BLOWDOWN AT PEAK POWER LOCATION.

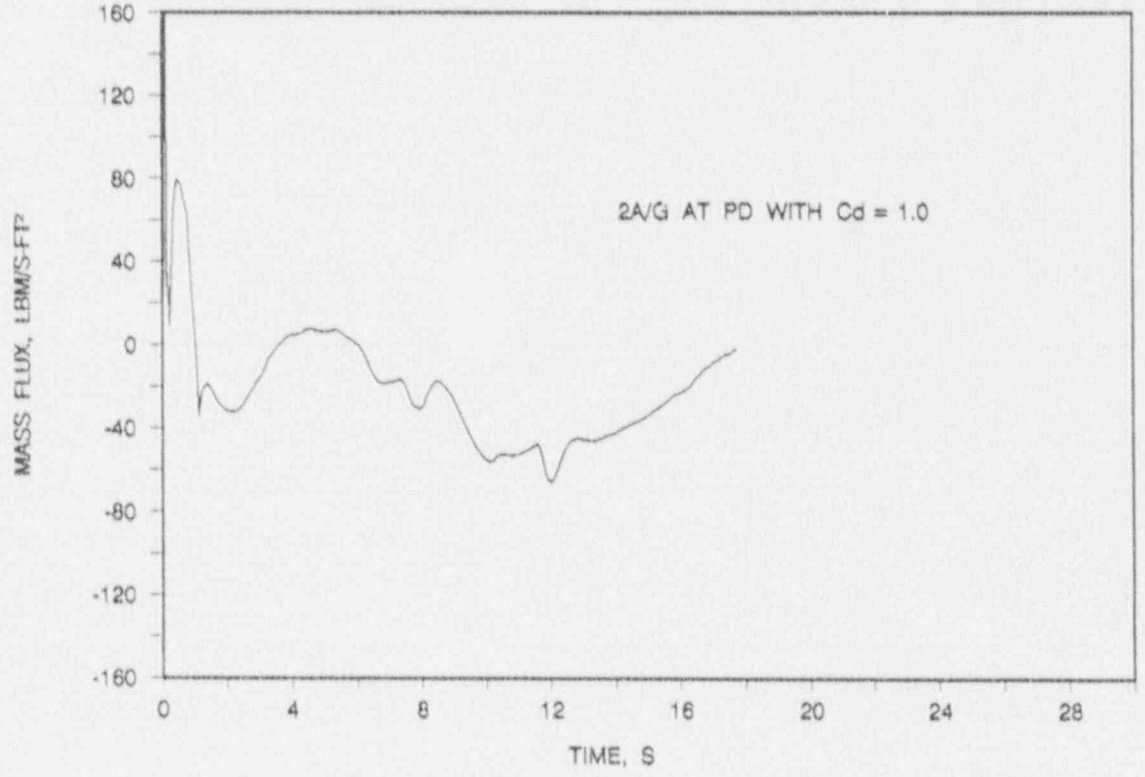

FIGURE 7-17. LOCA LIMITS STUDY - 8.0 FOOT CASE
CLADDING TEMPERATURES.

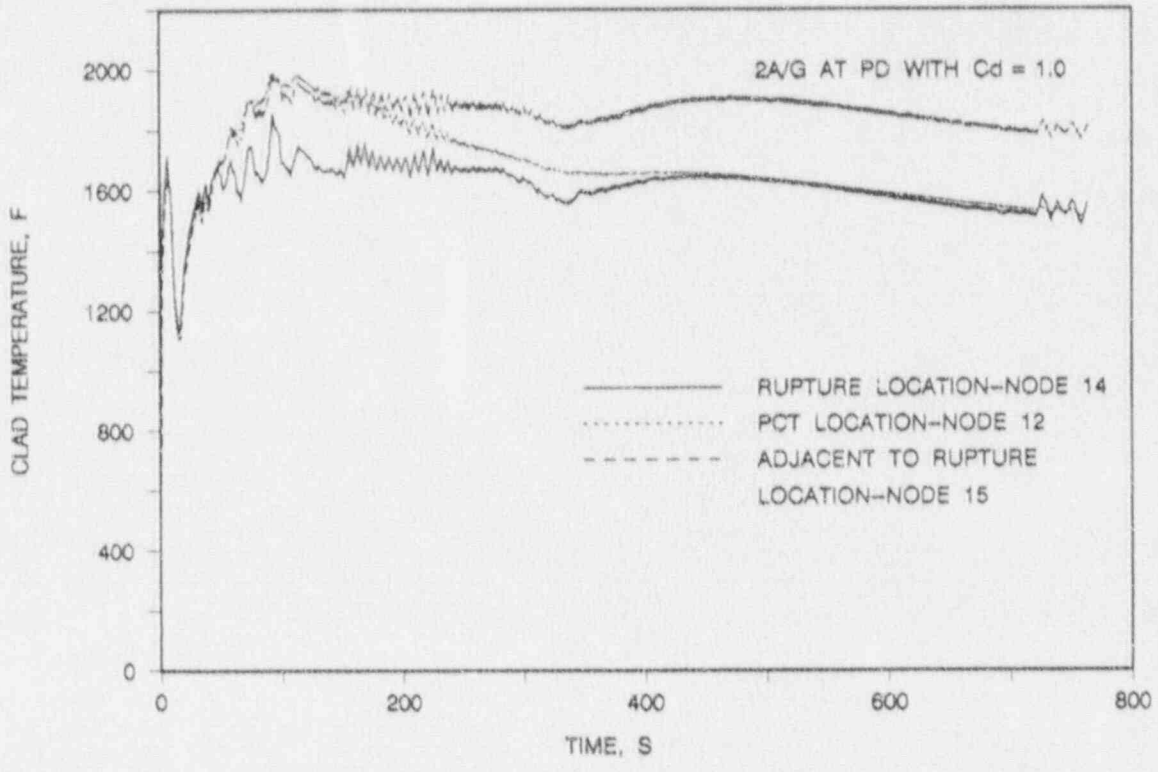

FIGURE 7-18. LOCA LIMITS STUDY - 8.0 FOOT CASE
HEAT TRANSFER COEFFICIENT AT PCT LOCATION.

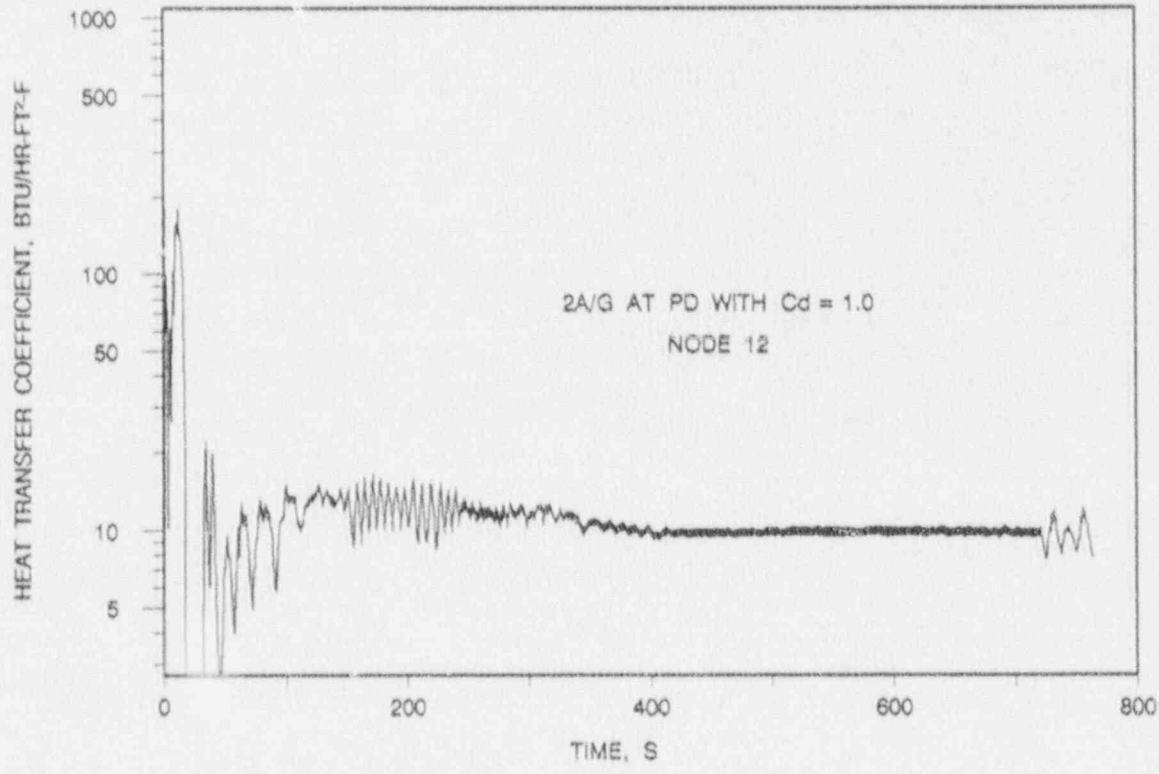

FIGURE 7-19. LOCA LIMITS STUDY - 8.0 FOOT CASE
LOCAL OXIDATION.

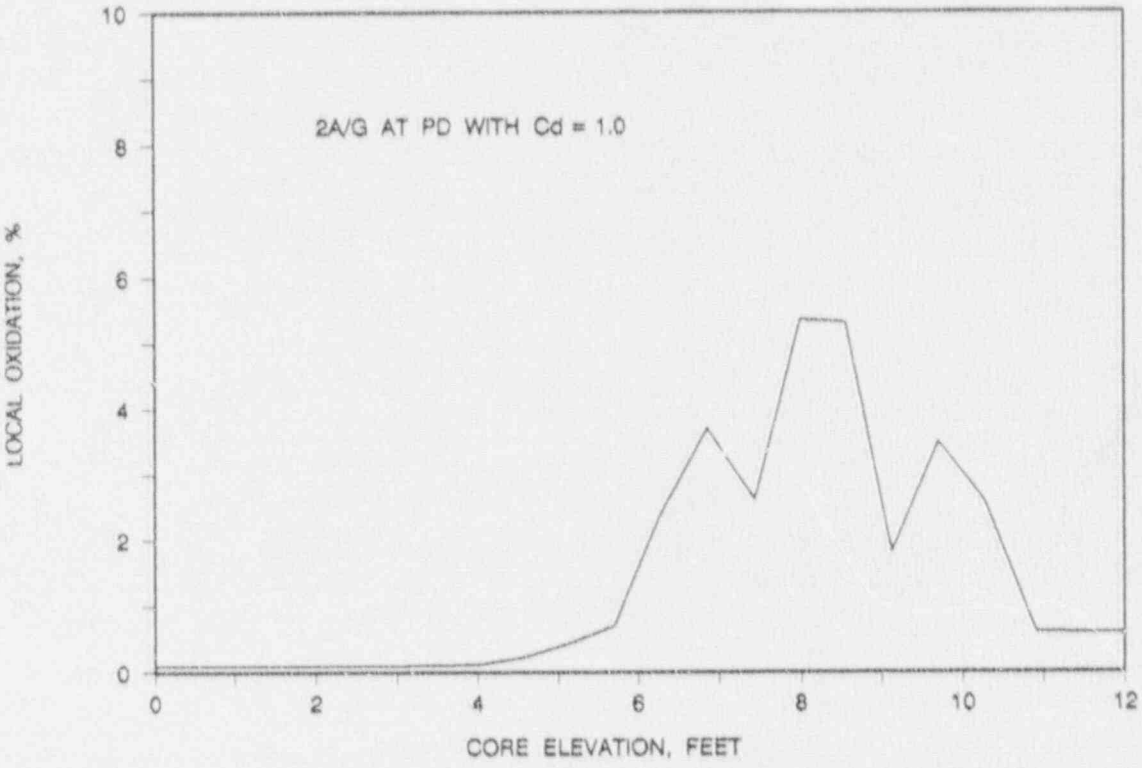

FIGURE 7-20. LOCA LIMITS STUDY - 9.7 FOOT CASE
MASS FLUX DURING BLOWDOWN AT PEAK POWER LOCATION.

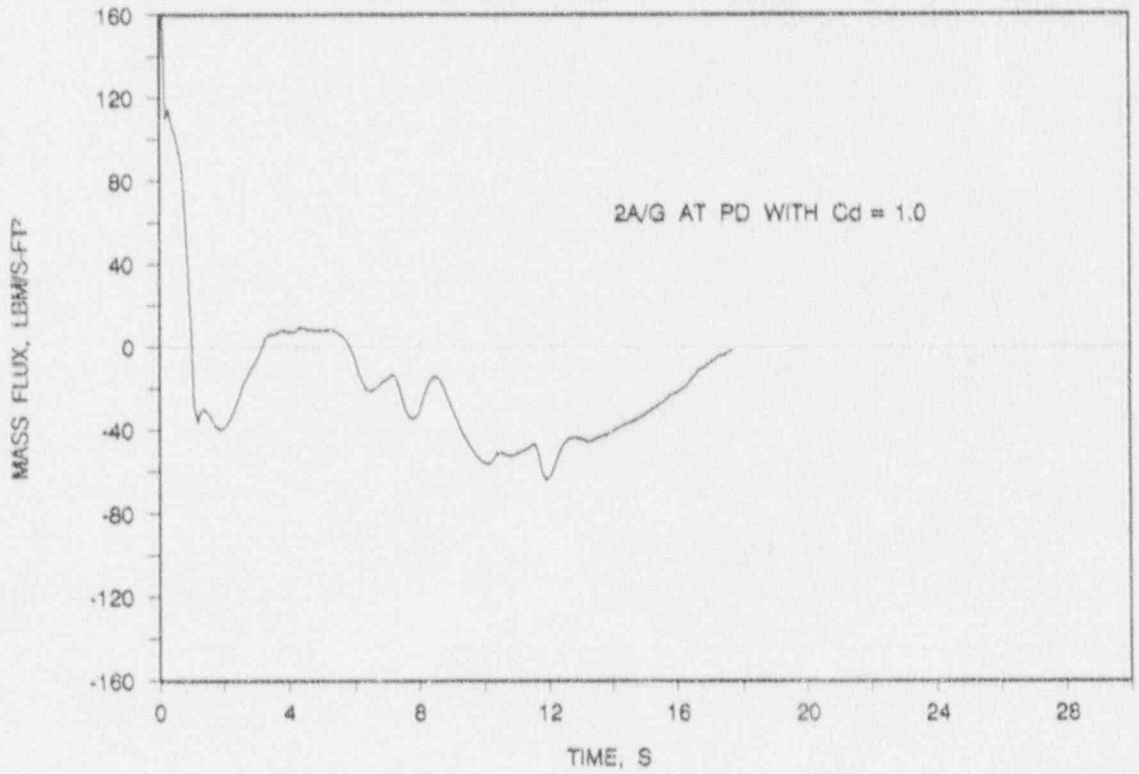

FIGURE 7-21. LOCA LIMITS STUDY - 9.7 FOOT CASE
CLADDING TEMPERATURES.

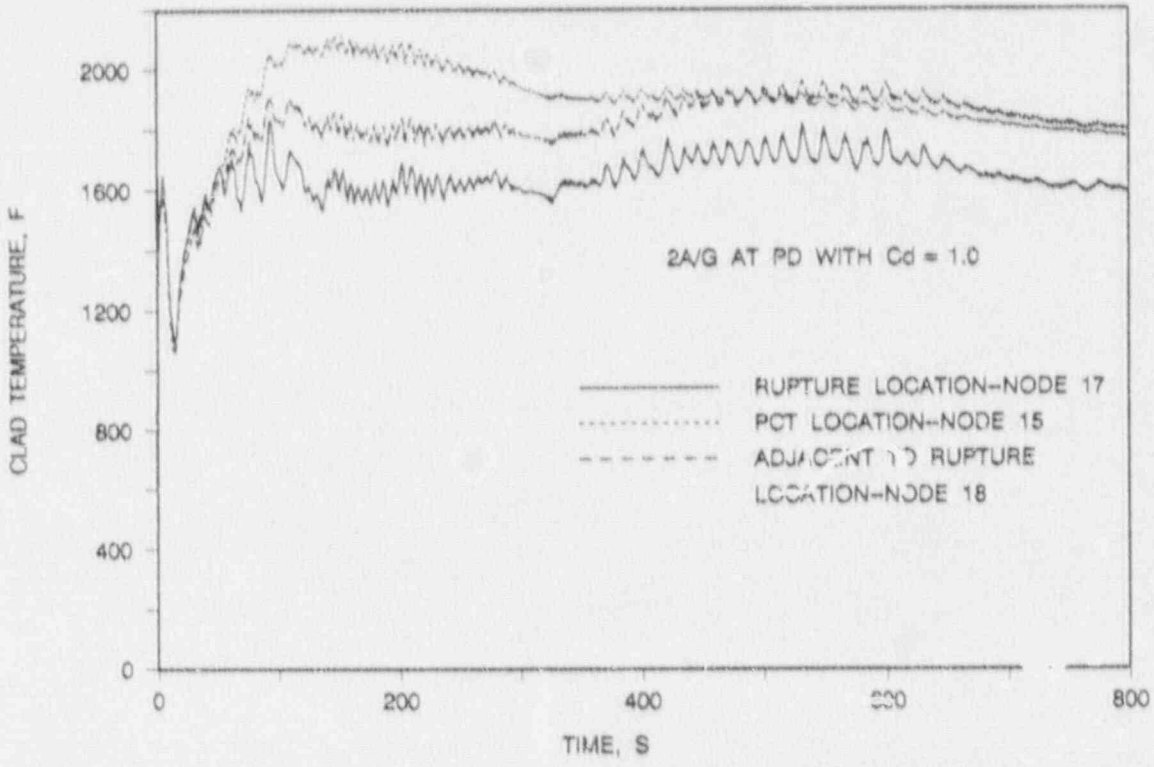

FIGURE 7-22. LOCA LIMITS STUDY - 9.7 FOOT CASE
HEAT TRANSFER COEFFICIENT AT PCT LOCATION.

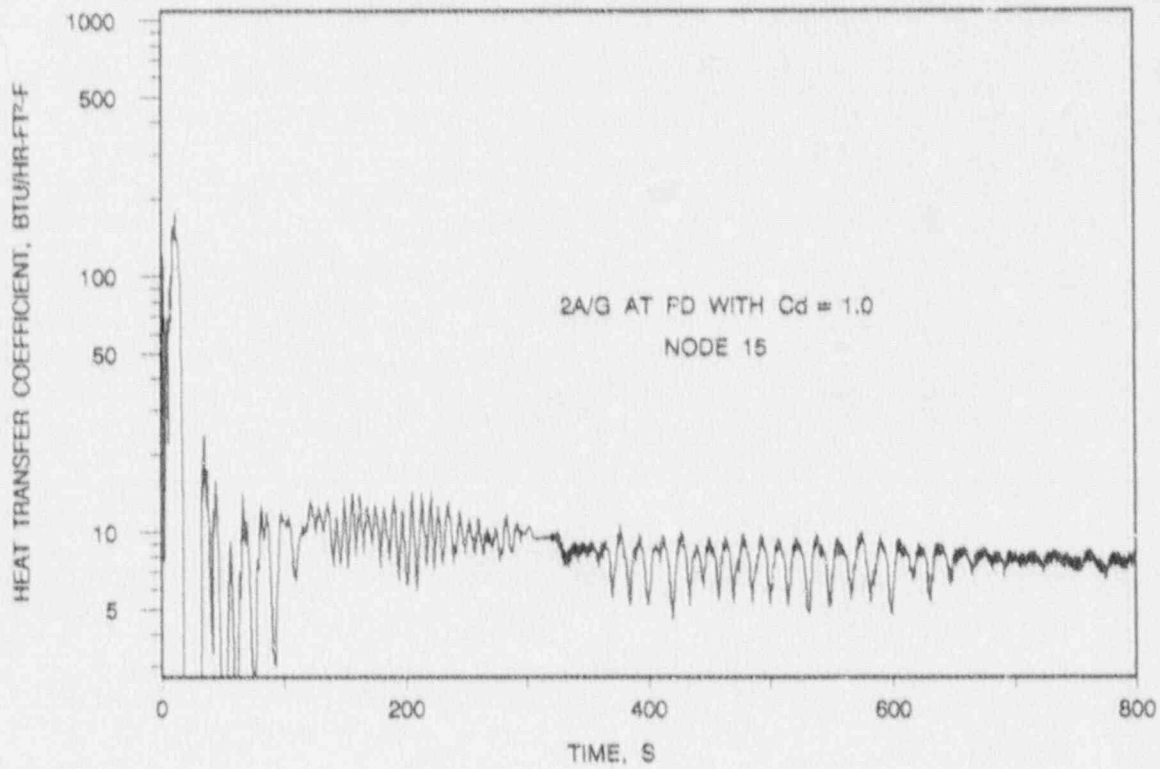

FIGURE 7-23. LOCA LIMITS STUDY - 9.7 FOOT CASE
LOCAL OXIDATION.

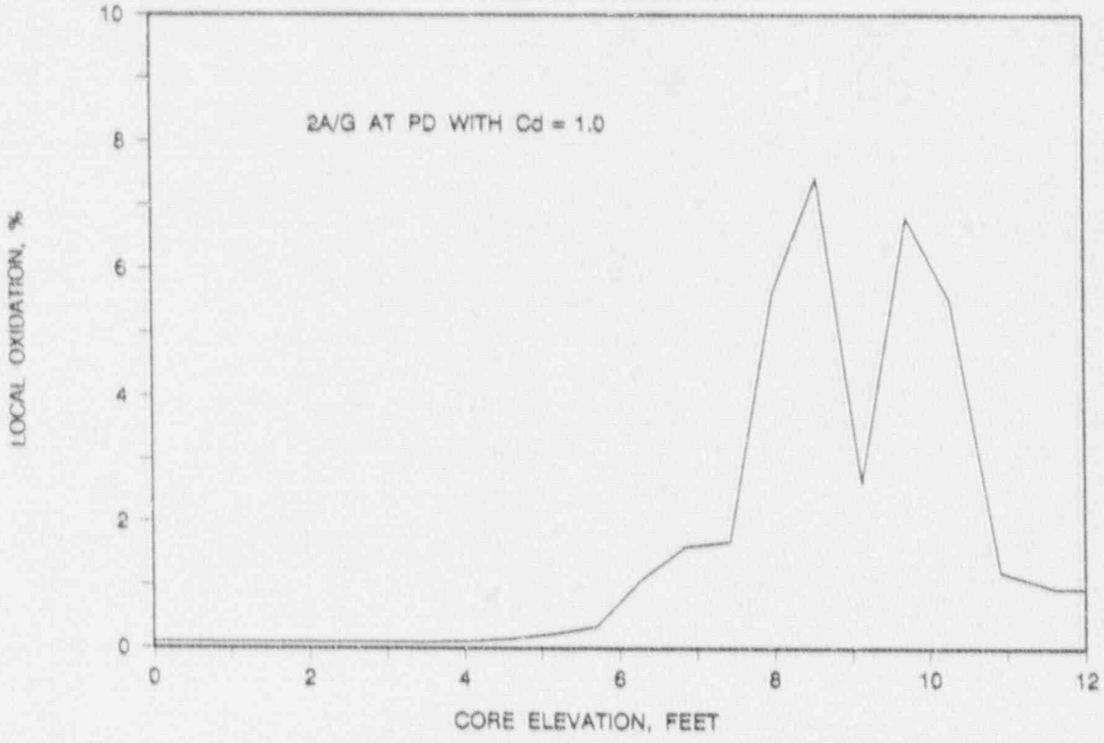

8. Whole-Core Oxidation and Hydrogen Generation

The third criterion of 10 CFR 50.46 states that the calculated total amount of hydrogen generated from the chemical reaction of the cladding with water or steam shall not exceed 0.01 times the hypothetical amount that would be generated if all of the metal in the cladding cylinders surrounding the fuel reacted, excluding the cladding surrounding the plenum volume. The method provided in the BWFC evaluation model, as amended by Question 2 on Revision 1 of BAW-10168, has been applied to determine corewide oxidation for each of the LOCA limits cases. In these calculations, local cladding oxidation was computed so long as the cladding temperature remained above 1000 F, and the REFLOD3B analysis did not show that the fuel at that elevation had quenched. These local oxidations were summed over the core to give the core-wide oxidation. Figures in Chapter 7 give the local oxidation for the hot pin including the initial oxide layer. The only difference between these distributions and the ones used for the whole core calculation is that the initial oxide layer is subtracted before the integration to provide a measure of the hydrogen produced during the LOCA. The results of these calculations for each of the power distributions of the LOCA Limits cases are:

Case	Whole Core Oxidation, %
2.9-ft Peak	0.43
4.6-ft Peak	0.63
6.3-ft Peak	0.79
8.0-ft Peak	0.74
9.7-ft Peak	0.84

Because these cases represent a range of the possible power distributions that can occur in the plant, the maximum possible oxidation that can occur during a LOCA at the Trojan plant is calculated to be less than 0.84 percent. Thus, the third criterion

of 10 CFR 50.46, which limits the reaction to 1 percent or less, is met.

9. Core Geometry

The fourth acceptance criterion of 10 CFR 50.46 states that calculated changes in core geometry shall be such that the core remains amenable to cooling. The calculations in Chapter 7 directly assess the alterations in core geometry, which result from the LOCA, at the most severe location in the core. These calculations demonstrate that the fuel pin cooled successfully. As discussed in Section 7 of the BWFC evaluation model report (BAW-10168), clad swelling and flow blockage due to rupture can be estimated based on NUREG-0630. For the Trojan plant, the hot assembly flow area reduction at rupture is less than 50 percent for all LOCA Limits cases. Furthermore, the upper limit of possible channel blockage, based on NUREG-0630, is less than 90 percent. Neither 90 percent blockage nor 50 percent blockage constitutes total subchannel obstruction. As the position of rupture in a fuel assembly is distributed within the upper part of a grid span, subchannel blockage will not become coplanar across the assembly. Therefore, the assembly retains its pin-coolant channel-pin-coolant channel arrangement and is capable of passing coolant along the pin to provide cooling for all regions of the assembly.

The effects of fuel rod bowing on whole core blockage are considered in the BWFC fuel assembly and fuel rod designs, which minimize the potential for rod bowing. The minor adjustments of fuel pin pitch due to rod bowing do not alter the fuel assembly flow area substantially and the average subchannel flow area is preserved. Therefore, due to the axial distribution of blockage caused by rupture, no coplanar blockage of the fuel assembly will occur and the core will remain amenable to cooling. Deformation of the fuel pin lattice at the core periphery can occur from the combined mechanical loadings of the LOCA and a seismic event. These loads have been analyzed separately in the original plant structural designs to ensure that they have no adverse effect on the core cooling processes. The loadings and effect on the Mark-BW

assembly are presented in the Mark-BW fuel mechanical design report (BAW-10172, Reference 7). Although deformations can occur, they are limited to the outer two or three points on the lattice structure of the core and do not cause a subchannel flow area reduction larger than 35 percent. The fuel pins at these lattice points do not operate at power levels sufficient to produce a cladding rupture during LOCA. Therefore, the only reduction in channel flow area is from the mechanical effect, and the assemblies retain a coolable configuration.

The consequences of both thermal and mechanical deformation of the fuel assemblies in the core have been assessed and the resultant deformations have been shown to maintain coolable core configurations. Therefore, the coolable geometry requirements of 10 CFR 50.46 have been met and the core has been shown to remain amenable to core cooling.

10. Long-Term Cooling

The fifth acceptance criterion of 10 CFR 50.46 states that the calculated core temperature shall be maintained at an acceptably low value and decay heat shall be removed for the extended period of time required by the long-lived radioactivity remaining in the core. Successful initial operation of the ECCS is shown by demonstrating that the core is quenched and the cladding temperature is returned to near saturation temperature. Thereafter, long-term cooling is achieved by the pumped injection systems. These systems are redundant and able to provide a continuous flow of cooling water to the core fuel assemblies so long as the coolant channels in the core remain open. For a cold leg break, the concentration of boric acid within the core might induce a crystalline precipitation which could prevent the coolant flow from reaching certain portions of the core. This chapter presents the evaluation of the final stages of the initial operation of the ECCS, a discussion of the long-term supply of water to the core, and a discussion of the procedures to prevent the build-up of boric acid in the core.

10.1 Initial Cladding Cooldown

The heat transfer models used to determine the peak cladding temperature are most conservative following the initiation of cladding cooldown and cannot be used directly to predict cladding quench. Rather, the occurrence of core quenching is determined from the core quench height as predicted by the REFLOD3B code. After quenching, core heat transfer is by pool nucleate boiling or by forced convection to liquid, depending on the location of the break in the reactor coolant system (cold leg breaks are in pool nucleate and hot leg breaks in forced convection). Either mechanism is fully capable of maintaining the core within a few degrees of the saturation temperature of the coolant. Thus,

within ten to fifteen minutes following the LOCA, the core has been returned to an acceptably low temperature level.

10.2 Extended Coolant Supply

Once the core has been cooled to low temperatures, maintaining that condition relies upon the systems available to provide a continuous supply of coolant to the core. Detailed descriptions of the plant systems and functions are provided in the safety analysis report for the Trojan plant (Reference 8). Provision for long-term core cooling with the ECCS as demonstrated in the FSAR is independent of the fuel design. Thus, the licensing basis for previous operation remains valid for Mark-BW reload fuel.

10.3 Boric Acid Concentration

As previously discussed, the long-term cooling mechanism for a hot leg break is by forced convection to liquid; once established, the coolability of the core is assured and need not be further considered. For the cold leg break, however, there is no forced flow through the core. The liquid head balances between the core and the downcomer prevent ECCS water from entering the core at a rate faster than the rate of core boiling. Extra injection simply flows out of the break and spills to the containment. With no throughput, boiling in the core region acts to concentrate boric acid. To limit the concentration of boric acid, the operator is required to establish a hot leg recirculation mode of operation within 13 hours of the initiation of the accident.

In this mode, the piping is aligned so that injection takes place in both the hot and cold legs. By doing so, the amount of injection to the hot leg becomes a through-flow that can control the concentration of boric acid. The timing and effectiveness of the hot leg injection is established by demonstrating that the in-vessel concentrations are well below the solubility limits for the

dissolved solids. Therefore, there is no dependency on the fuel element design as the concentrations depend only on the injection rate, the reactor coolant system geometry, and the core power level. Since none of these factors have been altered by the fuel change, the evaluation in the referenced FSAR remains valid for the plant. The operator actions and procedures to establish the operation are also described in the FSAR.

10.4 Adherence to Long-Term Cooling Criterion

Compliance to this criterion is demonstrated for the systems and components specific to the Trojan plant in the referenced FSAR and is not related to the fuel design. The initial phase of core cooling has been shown to result in low cladding and fuel temperatures. A pumped injection system capable of recirculation is available and operated by the plant to provide extended coolant injection. The concentration of dissolved solids has been shown to be limited to acceptable levels through the timely implementation of hot leg recirculation. Therefore, the capability of long-term cooling has been established and compliance to 10 CFR 50.46, demonstrated.

11. Small Break LOCA

The current licensing bases for the Trojan plant comprise a spectrum of large and small break loss-of-coolant accidents (LOCAs) analyzed by Westinghouse and documented in the plant final safety analysis report (FSAR). For operation of Trojan with BWFC-supplied fuel, BWFC has reanalyzed the large break LOCA transient as presented in the foregoing chapters. Reanalysis was considered necessary since the large break results can be sensitive to changes in fuel design. By the same consideration, reanalysis of the small break LOCA for operation with Mark-BW reload fuel is not required since SBLOCA evaluations are unaffected by the design differences between the Mark-BW and Westinghouse fuel assemblies. Thus, the referenced FSAR analyses, performed by Westinghouse, remain the bases for plant licensing even after the cores are loaded with BWFC-supplied fuel assemblies. The remainder of this chapter discusses the independence of SBLOCA results from fuel assembly design.

11.1 SBLOCA Transient

SBLOCA transients can be generally characterized as developing in five distinct phases: (1) subcooled depressurization, (2) pump/loop flow coastdown and natural circulation, (3) loop draining, (4) vessel/core boil-off, and (5) long-term cooling. These phases are examined in the following paragraphs as a lead-in to a discussion in the next section of the effects, if any, of fuel design differences--between the resident Westinghouse fuel and the Mark-BW reload assemblies--upon the sequence of events and consequences of the small break LOCA transient for the Trojan plant.

The limiting SBLOCA events begin with a subcooled reactor coolant system (RCS) depressurization until the primary system pressure reaches the initial hot leg temperature saturation pressure. During this depressurization phase, the low pressure reactor trip,

ECCS injection, and reactor coolant pump trip signals are generated. Tripping of the pumps begins t' ump and loop flow coastdown period.

Following reactor trip, the core power drops sharply. The initial forced flow and subsequent coastdown flow provide continuous heat removal via the steam generators. Thus, the initial stored energy, core power, and decay heat during this phase are transferred directly to the steam generators. The pump coastdown and natural circulation flows during this period are sufficient to prevent critical heat flux (CHF) from occurring in the core. As a result, the fuel pins are cooled toward the quasi-steady temperature distribution required to simply conduct and convect the decay heat energy out of the pins. These pin temperatures approach the RCS saturation temperature. Loss of continuous loop flow marks the end of this period.

The third phase in the transient is characterized as a period of loop draining. During this period, the system reaches a quiescent state in which the core decay heat, leak flows, pumped ECCS injection, and steam generator heat transfer combine to control the development of steam-water mixture levels within the RCS. The system inventory distribution is a strong function of the system geometry and break location. RCS liquid inventory will continue to decrease until component mixture levels provide a continuous vent path for core steam production. Relief of core steam production allows the RCS to further depressurize and enter the boil-off mode.

The development and timing of events that mark the end of the loop draining and onset of core boil-off are governed by the break location. For hot leg breaks, the continuous core steam venting path is readily established. A significant system inventory loss is required to establish the vent path for steam generator downstream piping breaks. The most severe of all SBLOCAs occurs in cold leg pump discharge breaks. In these breaks, liquid inventory

is lost until the primary levels descend to the spill-under elevation at the low point in the cold leg pump suction piping. This liquid trap or loop seal must be cleared of liquid to establish the steam venting path to the leak. Since the loop seal elevation is located slightly above the middle of the core, the core collapsed liquid level will be depressed by the manometric pressure balance imposed by the RCS geometry. Once the loop seals clear, the steam venting path is established and the residual liquid inventory in the pump discharge and downcomer regions drains into the core region.

The onset of the boil-off period typically coincides with the beginning of a final saturated depressurization. Voiding at the break increases the leak volumetric flow rate which ultimately depressurizes the system until the accumulator fill pressure is reached or the pumped ECCS injection matches core steaming. During this period, the reactor vessel mixture levels may drop into the core heated region. Pin temperature excursions calculated for the upper elevations are maximized by the assumption of a bounding, core outlet-skewed peaking. During these heatups, the cladding may swell and even rupture if the temperature approaches 1500 F.

Swelling and rupture produce three primary effects on the temperature calculation: First, the cladding expansion increases the fuel pin gap allowing a momentary cooling of the clad. This condition is temporary; however, it delays the temperature excursion, resulting in a lower peak cladding temperature because the decay heat level has decreased slightly. Second, the rupture introduces a blockage in the flow channel. The blockage affects local heat transfer positively through turbulence enhancements of heat transfer coefficients. The blockage negatively affects local heat transfer through diversion of flow from the subchannel. Locally, the increase in heat transfer area at the rupture and the turbulence enhancements more than compensate for any flow diversion. Downstream, there is no flow diversion impact because

rupture within a fuel assembly is an axially distributed phenomenon. Any rupture-induced subchannel flow diversion will be recovered just downstream of the rupture location through the action of ruptures in adjacent subchannels. Thus, the impact of rupture-induced blockage is a net local improvement in heat transfer with no remote or downstream consequence. Finally, the inside of the cladding is exposed to metal-water reaction which creates a new heat source. The metal-water reaction is exponential with the cladding temperature, becoming significant relative to decay heat levels as the temperature approaches 1800 F. Below 1800 F the metal-water heating is a small fraction of the decay heat.

The temperature excursions are arrested as the combined ECCS flows exceed the core decay heat level and final core refill begins. The suppression of core steam production further depressurizes the RCS, and thus increases the ECCS injection flow and hastens core refill. Eventually the RCS system will be depressurized to the containment pressure and the core will be refilled. At this point, the start of a long-term cooling configuration has been established and the transient is mitigated.

11.2 Fuel Design Effects

SBLOCA transients are affected primarily by system design and core decay heat levels. Fuel assembly design influences the calculated sequence of events only to the extent that it affects overall system behavior. In that regard, differences between the Mark-BW reload fuel assemblies and the resident Westinghouse assemblies should not materially affect the bounding SBLOCA sequences of the reference FSAR. The BWFC and Westinghouse assemblies differ in the following areas: unrecoverable pressure drops across the assemblies, initial fuel temperatures, and initial pin internal gas pressure. The potential impacts of each of these differences, with respect to the controlling aspects of the SBLOCA transient, will be evaluated in the following paragraphs.

Mark-BW fuel assemblies have unrecoverable pressure drops that are approximately the same as those of the Westinghouse assemblies. The associated effect of small changes in overall loop pressure drop would translate to less than 1 percent difference in the initial forced flow. At the same steady-state core power and effectively identical loop flows, the controlling hot leg initial temperature is also essentially unaffected. The maximum hot leg temperature variation will be less than 1 F. Thus, the initial subcooled depressurization phase of the SBLOCA will be unaltered. The reactor trip signal and pump trips will occur at the same time in the transient as in the reference FSAR calculations.

The impact of the fuel bundle resistance will be even less during the pump coastdown and natural circulation phase because the flows during this phase are much reduced. Significant margins exist such that CHF will not be exceeded. All of the initial stored energy in the fuel will still be transferred to and removed by the steam generators. Therefore, core resistance variations will not change the fuel thermal transient or impact the existing evaluations.

Changes in the initial fuel temperature add or subtract overall energy from the RCS. The initial fuel energy is removed from the fuel pin during the reactor coolant pump coastdown phase and rejected from the system via the steam generators. Therefore, the initial fuel enthalpy at operation has virtually no impact beyond the loop coastdown period. The core energy content during the loop draining and boil-off mode will be identical to the current licensing base.

The fuel pin internal gas fill pressures are similar to the Westinghouse values, but may differ slightly. The internal gas pressure could affect the fuel/cladding gap dimensions and rupture time. The fuel temperatures approach the system saturation temperature within a fraction of a minute following reactor trip, and the impact of gap differences at low temperatures is

negligible. Therefore, the impact of the internal pressure differences prior to the boil-off phase is negligible.

The difference in internal pressure between the Westinghouse assemblies and the Mark-BW is such that the Mark-BW will have a slightly higher internal pressure both initially and during the transient. This will lead to a rupture of the Mark-BW fuel assembly at a somewhat earlier time than would occur for the Westinghouse fuel. As discussed in Section 11.1, the only effect of rupture on the S3LOCA transient is associated with the possibility of an additional heat load on the cladding due to oxidation of the inside surface of the cladding. The extra heating is inconsequential relative to the rest of the core or the other locations on the ruptured fuel pin, but it can effect the local cladding temperature. Because of the inverse relationship between the oxide layer and the rate of oxidation, the effect is most severe when the oxidation layer is thin. Therefore, the most severe consequences of a rupture during a small break LOCA occur when the timing of peak cladding temperature and rupture coincide. Because the occurrence of rupture for the Mark-BW fuel will precede that for the Westinghouse fuel, the Mark-BW will have ruptured and built-up an oxide layer at the time of peak cladding temperature that is thicker than that for the Westinghouse fuel. Therefore, the heating rate for the Mark-BW at the time of peak cladding temperature will be slightly lower than that of the Westinghouse fuel and the evaluation of the Westinghouse fuel will bound that of the BWFC fuel. Thus the Westinghouse evaluation along with its treatment of rupture remains bounding for the Mark-BW even with the increase in internal pin pressure.

As a final point, the technical specifications for allowable local power levels, core peaking, for core elevations at or above 8 feet will not be increased due to the use of BWFC-supplied fuel. Thus, the axial power profile used by Westinghouse in the SBLOCA analyses remains bounding. This assures that the thermal power imposed on

the fuel during a temperature excursion remains conservatively modeled. The thermal results, cladding temperatures, for the present FSAR evaluations are, therefore, conservative for Mark-BW fuel.

In summary, the core resistance variations will not affect the loop flows such that the controlling hot leg temperature or CHF points are altered. The steam generator heat removal rate during the flow coastdown period will compensate for any initial fuel stored energy fluctuations. All but one controlling parameter in the phases following the pump coastdown and natural circulation phase will be unchanged and that one, rupture timing, has been conservatively evaluated in the previous analyses. Therefore, since the overall RCS geometry, initial operating conditions, licensed power, and governing phenomena are effectively unchanged, the existing FSAR calculations should remain bounding for operation of the Trojan plant with BWFC-supplied fuel.

11.3 Current FSAR Results

The Westinghouse calculations of SBLOCA accidents for the Trojan plant are based on predictions by the NOTRUMP and LOCTA-IV computer codes. All parameters are within the acceptance criteria limits of 10 CFR 50.46. Small variations in SBLOCA results would not cause the SBLOCA to exceed the criteria of 10 CFR 50.46.

11.4 Compliance with Acceptance Criteria

The existing SBLOCA calculations for the Trojan plant are valid and bounding for the BWFC Mark-BW fuel. The reactor coolant system, decay heat levels, and other system controlling parameters remain unchanged by the reload fuel. The fuel design differences between the Westinghouse standard 17 x 17 and the BWFC Mark-BW do not substantially alter the results of SBLOCA evaluations. Adequate core cooling has already been demonstrated and does not need to be

repeated because of the change in fuel design. Thus, the present SBLOCA evaluation calculations are applicable to the Mark-BW reload fuel for demonstrating compliance with the criteria of 10 CFR 50.46.

12. References

1. RSG LOCA-B&W LOCA Evaluation Model for Recirculating Steam Generator Plants, BAW-10168 Revision 1, B&W Fuel Company, September, 1989.

2. RELAP5/MOD2-B&W, An Advanced Program for Light Water Reactor LOCA and Non-LOCA Transient Analysis, BAW-10164 Revision 1, B&W Fuel Company, October, 1988.

3. SAVER, Digital Computer Code to Determine Pressure Drops, BAW-10072-A, Babcock & Wilcox, July, 1973.

4. CRAFT2-FORTRAN Program for Digital Simulation of a Multinode Reactor Plant During Loss-of-Coolant, BAW-10092, April, 1975.

5. V. H. Ransom et al., RELAP5/MOD2 CODE MANUAL, Volumes 1 and 2, NUREG/CR-4312, EGG-2396, August 1985.

6. BEACH, Best Estimate Analysis Core Heat Transfer, BAW-10166 Revision 3, B&W Fuel Company, October, 1990.

7. Mark-BW Mechanical Design Report, BAW-10172, B&W Fuel Company, July, 1988.

8. Trojan Nuclear Plant Upgraded Safety Analysis Report, Portland General Electric Company, 1989 Update.

Appendix A. Evaluation of Transition Cores

During the period of transition from a full Westinghouse core to a full Mark-BW core, the two types of fuel assemblies will reside next to each other in various mixes for several cycles of operation. This appendix addresses the LOCA and ECCS aspects of both types of fuel assemblies in the mixed core configuration. As will be shown, the two fuel assemblies are so similar that there will be no feed back between them to alter the results of LOCA evaluations and either assembly could be evaluated with the other assembly occupying the remainder of the core with no consequence. Thus, the mixing of the fuel assemblies will not alter the LOCA evaluations and the evaluations of the fuels, performed as full cores, remain valid for the mixed core condition.

A.1 Westinghouse Standard 17 x 17 and Mark-BW Design Differences

Table A-1 presents a comparison of design parameters between the Westinghouse standard 17 x 17 and the Mark-BW fuel assemblies. There are no essential differences between the two fuels from the LOCA calculational standpoint. The only change that could cause fuel assembly interaction during a LOCA evaluation is the slight change in the unrecoverable pressure drop across the assembly.

Fuel Assembly Pressure Drop

The change in fuel assembly unrecoverable pressure drop, less than 0.3 psi, is too small to produce a meaningful and discernable change in LOCA results. In BAW-10174, Reference A.1, the effect of mixing fuel assemblies with up to a 1 psi difference in pressure drop (Westinghouse OFA to Mark-BW) was evaluated on large break LOCA results. The effect during blowdown was to divert some flow away from the high pressure drop assemblies and towards the low pressure drop assemblies. During reflood the impact was on the

whole core pressure drop which allows a gradual increase in the flooding rate as the core transitions from high pressure drop to low pressure drop assemblies. The high pressure drop assembly was shown to experience a possible 30 F temperature increase due to the mixed core during blowdown and a compensating 30 to 50 F decrease in temperature during reflood. The low pressure drop core experienced the opposite effects with the end conclusion of the study being that there were no adverse consequences during the mixed core period. The differences in design are considerable smaller for the switch from Westinghouse standard 17 x 17 to the Mark-BW and the resultant impact on the LOCA evaluations will be smaller. In fact it is probably not possible to evaluate the effect fairly as they lie well within the uncertainties of the evaluation models.

The impact of a fuel assembly pressure drop difference on small break LOCA was addressed in the BWFC response to Question 24 on BAW-10174, Reference A.1. Because of the abundant coolant flow available during the pump coastdown phase of the transient and because gravity heads rather than friction flow losses control system evolutions during the core uncovery phase of a small break, a difference in fuel assembly frictional pressure drop even much larger than that between the Westinghouse and BWFC fuels will not impact small break LOCA results.

A.2 Conclusions

An assessment of the design differences between the Westinghouse standard 17 x 17 and the Mark-BW assemblies has concluded that the LOCA cladding temperatures for mixed core operation will not vary from those calculated for the two designs in pure core operation. Furthermore, the calculations for each of the designs show margin to 10 CFR 50.46 criteria. The peak cladding temperature reported for the Mark-BW in Chapter 7 of this report is 2119 F. Therefore, the full core evaluations of the respective fuel assemblies can be

applied for licensing during mixed core operation. The analysis contained in the current FSAR will justify the use of the Westinghouse standard 17 x 17 assemblies, and the technical specifications applied to those assemblies will be based on those analyses. The analysis presented in the main body of this report will be applied to the licensing of the Mark-BW during the mixed core period, and the technical specifications applied to the Mark-BW assemblies can be based on the assumptions of this analysis. Operational limits or technical specifications required by either analysis that are not directly applied to the fuel assemblies will be based on the analysis which generates the most stringent limit.

A.3 References

1. Mark-BW Reload LOCA Analysis for Catawba and Mcguire, BAW-10174, B&W Fuel Company, September, 1989.

TABLE A-1 WESTINGHOUSE STANDARD 17 x 17 / MARK-BW
DESIGN DIFFERENCES

	Mark-BW	Westinghouse 17 x 17
Guide Thimbles:		
Upper Section OD/t, in	0.482/0.016	0.482/0.016
Lower Section OD/t, in	0.429/0.016	0.429/0.016
Instrument Tube:		
OD/t, in	0.482/0.016	0.482/0.016
Fuel Pin:		
Pin OD, in	0.374	0.374
Clad Thickness, in	0.024	0.0225
Pellet OD, in	0.3195	0.3225
Pellet Length, in	0.400	0.530
Diametral Gap, in	0.0065	0.0065
Pressure Drop Across Core, psi (at full flow)	22.7	22.5